12-2017

Naturally Derived Anti-Inflammatory and Antibacterial Coatings for Surgical Implants

Dmitry Gil
Clemson University

NATURALLY DERIVED ANTI-INFLAMMATORY AND ANTIBACTERIAL COATINGS FOR SURGICAL IMPLANTS

A Dissertation
Presented to
the Graduate School of
Clemson University

In Partial Fulfillment
of the Requirements for the Degree
Doctor of Philosophy
Bioengineering

---

by
Dmitry Gil
December 2017

Accepted by:
Dr. Alexey Vertegel, Committee Chair
Dr. William Cobb
Dr. Melinda Harman
Dr. Robert Latour
Dr. Kenneth Webb

ABSTRACT

The evolution of surgical approaches and procedures over the past century is remarkable. The brutality and risks associated with operations has substantially decreased, whereas the procedures themselves became safe and efficient. Nevertheless, none of the surgical procedures is completely safe, reliable and painless, which often leads to the patients experiencing post-operative discomforts. These discomforts are usually resolved within several days after the operation, and do not require any additional prophylaxes or treatments. However, in some cases, surgeries are followed by post-operative complications that cannot be resolved without additional medical attention. Shock, hemorrhage, deep vein thrombosis, pulmonary complications, urinary retention, reaction to anesthesia are among the most devastating post-surgical complications. However, the most important ones are infections and chronic pain. The emergence of these complications becomes more acute when surgical implants are used during the operation. Implant-associated complications often require specific medical treatment; in some cases, additional surgery or implant removal is necessary to resolve the complication. All these negatively affect patients' quality of life and put an additional economic pressure on a healthcare system. Therefore, the development of approaches to decrease the burden of surgical implant-associated complications, in particular chronic pain and infections, is an important objective and was addressed in the present study.

The first part of the dissertation is focused on the post-surgical infections. We addressed this problem in the example of orthopaedic Kirchner wires, bearing in mind high incidence rate of the pin-site infections, which can reach up to 100% for longer implant residence times. Therefore, novel approaches to prevention of microbial infections after insertion of orthopedic external fixators are in great demand. Monolaurin is an antimicrobial agent with known safety record, broadly used in food and cosmetic industries; however, its use in antimicrobial coatings of medical devices has not been studied in much detail. Here, we report the use of monolaurin as an antibacterial coating on external fixators for the first time. The monolaurin-coated Kirschner wires (K-wires) showed excellent antibacterial properties against three different bacterial strains - *Staphylococcus aureus*, methicillin-resistant *Staphylococcus aureus* (MRSA) and *Staphylococcus epidermidis*. Both planktonic and adherent bacteria were completely eliminated, when brought in contact with monolaurin-coated K-wires. At the same time, monolaurin-coated K-wires did not show any observable cytotoxicity with mouse osteoblast cell cultures. Overall, monolaurin-coated K-wires could be promising as potent antimicrobial materials for orthopaedic surgery.

In the second part of the dissertation we address post-operative chronic pain in the example of hernia repair meshes. First, we focused on studying the mechanism of the development of post-hernioplasty chronic pain. Despite the relative safety of the procedure, hernia repairs are often associated with chronic post-operative pain. While this complication has been linked among others to mesh

deterioration, details of the processes that lead this deterioration are still unknown. Here, we aimed to bridge this gap by analyzing the chemical, physical and structural alterations in hernia repair meshes exposed to oxidative stress *in vitro*. We developed a methodology to characterize effect of oxidation stress on structure and properties of polymeric hernia repair meshes. It was shown that structural changes in polypropylene meshes exposed to oxidative stress may involve formation of cross-links between the polymer chains, chain scissions, and hydrogen bonds between the carboxyl groups, which are formed in the material during the oxidation. These effects result in mesh stiffening, ultimately leading to chronic post-operative pain. Moreover, we demonstrated that Composix™ meshes are more vulnerable to the oxidative stress when compared with UltraPro® meshes.

Consequently, we focused on coating polymeric hernia meshes with anti-inflammatory agents in an attempt to mitigate the oxidative stress and improve long-term outcomes of the surgery. In particular, polypropylene hernia repair meshes coated with vitamin E (α-tocopherol), a known antioxidant, were prepared and characterized. The adsorption isotherm of vitamin E on the mesh was characterized and a release profile study yielded a promising results, showing sustained release of the drug over a 10-day period. An animal study was conducted, and histological analysis 5 weeks after implantation exhibited a reduced host tissue response for a modified mesh as compared to a plain mesh, as evidenced by a higher mature collagen to immature collagen ratio, as well as

lower level of fatty infiltrates, neovascularization and fibrosis in the case of modified mesh. These results support the use of α-tocopherol as a potential coating in attempt to reduce the extent of post-operative inflammation, and thereby improve long-term outcomes of hernioplasty.

DEDICATION

I would like to dedicate this work to my first scientific advisor, Dr. Aleksey Shaporev, who put a great deal of effort and invested a lot of his time in me, and introduced me to a fascinating realm of scientific research.

ACKNOWLEDGEMENTS

First of all, I would like to thank my current advisor, Dr. Alexey Vertegel, for inviting me to join his lab and giving me an opportunity to start the journey of my PhD research. I thank him for the wisdom he has shared, inspiration he has provided, and encouragement he has offered throughout the years.

Next, I would like to thank members of my lab, especially Dr. Vladimir Reukov, whose kindness, guidance, and support have been invaluable in every aspect during all these years. Also, I would like to thank Dr. Victor Maximov, Dr. Raisa Kiseleva, Dr. Yun Xiang, James Rex, Jeannette Rodriguez, Mikhail Bredikhin, and Anastasia Frank-Kamenetskii for their help and support.

I would like to express my gratitude to the members of my committee, Dr. William Cobb, Dr. Melinda Harman, Dr. Robert Latour, and Dr. Ken Webb for providing me assistance and guidance with regard to my projects. Also, I want to thank Dr. Martine Laberge and all other members of the Department of Bioengineering at Clemson University for giving me all the necessary support and help.

I would like to thank Dr. Christopher Gross, Dr. George Chumanov, Dr. William Richardson, and Dr. Igor Luzinov for helping me with the design of my experiments. Also, I want to acknowledge Kimberly Ivey, George Wetzel, Chad McMahan, Cassie Gregory, Dr. Shuguo Ma, Dr. Gulya Korneva and Olga Reukova for assisting me throughout the time spent in Clemson. I also want to thank my former advisors and members of Kurnakov Institute of General and Inorganic

Chemistry, and Lomonosov Moscow State University, particularly Dr. Vladimir Ivanov, Dr. Alexander Baranchikov, Dr. Alexander Vanetsev, Dr. Olga Ivanova, Dr. Natalia Kuzmina, Dr. Yulia Gorbunova, and Dr. Dmitry Petuhov.

I would like to sincerely thank my dear friends, in particular Sergey Shuvaev, Alexander “Sanechka” Samuel Polman (פולמאנ אלכס), Ekaterina Dolgopolova, Nikolay Borodinov, Anton Gavrilov, Artem Trofimov, Katie Trofimov, Pavel Aprelev, Dmitry Davydovich, Nick Erdman, Samuel Bearden, Tigran Abramyan, etc. Finally, I would like to thank and express my deepest love to my wife, Arina, and my family, whose unconditional support and care fueled this journey.

TABLE OF CONTENTS

Page

Table of Contents (Continued)

Page

Table of Contents (Continued)

Page

CHAPTER 1

INTRODUCTION

Nowadays, implantation of medical devices has become a conventional treatment modality for numerous medical conditions. Implants are artificial structures, which are placed inside or on the surface of the human body in an attempt to replace a missing biological part, or to restore its original functions. Currently, tens of millions of Americans have medical implants in their bodies. Examples of implants are catheters, orthopaedic and cardiovascular devices, neurological and contraceptive implants, etc. Despite being made of highly biocompatible materials, surgical implants trigger the host response, which can lead to implant-associated complications. Rejection, chronic inflammation, hemorrhage, implant migration and failure, and tissue damage are among the most common implant-associated complications [1,2]. However, the most impactful complications are post-surgical infections and post-operative chronic pain, as they result in the highest morbidity and mortality rates. These complications place a significant burden on the healthcare system, as in many cases revision surgery is the only treatment option for the patients. Therefore, developing approaches to prevent and treat post-surgical complications appears to be an important research direction.

The ultimate goal of the present study was to develop strategies to decrease the burden of medical implant – associated complications, thus improving long-

term surgical outcomes. A particular focus of this study was on two most significant complications: implant-associated infections, and post-operative chronic pain.

In the first part of the dissertation (chapter 3) we address post-surgical infections in the example of orthopaedic Kirchner wires (K-wires). Despite all recent improvements in orthopaedic surgery techniques and post-operative care, clinical infections continue to be one of the most serious complications, particularly when external fixators, such as K-wires, are used. In fact, multiple evidence suggests that the infection rate following K-wiring procedures is high and can reach 30 - 100% [3,4]. Therefore, the search for an optimal approach to mitigate pin-site infections is an important objective.

In the second part of the dissertation (chapters 4, 5) we address post-operative chronic pain in the example of hernia repair meshes. Hernia repair is the most common surgery in the US with over a million procedures performed annually. Post-hernioplasty chronic pain is a major complication affecting 20 - 30% of patients undergoing hernia repair. Therefore, development of the strategies to prevent or reduce the extent of post-hernioplasty chronic pain is of particular importance.

Current clinical strategies to reduce the burden of these complications rely heavily on the systemic administration of various drugs (antibiotics or pain-relievers), as well as appropriate wound care. However, these approaches are far from being perfect. For instance, systemic drug administration often results in adverse side effects. Additionally, appropriate wound care has limited efficiency

and is often neglected by the patients when needed for a prolonged period of time. Therefore, much research effort these days is focused on the development of novel approaches to reduce the emergence of implant-associated complications. Surface modification is among the most widely used and prominent strategies. Coating medical implants with various therapeutic agents provides drug delivery directly to the surgical site, improving outcomes of the operation. Moreover, since systemic administration is avoided, drug doses can be reduced; therefore, this approach promises a reduction of possible systemic side effects. However, in certain cases implant surface modification can cause undesirable effects upon implantation. For example, several therapeutic agents incorporated into antimicrobial coatings were shown to lack biocompatibility and possess feasible cytotoxicity, which can substantially impair the healing process [5]. Furthermore, since many therapeutic agents are water-soluble, it is difficult to provide and control sustained drug release in the vicinity of the implant. Therefore, development and optimization of the modification protocols, as well as the search for novel therapeutic agents appear to be critical objectives. In the present dissertation, we proposed to use water-insoluble, naturally-derived compounds as therapeutic agents to coat medical implants in an effort to improve long-term outcomes of surgeries.

The first specific aim of the present study was to develop a novel antimicrobial coating for orthopaedic implants, which combines pronounced antibacterial activity against common pathogens along with minute cytotoxicity.

Given that emergence of post-operative infections is particularly common for external fixators, we focused on studying Kirschner wires (K-wires) - the most widely used external fixators. In the first part of the study we proposed coating K-wires with monolaurin — natural compound found in coconut oil. Being widely used in food and cosmetic industries, monolaurin was shown to exhibit excellent antimicrobial properties against various microorganisms, including *Staphylococcus aureus* (both methicillin-resistant, MRSA, and methicillin-sensitive, MSSA, species) and *Staphylococcus epidermidis*, which combined are responsible for more than 80% of K-wire infections [6,7]. In spite of this fact, the use of monolaurin in biomedical applications was somewhat limited. In the present dissertation, K-wires were coated by monolaurin, followed by the detailed physicochemical characterization of the coating and assessment of the antimicrobial properties of the modified K-wires against *Staphylococcus aureus* strains (both, MSSA and MRSA) and *Staphylococcus epidermidis*. Additionally, cell culture experiments with mouse 7F2 osteoblasts were conducted to test cytotoxicity of the coated wires.

In the second part of the dissertation we focused on post-surgical pain. As stated above, post-operative chronic pain is a major complication, particularly common for hernia repair surgeries. A consensus has not yet been reached on the exact cause for this pain, however there are indications that oxidative stress, a result of the body's inflammatory response, may play a key role. For instance, enhanced activity of inflammatory cells was shown to induce oxidative stress in the

vicinity of the implant [8]. Moreover, physical and chemical integrity of hernia repair mesh can also be compromised. In particular, experiments with explants demonstrated that changes of mesh shape, as well as implant shrinkage can occur after the surgery leading to severe discomfort [9]. However, there is still a lack of understanding of the mechanism of hernia repair mesh deterioration in human body.

Therefore, the second specific aim of the present dissertation was to study the mechanism of oxidative deterioration of hernia repair meshes. Pursuing this aim, we focused on simulating the effect of reactive oxygen species (ROS) and hypochlorite anions on hernia repair meshes. We treated mesh samples in model environments that contained either H_2O_2 (in the presence of$CoCl_2$ and glass wool), or hypochlorite. The samples were then analyzed by means of several physicochemical techniques, including FTIR, DSC, SEM, XPS. Tensile strength testing was performed to evaluate mechanical properties of the analyzed meshes before and after the treatments. Results of these studies were used to determine the role of oxidative stress in the deterioration of hernia mesh in the body.

The third specific aim of this study was to develop anti-inflammatory coating for hernia repair meshes in an attempt to mitigate oxidative stress and reduce the incidence rate of post-hernioplasty chronic pain. In this part we hypothesized that vitamin E-coated polypropylene mesh would promote reduced inflammatory response around the implant, improve its mechanical durability, and decreased connective tissue formation, resulting in a more robust hernia repair with better

surgical outcomes. Utilizing a retromuscular approach to hernia repair, we assessed the characteristics of vitamin E as an anti-inflammatory coating through both *in vivo* and pilot *in vitro* studies.

Organization of the dissertation:

- Chapter two provides a comprehensive literature review that embodies the following topics:
  - Orthopaedic implants – associated infections and current strategies to address this problem;
  - Overview of hernia repair surgeries and post-hernioplasty complications;
  - Current approaches to prevent and treat post-hernioplasty complications.
- Chapter three discusses the novel antibacterial coatings on orthopaedic implants;
- Chapter four describes the *in vitro* study on polypropylene hernia repair mesh deterioration;
- Chapter five focusses on the development of anti-inflammatory coating on hernia repair meshes;
- Chapter six draws final conclusions and provides recommendations for further studies.

CHAPTER 2

LITERATURE REVIEW

2.1. Orthopaedic implant-associated infections

The potential for post-operative infection exists for all areas of medicine involving the implantation of foreign objects. Orthopaedic implant-associated infections (Fig. 2.1) are of particular importance as they result in high rates of morbidity and mortality. [10–13]. The present chapter focuses on orthopaedic infections, and the most common strategies to treat and prevent its emergence.

Fig. 2.1. Photograph of the superficial pin site infection*.

In terms of susceptibility to infections, orthopaedic implants can be divided into two groups. The first group includes the implants used for major orthopaedic surgeries, such as total hip, knee, and shoulder replacements. The infection rate for these types of implants is relatively low: according to several reports, the incidence rate of post-arthroplasty infections is 1-2% [14,15]. An average rate of infections following these major orthopaedic surgeries was estimated below 5%

* Photograph is provided by Dr. Christopher Gross, Department of Orthopaedics, Medical University of South Carolina, Charleston, SC, USA

[10]. However, if an infection emerges, it resides in the bone tissues causing high morbidity, and in some cases mortality. The second group is comprised of temporary orthopaedic implants, such as screws, pins, plates, wires, etc. The infection rate for those devices is considerably higher. For instance, the infection rate following external fixator surgeries was shown to exceed 30% [3]. For longer implant residence time and in the case of devastating traumas, the pin-site infection rate was shown to reach 100% [4]. Fortunately, the emergence of infections does not lead to the high morbidity and mortality, although revision surgeries are required to eradicate the contaminants.

Upon implantation, foreign bodies get exposed to numerous plasma proteins that absorb on implant surfaces in a matter of minutes. Although these proteins are necessary to promote cell adhesion and wound healing, multiple pathogens can also adhere and colonize on the protein-coated surfaces [16]. There are three general mechanism of the emergence of orthopaedic infections: 1) bacterial pathogens migrate from external sources; 2) bacteria are carried by blood from other parts of the body; 3) recurrent infections [11]. The first mechanism is particularly relevant for external fixator infections, as these implants provide an accessible passage for external contaminants.

Following bacterial adhesion, pathogens proliferate rapidly and are capable of secreting exopolysaccharides, thus, forming a biofilm—a robust structure that shields microorganisms from the host inflammatory response, and systemically administered antibiotics [11]. Therefore, if a biofilm is formed, treatment of an

infection often becomes difficult and, in some cases, a revision surgery is required [10].

Pathogens that cause orthopaedic implant-associated infections vary between countries. In the US, more than 80% of those infections are caused by methicillin-resistant and methicillin-sensitive *S. aureus* (MRSA and MSSA, respectfully) and *S. epidermidis* (MRSE and MSSE, respectfully) [15]. In European countries, considerable fraction of infections (ca. 90%) is associated with *Staphylococcus* spp. In their turn, *Enterococcus* and *Streptococcus* spp. account for approximately 8% of cases [17]. The infections caused by methicillin-resistant species is of particular importance, since they require specific prophylaxes and treatment modalities[11].

Management of musculoskeletal infections puts an additional economic burden on the healthcare system. In fact, treatment of necrotizing fasciitis, a type of infective complication associated with external fixations, was estimated in the range of $20,000 - $866,000 per patient [18]. Parvizi et al. reported the cost of care of periprosthetic joint infection to be ca. $68,000. Treatment of methicillin-resistant infections was shown to further increase hospital charges [19]. The total economic burden of orthopaedic infections is expected to reach $1.6B by 2020 in the US [10].

If not treated properly, orthopaedic implant-associated infections may substantially lower patient quality of life, and may even lead to mortality [20]. According to Bhattacharyya et al. a risk of infection-caused mortality after an

orthopaedic surgery was estimated to be 1.62% [13]. However, for total hip revisions for infections, a mortality rate of 26% within 2 years was reported [21]. Furthermore, osteomyelitis is claimed to be the leading cause of death in hand surgery and sports medicine [13].

Therefore, prophylaxes and treatment of orthopaedic infections appear to be of a paramount importance. Over the past years multiple strategies to manage orthopaedic infections have been developed.

2.1.1. Clinical strategies to address orthopaedic infections

Current clinical strategies to prevent orthopaedic implant - associated infections can be divided into three categories: preoperative, intraoperative, and postoperative methods.

Preoperative methods rely heavily on patient skin disinfection using various antimicrobial agents, such as iodine-based antiseptics, antiseptic soaps, and chlorhexidine gluconate-based drugs [11]. The latter compounds were shown to possess superb antibacterial activity, significantly reducing post-surgical infection rates [22]. Moreover, other cutaneous preparations, including hair removal and surgical draping, are conducted before surgery, and appear to be essential for infection prophylaxes [11].

During the surgery, antibiotic prophylaxis is the major infection preventive measure. In fact, it was shown that the absolute risk of infection is reduced by 8% if antibiotics are administrated during the operation. Cefazolin, clindamycin and

vancomycin are the most widely used antibiotics for this application [23]. Another preventive measure involves the use of intraoperative lavage. Brown et al. showed the significant decrease of the infection rate when dilute betadine lavage is used during arthroplasty [24].

Postoperative prevention methods include antibiotics prophylaxis and evacuation drains. According to the American Association of Orthopaedic Surgeons (AAOS), antibiotic administration should remain during the first 24 hours after a major orthopaedic surgery [11]. Although multiple reports show the efficacy of evacuation drains in terms of infection prophylaxis, superficial bacteria can use drain tubes as a passage to the injury site. Therefore, drain tracts are recommended to be removed between 24h and 48h [25].

However, currently used clinical strategies lack efficiency due to several factors. Among these is the development of drug resistance, inability to eradicate all the microorganisms lodging in patient's skin, and insufficient wound care. These translate to the relatively high incidence rate of orthopaedic implant – associated infections. Therefore, much research focuses on the development of novel approaches to prevent orthopaedic infections.

2.1.2. Research strategies to fight orthopaedic infections

In the search for an optimal strategy to prevent and treat orthopaedic infections, multiple approaches are currently being developed and tested. Most of the studies published in this area can be divided into two categories: development

of an antibiotic-loaded bone cement, and modification of orthopaedic implants with antibacterial agents.

Bone cement is a polymeric material that consists of poly(methyl methacrylate) (PMMA) micro-beads cross-linked by PMMA chains. This material is primarily used to secure joint-replacement implants [26]. Due to its relatively high porosity, bone cement appears to be an excellent matrix for antimicrobial agents. The ultimate aim of the antibiotic-loaded cement is to deliver antimicrobial drugs directly to the implant surface and surrounding bone [12]. In 1979 Klemm et al. demonstrated excellent antimicrobial properties of the gentamicin-loaded cement, and since then, various antibiotics have been tested as additives to the bone cement [26]. Scott et al. showed that tobramycin-loaded cement exhibited pronounced antibacterial activity against the pathogens causing 98% of orthopaedic infections [27]. Several studies demonstrated excellent activity of vancomycin and amphotericin B impregnated into the cement [11,28].

Despite the success of *in vitro*, animal and clinical studies of antibiotic-impregnated bone cements (AIBC), a number of scientists and physicians oppose the use of these compounds in joint replacement surgeries [12]. Their major concern is the alteration of mechanical properties of the cement when antibiotics are loaded. Moreover, control and adjustment of the drug release kinetics from AIBC is often difficult. Insufficient drug release can also contribute to the development of antibiotic resistance. However, feasible progress has been made in this area by optimizing cement composition [26].

It is important to note that the use of AIBC is somewhat limited, as many orthopaedic surgeries do not require cement for implant fixation. Therefore, the use of AIBC cannot be considered as a universal approach to address the incidence of orthopaedic infections.

Another research strategy to eliminate orthopaedic infections involves the development of antimicrobial coatings on the implants. Various antibacterial agents are either covalently grafted to the surface, or physically adsorbed, or incorporated into polymeric matrices to achieve prolonged drug delivery [12]. Moreover, several studies focused on “hybrid antibacterial surfaces”, which combine covalently attached antibiotics and controlled release systems [29,30].

Most research dealing with covalent modification of metallic implants focuses on grafting vancomycin using various linkers, such as diphosphonic acid, various silanes, glycidyl-containing groups, etc [12]. Besides vancomycin, several other antibiotics, including daptomycin, kanamycin and tetracycline, were successfully tethered to metallic surfaces [31,32]. Additionally, metallic surfaces modified with silver nanoparticles have also been extensively tested [33]. Multiple *in vitro* and animal studies showed feasible antibacterial activity of the modified implants against orthopaedic device-related pathogens [33]. However, when covalently grafted, antimicrobial agents often exhibit reduced antibacterial activity due to the alterations of their chemical structure. Moreover, therapeutic compounds that interact with bacterial DNA lose their activity completely when grafted to the surface due to diffusion limitations. Furthermore, sustained drug

release cannot be achieved when therapeutic compounds are covalently linked to or immobilized on the surface of the implant. Another concern is associated with high cytotoxicity of the surfaces modified with silver nanoparticles.

Several studies focused on physical adsorption of antibiotics and antiseptics on orthopaedic implants. Surfaces modified with various conventional antimicrobial agents (e.g. chlorohexidine, gentamycin, vancomycin, etc.) have been tested *in vitro* and demonstrated prominent antibacterial properties. At the same time, successful animal studies with physically adsorbed antibiotics were not reported in the literature, potentially due to the insufficient mechanical stability of the coatings [20,33]. Therefore, additional studies are required to establish if physically adsorbed drugs can be used in orthopaedic applications.

Controlled drug delivery is a powerful treatment modality drawing the attention of scientists in various areas of medicine. However, only few studies dealt with drug eluting coatings on orthopaedic implants [34–36]. Low work of adhesion between the metallic surface and polymeric matrix, which provides controlled drug release, makes it difficult to adhere a drug-eluting layer to the implant. Nevertheless, several studies focused on the modification of titanium and stainless steel orthopaedic implants with polylactide and polyglycolide coatings loaded with different antibiotics, such as gentamicin, triclosan and teicoplanin [36,37]. Preliminary *in vitro* and animal experiments demonstrated the pronounced antibacterial activity of the modified implants against MSSA, MSSE and *P.aeruginosa*. Other studies focused on the incorporation of antimicrobial agents

into a hydroxyapatite layer. Coatings loaded with tobramycin, vancomycin, amoxicillin, silver nanoparticles, etc. were tested against most of the orthopaedic-related infections [38–40]. Animal studies suggested that ceramic coatings impregnated with antibiotics can not only prevent orthopaedic infections, but also significantly improve osseointegration.

Despite current achievements in the development of antimicrobial coatings on orthopaedic implants, this approach possesses several important shortcomings. In particular, most antibiotics and antimicrobial agents (such as silver nanoparticles) exhibit feasible cytotoxicity, which was shown to impair fracture healing [41]. Moreover, modification of orthopaedic implants often requires physical and/or chemical treatments, which can alter implant characteristic, ultimately affecting osseointegration [42]. Therefore, the search for an optimal strategy to prevent and treat orthopaedic infections is still ongoing.

2.2. Hernia repair

2.2.1. Historical aspects of hernia

The word *hernia* comes from Latin and means rupture of a portion of a structure. One can define hernia as a bulging of an organ (or a portion) through an abnormal hole or opening into an area where it should not be originally located. Hernias have been drawing attention of physicians since the dawn of the surgical era, primarily due to the high prevalence of this medical condition [43]. In 1892 Dr. William Halsted, professor of surgery at John Hopkins University, claimed: “There

is perhaps no operation which has had so much of vital interest to both physician and surgeon as herniotomy, and there is no operation which, by the profession as large, would be more appreciated than a perfectly safe and sure cure for rupture" [44]. This statement demonstrates the profound impact of hernia formation and hernia repair surgeries.

According to Lyons et al. hernias were first mentioned in the Egyptian Papyrus of Ebers at ca. 1552 BC, where ancient physicians characterized this condition as an abdomen swelling caused by coughing or other physical activities [45]. The next significant reference to hernias was made in the book "On the Surgery" written by Hippocrates in 352 BC, where he speculated about the susceptibility of young children to hernias [46]. Hippocrates followers, who are claimed to be the founders of anatomy and physiology, were shown to practice hernia repair among other surgeries.

Aulus Cornelius Celsus, one of the most ardent followers of Hippocrates, brought his knowledge to the Roman Empire, where he did much to advance the techniques [47]. Celsus provided the first detailed descriptions of hernia defects, hernia repair techniques, and records of the operations conducted in "Alexandrian traditions". State-of-the-art procedures introduced by Celsus were further developed by Heliodorus and Gallen of Pergamum. The most advanced technique involved litigation of the hernia sac, followed by the amputation of the testicles, in the case of groin hernias [48].

Unfortunately, the major improvements to hernia repair of hernia repair surgeries were lost and forgotten during the middle ages. Not until the 13th century a novel herniotomy technique was described and successfully implemented [43]. William of Salicet, a talented surgeon from the medical school of Salerno, modified Celsus's approach and managed to both close the hernia sac and preserve the testicles.

The next significant development of hernia repair was made by Ambroise Pare in the16th century; he proposed for the first time to separate the peritoneum, and use it to close the hernia defect [49]. If the proposed technique was not possible, Pare suggested to use the Golden Ligature to close the opening. Pierre Franco introduced further improvements to the Pare's technique completely eliminating the necessity to excise testicles and spermatic cord in the case of groin hernias. Kaspar Stromayr, in his turn, was the first surgeon to describe the differences between direct and indirect hernias. Moreover, he developed multiple surgical approaches for both types of hernias [47].

Hernia research in the 18th century was primarily focused on the study of its pathogenesis. Drs. Cooper and Richter conducted the most advanced research of their time, and were the first to recognize the role of transversalis fascia in the development of hernias [43].

Despite the number of herniotomy techniques developed by the beginning of the 19th century, none of them was flawless leading to a high incidence of failures and recurrences [45]. An Italian surgeon, Eduardo Bassini, addressed these issues

by introducing a pioneering technique called the Bassini repair [50]. This approach involved sewing the hernia defect followed by reconstruction of the abdominal floor. This was done by approximating the conjoined tendon to the inguinal ligament. The Basini repair revolutionized hernia repair surgeries resulting in a substantially lower complication rate [50]. Up until the late 1950s, the Basini repair appeared to be a gold standard for hernia repair surgeries. Nonetheless, several surgeons further developed the approach improving the efficacy of the methodology. For instance, Harvey Cushing pioneered the use of local anesthesia while performing the Basini repair [51].

Although several essential modifications to the original Basini repair technique were developed and successfully implemented, the rate of post-surgical complications was still relatively high [47]. Post-operative chronic pain and hernia recurrence was among the most devastating complications. This was perhaps due to the additional stress that was put on the adjacent tissues when the edges of the defect were stitched together. It is important to emphasize that despite all the advancements introduced by that time, the general concept of hernia repair remained the same since the middle ages.

In the late 1950s the development of novel anesthetics gave rise to two major hernia repair techniques: the tension-free hernioplasty and the Canadian Shouldice repair [47]. These two novel approaches revolutionized hernia repair surgeries resulting in more efficient and safe operations. This was done by reconstructing the hernia defect and abdominal cavity by means of surgical mesh.

In 1959 Dr. Usher and his colloquies conducted the first hernia repair surgery involving polyethylene (Marlex) mesh being used for an additional reinforcement of the ligation of the hernia sac [52]. Later that year, Usher proposed the use of polypropylene mesh for closing hernia defects for patients with large protrusions [53]. The choice of polypropylene mesh was dictated by: 1) the ability of polypropylene to resist infections; 2) low immunogenicity; 3) mechanical characteristics of the material. Outcomes of the surgery were remarkable; Usher later stated: “The postoperative course of these patients has been remarkable. They are quite free of postoperative pain, catheterization is seldom necessary and they are able to walk in an erect position without discomfort’’ [53]. Another important innovation of the Usher’s technique was the retention of a normal shape, position and direction of the spermatic cord, in contrary to what was observed in herniorrhaphies. By the beginning of the 1980s, Usher’s approach was successfully optimized for all types of hernia defects, and since then the prosthetic tension-free repair has been dominant in hernia repair surgeries [54]. However, it is important to note that herniorrhaphies are still performed when operating infants, repairing small and minor hernias, and in some developing countries, where there is a lack of prosthetic meshes [55].

The emergence of laparoscopic surgeries positively affected hernioplasty and resulted in a safer hernia repair. Filipi et al. reported the substantial advantages of laparoscopic hernia repair over conventional hernioplasty [56]. The

recovery time and long-term outcomes of the repair were shown to significantly improve with the laparoscopic approach.

2.2.2. Biological aspects of hernia formation

Prior to discussing hernioplasty-related complications, it is important to reveal and understand the processes preceding and causing the initial formation of hernia. As mentioned earlier, hernia appears to be a defect in the form of a weakening or a hole in a muscle wall, through which an organ or its part protrudes to an area where it should not be originally located. Depending on the location of the defect, physicians distinguish several types of hernia, including femoral, inguinal, spigelian, umbilical, ventral, hiatus (Fig. 2.2).

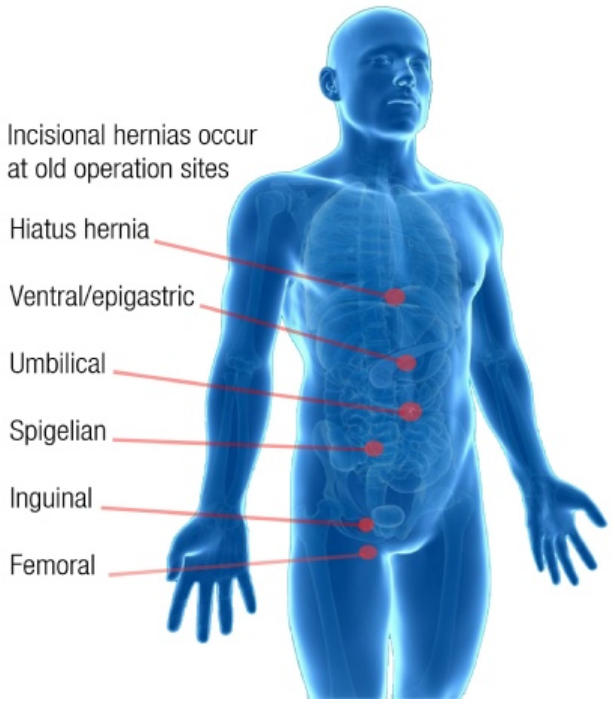

Fig. 2.2. Types of hernia defects [57].

Moreover, there are also incisional hernias, which emerge in the areas where an incision or trauma previously occurred. Although there is no general consensus regarding the mechanism of hernia development, many scientists believe that a hernia is a disease of an extracellular matrix (ECM) [58,59]. Despite technological advancements and developments in hernia repair surgeries, several reports suggest that the decrease in hernia recurrence rate following the repair is marginal [60].

Thus, it was proposed that the external factors (endogenous and exogenous) may have more influence on the healing process than the surgical procedure (Fig. 2.3) [61].

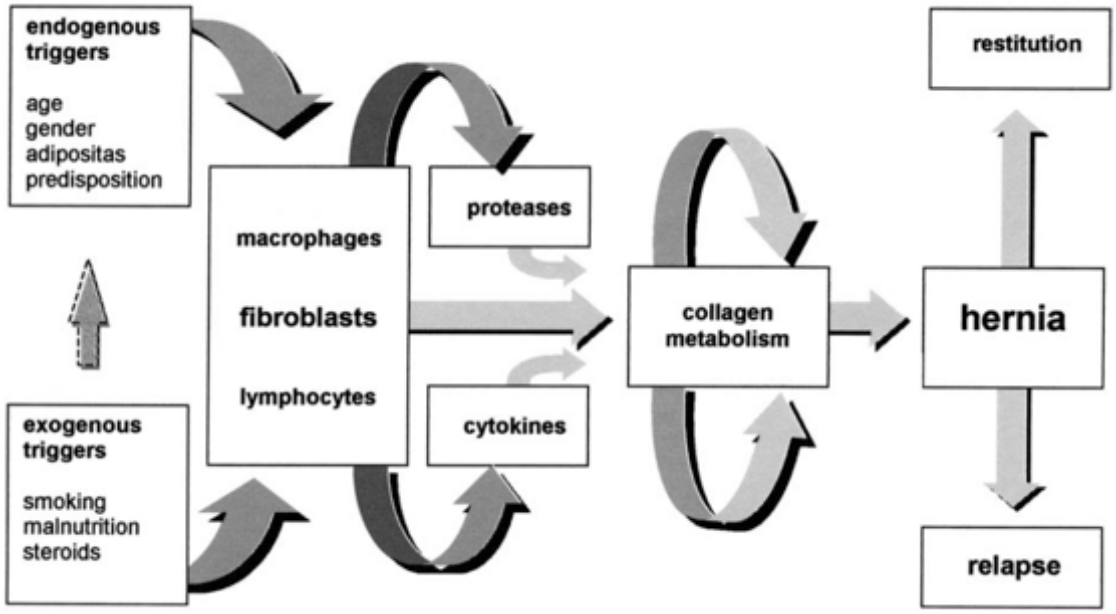

Fig. 2.3. The mechanism of hernia formation [59].

These factors were shown to affect collagen turnover in hernia patients [62]. There is a growing body of evidence suggesting that deviations in collagen

production and metabolism contribute to both the initial formation of hernia defect and the opening recurrence [58,62,63]. If collagen structure and integrity is compromised, the process of tissue remodeling and wound healing is affected, ultimately resulting in the deterioration of the ECM mechanical properties. This claim was confirmed in papers studying tissue samples taken from the hernia patients [58,62,64,65]. In the case of direct inguinal hernias, the rectus sheet was shown to contain irregular collagen fibrils, making the tissue more compliant and compromising biomechanical properties [66]. These observations were also confirmed for incisional and recurrent hernias [67].

Another abnormality found in the analyzed tissue samples was the decreased ratio of collagens type I/III in the fascia [59]. Moreover, in the case of incisional hernias, significant alterations in the morphology of collagen fibers were observed in the samples taken from the hernia sac, and newly formed tissues in the vicinity of the defect [68]. These results are indicative of the compromised metabolism of collagen.

Although the factors causing alterations in collagen metabolism are still a subject of debates, there is a theory that overexpression or underexpression of the matrix metallo-proteinases (MMPs) play a role in collagen deterioration [59]. MMPs are a class of enzymes capable of degrading components of ECM, specifically collagen. MMPs play an important role in tissue remodeling and wound healing processes. With regard to hernia formation, Bellon et al. demonstrated an increased concentration of MMP-2 in the tissue samples taken from the patients

with inguinal hernia [69]. Other studies showed overexpression of MMP-1 and MMP-13 in fibroblasts in the case of recurrent inguinal hernias [70,71]. Antoniou et al. confirmed previous observations showing high levels of MMP-9 and MMP-2 in the patients with inguinal hernias [72]. At the same time, concentrations of MMP's inhibitors, TIMP metallopeptidase inhibitor (TIMP), was found to be significantly lower when compared to the healthy patients [58,72]. Therefore, MMP and TIMP may play an important role in the development of hernia defects. However, there are other factors leading to hernia development.

In the case of incisional and recurrent hernias, alterations in the architecture of a newly-formed tissue was shown to play a significant role in the development of an opening [73]. Type I and type III collagen are major components of scar tissue. Collagen type I is composed of highly-organized fibrils, aligned towards the stress lines, and possesses robust biomechanical properties. Type III collagen is significantly softer and more compliant when compared with the type I [59]. It consists of thin tropocollagen fibrils secreted by fibroblasts during the remodeling phase of the wound healing [74]. Type III collagen is often called "immature", and after being produced, it is then transformed into type I ("mature") collagen at a later stage of wound healing [75]. Thus, the decrease of type I/III collagen ratio can cause deterioration of the ECM biomechanical properties, ultimately resulting in the formation of a hernia defect [68].

Klinge et al. confirmed this theory, demonstrating a significant increase in type III collagen content in hernia patients [76]. Another study showed an

increased level of type III collagen production in patients with pronounced herniation [77]. These observations were additionally confirmed in the literature [68,71,78]. Animal studies reviewed by Deeken e. al. showed a significant drop of the ECM biomechanical strength, as well as high content of collagen type III [79].

There are several factors causing alterations in type I/III collagen ratio. Several studies suggested that modified expression of various collagenase, in particular MMP-2 and MMP-13, is a key reason for the high type III collagen content in hernia patients [71,80,81]. At the same time, Ajabnoor et al. showed little to no difference in the activity of various MMPs in hernia and control patients [54]. Therefore, the predominance of type III collagen in the hernia group can be ascribed to the alterations of collagen expression.

Genetic factors can also be responsible to the overproduction of collagen type III in hernia patients. Jansen et al. showed that impaired regulation of the collagen gene can result in significant alterations during injury-related wound healing [82]. In particular, the transition of collagen type III to type I can be severely compromised.

With regard to recurrent hernias, several studies showed that herniation can be caused by post-operative chronic inflammation, ultimately causing impaired mesh tissue integration [58,83]. Although mesh materials are believed to be highly inert, in ca. 20% of cases post-hernioplasty inflammation does not resolve, accelerating macrophage and neutrophil recruitment to the injury [54]. These non-lymphatic white blood cells produce a myriad of oxidants and enzymes, which were

shown to affect the fibrillogenesis [54,58]. As such, type I/III collagen ratio may be significantly lower in inflammatory conditions when compared to the resolved inflammation (Fig 2.3).

Exogenous factors can also play a role in the development of herniation. Lifestyle diseases, in particular diabetes, obesity, smoking, and drug abuse, were shown to substantially affect fibrillogenesis, causing a decrease of the type I/III collagen ratio and, thus, increasing the chance of hernia formation [54].

2.2.3. Overview of hernia repair meshes

As stated previously, prosthetic hernioplasty is currently a gold standard for surgical hernia repair. These operations imply the use of surgical mesh for tissue reinforcement. Over the past decades, a variety of different hernia meshes have been developed.

Initial development of hernia meshes aimed to create an implant capable of withholding intra-abdominal pressure and providing tissue ingrowth. These requirements dictated the shape and structure of hernia meshes, and resulted in the development of implants with thick polymeric filaments. These meshes are called heavy-weight due to the high density and amount of the polymer used in production. However, multiple evidence showed that the host-tissue response provoked by heavyweight meshes was relatively high, resulting in impaired healing [64,84,85]. As discussed previously, excessive inflammatory response following hernioplasty can result in post-hernioplasty complications. Moreover, movement

constraints and increased chances of hernia recurrence were also recorded for patients with heavyweight meshes [83,86].

After the value of intra-abdominal pressure was determined, it became clear that the amount of polymer composing the meshes could be substantially decreased [75]. In 1998, a Vypro® mesh was introduced and became the first lightweight hernia repair mesh. This type of implant consists of thin polymeric fibers and large pores that facilitate tissue ingrowth. Implantation of the lightweight meshes was shown to reduce host-tissue response when compared with the heavyweight meshes [55,79]. Moreover, lightweight hernia repair meshes are significantly more compliant, and do not generally shrink after implantation [87]. These characteristics were shown to substantially improve the outcomes of hernioplasty as well as patients' quality of life after the surgery. However, multiple reports suggest that implantation of the light-weight meshes can still lead to post-hernioplasty complications, including recurrences, chronic pain, infections, etc. [75,85]. Therefore, minimizing mesh density is not sufficient to eliminate the burden of post-hernioplasty complications.

Lake et al. used a porcine model to study the influence of pore size and shape on tissue integration and wound healing following hernioplasty [85]. Meshes with square, diamond and hexagonal pores were implanted, and the T-peel test was used thereafter to quantify mesh tissue ingrowth. Meshes with hexagonal pores were shown to possess the most pronounced tissue integrative properties, followed by diamond-like and square pores. With regard to the pore size, it was

shown that meshes with medium pores (3.8X3.9mm) exhibited the best tissue integration and ingrowth when compared to the large (4.9X5.1mm) and small (1.7X3.6mm) pores. However, previous reports suggested that implantation of the meshes with ultra-large diamond-like pores led to the best outcomes in terms of tissue integration and compliance, as well as post-operative chronic pain [88,89]. Large-pore meshes were also shown to reduce foreign body sensation [88]. Therefore, the ideal pore shape and size is still subject of a debate, however, most studies suggest that small pore hernia meshes provoke significant host-tissue response, culminating in impaired healing.

Over the past decades, many researchers have been involved in a search for an ideal material for hernia repair implants. All meshes developed currently can be divided into three categories: non-absorbable, absorbable, and biological.

The following polymers are commonly used to produce non-absorbable meshes: polypropylene (PP), polyester, polytetrafluoroethylene (PTFE, Teflon), and polyvinylidene fluoride (PVDF). According to multiple reports, PP meshes are the most widely-used, primarily due to the favorable mechanical properties; these meshes also provide sufficient tissue ingrowth and incorporation [90–92]. Moreover, PP meshes are inexpensive and available in most institutions. At the same time, several studies suggest that PP meshes lose compliance upon exposure to oxidative stress [93,94].

Polyester meshes are also widely used in several European countries. These meshes provide excellent tissue integration and are less susceptible to the

foreign body reaction when compared with PP meshes [95]. At the same time, polyester meshes were shown to be more susceptible to infections, as well as losing their integrity and strength over time due to the material degradation [96,97]. Moreover, excessive tissue deposition and adhesions were shown to be an issue [97].

PTFE hernia repair meshes became widely used after the release of the Gore-Tex® Soft Tissue Patch. These meshes gained success due to their chemical and biological inertness, which significantly reduces tissue adhesions and foreign body reaction [98]. On the other hand, several studies suggest that PTFE meshes exhibit low tissue ingrowth and high recurrence rate due to having poor mechanical properties [99,100]. Moreover, implantation of the PTFE meshes is often associated with higher infection risks [101].

Although PVDF meshes are relatively new on the market, multiple clinical studies suggest that they possess excellent tissue integrative properties, sufficient mechanical properties, and do not provoke tissue adhesions [8,102]. Moreover, the risk of infections is low when compared with PP and polyester meshes [103]. Host-tissue response was also shown to be mild, and comparable with that of PTFE meshes [103]. However, another meta-analysis showed a high recurrence rate associated with the PVDF meshes [104]. Therefore, further studies are required to establish clinical outcomes of the PVDF hernia meshes.

Most of the absorbable meshes are made of polyglycolic acid or polylactic acid. The first absorbable meshes were introduced in 1983 and were expected to

become a golden standard for hernia repair. However, it was later shown that these implants provoked pronounced host-tissue response leading to an impaired healing and increased chances of recurrence [54]. Therefore, modern absorbable meshes are used infrequently, and are substituted with composite meshes, such as UltraPro® mesh system that consists of polypropylene and poliglecaprone-25 fibers [100]. This type of implant combines the advantages of both absorbable and non-absorbable meshes. Composite meshes are widely used nowadays, and were shown to provide excellent tissue-integration [100]. The mechanical properties of these meshes are sufficient to avoid hernia recurrence. However, due to the degradation of the absorbable portion, composite meshes were shown to provoke mild to low host-tissue response [54]. Therefore, none of the polymeric meshes is without disadvantages.

Development of the approaches to obtain biological tissue grafts led to the emergence of bioprosthetic meshes, which are mainly composed of extracellular matrix (ECM). These implants were claimed to possess paramount tissue-integrative properties, match the mechanical properties of their predecessors, and resist contaminations [105]. The last quality—the ability to be used in infected or potentially infected areas—appeared to be a genuine breakthrough and was highly promoted in the literature [54].

Surprisingly, the performance of biological meshes was found to be below expectations. Cano et al. provided a comprehensive comparison of the clinical experience with biological and prosthetic hernia repair meshes [106]. Although

there are data suggesting that ECM - derived meshes are effective, there is still no consensus of how or when to use biological implants. Moreover, there is no long-term data showing long-term effects of biological meshes. Having analyzed clinical evidence, Cano et al. concluded that biological implants should be used only when the use of synthetic implants may be harmful. For instance, biological meshes were recommended for immunocompromised patients, in the case of contaminated surgeries, or for the patients with chronic infections without large bacterial inocula. It is important to note that the use of biological meshes is contraindicated in infected patients with large bacterial inocula. These results are in good correlation with those published by Bellows et al. [105]. They reported a lack of high-quality clinical evidence of the superiority of bioprosthetic hernia repair meshes over polymeric implants. Thus, the use of the ECM-based meshes in hernioplasty should be performed with caution. Le et al. performed a review on the use of different kinds of hernia repair meshes including conventional and bioprosthetic implants [107]. It was shown that the use of biological meshes is preferred in the high-risk clean cases such as morbid obesity, smoking, immune suppression and history of previous infections. Surgeons should strongly consider ECM-based implants in patients with an increased number of comorbidities or risk factors. Smart et al. showed that, despite the lack of clinical data for biological hernia repair meshes, the use of three implants, AlloDerm™, Permacol™ and Surgisis™, drastically decreased hernia recurrence rate [108].

Therefore, despite the quantity and diversity of hernia repair meshes on the modern market, none is flawless, resulting in complications following hernia repair. At the same time, it is important to note that polypropylene meshes continue to be a gold standard for hernioplasty.

2.2.4. Complications following hernioplasty

Although hernia repair meshes used nowadays are claimed to be safe, biologically inert and biocompatible, clinical practice shows that mesh implantation can initiate several undesirable processes (e.g. fibrosis, excessive inflammation, calcification, etc.), which lead to post-hernioplasty complications [109]. This chapter focusses on the most common complications following hernia repair surgeries.

Every hernia repair is followed by a host-body response [54]. This process involves migration of non-lymphatic white blood cells, particularly monocytes and neutrophils, and their subsequent activation. Once activated, macrophages and neutrophils release a myriad of oxidants (reactive oxygen and reactive nitrogen species) and enzymes that interact with both the implanted material and surrounding tissues [93]. This leads to the development of granuloma that can cause seroma formation, tissue adhesions, mesh migration, as well as chronic pain [75].

The risk of seroma formation is feasible only in the case of large and complicated incisional hernias [110]. The risk increases concurrently with

dissection extent. Seroma rates are generally higher for Teflon® meshes (5-15%) as compared with polypropylene implants (5-8%) [111,112]. Although in some cases seroma can resolve spontaneously, drains or catheters are often required to treat the complication [110].

A cascade of various cellular and humoral effects following hernia repair surgery can cause the formation of peritoneal adhesions (Fig. 2.4) [113]. This often results in chronic pain and movement constraints [54]. Once these symptoms are observed, and the adhesions are confirmed, a revision surgery is required. The rate of adhesions following hernioplasty was shown to be ca. 3.3% [114].

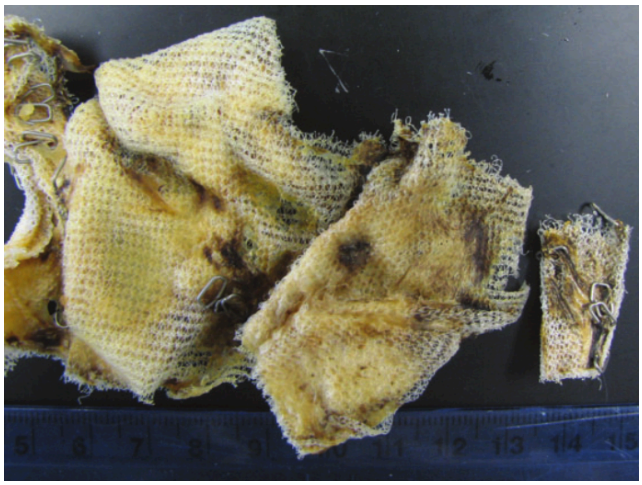

Fig. 2.4. Photograph of explanted hernia meshes showing tissue adhesions and mesh shrinkage [117].

There are several strategies to reduce adhesiogenesis. In particular, little to no tissue adhesions were observed after implantation of biological meshes and those made of Teflon [75,115]. Another strategy involves coating polymeric meshes with collagen, which was shown to significantly enhance tissue integration and eliminate adhesiogenesis [116].

While performing hernioplasty, surgeons typically use sutures to fixate the mesh. However, several studies showed that in ca. 1% of cases, hernia meshes can migrate due to an improper fixation or external displacing forces [118,119, 109,120]. Mesh displacement can also occur due to the trans-abdominal forces. Mesh migration was shown to trigger the inflammatory process, leading to chronic pain [54].

Along with post-operative chronic pain, mesh-related infections are the most devastating complications of hernioplasty. Many meta-analyses focusing on the prevalence of hernioplasty associated infections have been conducted over the past years [109]. An infection rate of up to 8% was reported in the literature [121]. For patients suffering from obesity and diabetes the rate was shown to be even higher [1].

Leber et al. studied the influence of surgical techniques on the infection incidence rate [122]. Interestingly, it was shown that there is no direct correlation between the surgical approach used for hernioplasty and the infection rate. Although, there is a general opinion that laparoscopic approach reduces post-operative complications, there is no data supporting this notion with regard to post-hernioplasty infections [1].

Several studies focused on the correlation between the mesh type and the infection incidence rate [122,123]. A significant increase in infection rate was shown when microporous meshes (e.g. Teflon meshes) are used. These implants possess pores with a diameter of ca. 10 μm, which enables bacteria to lodge on

them and form a biofilm [1]. At the same time, non-lymphatic white blood cells are too large to penetrate the pores, resulting in inability to provide sufficient immune response.

With regard to the pathogens causing post-hernioplasty infections, *Staphylococcal* species were reported to be responsible for most of the cases. Moreover, the incidence rate of methicillin-resistant *Staphylococcus aureus* (MRSA) infections following hernia repair was shown to reach up to 63% [124]. In rare cases, post-hernioplasty infections are caused by *Streptococcal* species, *Enterobacteriaceae* and *Peptostreptococcus* species [125].

2.2.5 Strategies to reduce post-hernioplasty complications

Despite being considered relatively safe and reliable procedure, hernioplasty is often associated with post-operative complications. As previously discussed, infections and chronic pain are among the most devastating complications following hernioplasty. Despite all recent improvements to mesh design and surgical procedures, complication rate is still approximately 25% [54]. Therefore, development of strategies to decrease the burden of post-hernioplasty complications is an important objective.

In an attempt to decrease the complication rate, several strategies focusing on modification of hernia meshes with various coatings have been developed over the past years. In particular, multiple studies focused on providing antibacterial activity to hernia meshes by coating the latter with antiseptic or antimicrobial

agents [116]. A variety of conventional antibiotics (e.g. vancomycin, gentamicin, rifampicin, etc.) and antiseptics (e.g. chlorohexidine, triclosan, etc.) have been extensively tested to modify commercially available meshes [78,126,127]. *In vitro* and *in vivo* experiments showed excellent results suggesting that antibacterial coatings can significantly reduce the burden of post-hernioplasty infections. However, several studies revealed that certain antibiotic and antiseptic coatings exhibit potential cytotoxicity, which can result in adverse side effects and impair healing [128,129]. Nonetheless, several antimicrobial coatings were shown to possess low cytotoxicity along with the pronounced antibacterial activity [116]. Some of the products successfully underwent clinical studies and were approved by the FDA. GORE became the first company to commercialize antibiotic loaded hernia repair meshes (MycroMesh™ Plus).

Several strategies were used to incorporate antimicrobial agents into the meshes. Dip-coating, electrospraying, and air brush spray techniques are among the most widely used approaches to modify hernia meshes with antimicrobials [78,130,131]. In particular, Yurko et al. demonstrated prominent antibacterial activity of the lysozyme-coated hernia meshes against *S. aureus* [131]. Moreover, multiple studies focused on drug incorporation into absorbable polymeric matrixes, including those based on polylactide and polyglycolide (PLA and PLGA, respectfully) [78,132]. These drug-loaded systems were then used to modify hernia meshes in order to achieve prolonged drug release. Besides polymeric-based systems, drugs were also incorporated into various hydrogels, including those

based on chitosan [132]. These drug delivery systems were shown to provide sustained drug release, enhancing the efficacy and reducing side effects of the antimicrobial therapy.

Besides coating with antimicrobial agents, multiple studies focused on modifying hernia mesh with anti-inflammatory drugs in an attempt to reduce foreign body reaction. As discussed previously, excessive inflammatory response following hernioplasty can cause various complications, in particular chronic pain [54]. Reduction of the foreign body response can be achieved by implanting biologically inert hernia meshes, such as those made of Teflon® or PET, as well as biological meshes [75,109]. However, multiple reports suggest that even those types of hernia meshes can trigger mild inflammatory response, resulting in an impaired healing and chronic pain [116]. Therefore, several approaches have been taken to modify hernia meshes with anti-inflammatory drugs. Many therapeutic compounds, including ibuprofen, cortisone, tetracycline, have been incorporated into hernia meshes [133,134]. *In vitro* and *in vivo* experiments revealed that modified meshes provoked significantly lower foreign body reaction, improved wound healing and resulted in a better architecture of a newly formed tissue. Moreover, reduced granuloma formation and increased neovascularization were also achieved by delivering anti-inflammatory drugs to the surgical site. Another work demonstrated that foreign body response can be mitigated if compastin, a C3 complement system inhibitor, is integrated into the PP hernia meshes [135].

Of particular interest is the C-QUR™ mesh developed and introduced to the market by Atrium Medical. This implant appears to be a polypropylene mesh coated with Omega 3 fatty acid gel, a well-known anti-inflammatory agent. Preliminary animal and clinical studies demonstrated excellent anti-inflammatory activity of the C-QUR™ meshes, which often resulted in an improved healing following hernioplasty [100,136]. This led to the FDA approval of the C-QUR™ meshes in March 2006. However, it was subsequently shown that these meshes are significantly more susceptible to post-surgical infections. Moreover, Kong et al. reported that Omega 3 fatty acid coating on the C-QUR™ mesh can provoke a pronounced host-body response [137]. Furthermore, handling characteristics of these meshes were found to be poor due to the coating stickiness, which often resulted in the mesh adherence to the package or gloves of the surgeons (Fig. 2.5). Therefore, C-QUR™ meshes are not currently widely used for hernia repair. Moreover, as of 2016, there were 16 lawsuits filed against Atrium medical with regard to the C-QUR™ meshes.

Fig. 2.5. Photograph of the C-QUR™ mesh adhered to the package [138].

Another strategy to reduce the extent of foreign body reaction involves camouflaging polymeric meshes with collagen-base hydrogels to avoid immunodetection. Wolf et al. used a rodent model to demonstrate that ECM hydrogel coating on PP meshes can significantly attenuate foreign body response by reducing the activity of M1 macrophages and promoting M2 macrophages [139]. Thus, the healing process following implantation was significantly improved. The results of this work are in a good agreement with other studies of collagen-based coatings on polymeric meshes [140,141].

Several studies demonstrated that the inflammatory response towards surgical meshes can also be reduced by promoting protein adsorption and enhancing cytocompatibility of ultra-hydrophobic meshes [116]. Chen et al. conducted animal studies showing that plasma treated PTFE meshes provide significant increase in tissue integration when compared with the untreated meshes [142]. At the same time, only minor encapsulation and granuloma formation was observed for the modified meshes. Another study dealt with dual-side PTFE meshes: one side was treated with plasma to increase the hydrophilicity and promote tissue ingrowth, whereas the opposite one remained intact to avoid tissue adhesions [143]. *In vitro* experiments confirmed the efficacy of that approach; however, results of the animal studies were inconclusive.

Several studies dealt with hernia meshes modified with biological coatings to enhance tissue integration. In particular, Gerullis et al. treated commercially

available PP meshes in human plasma and demonstrated significant increase in biocompatibility of the modified meshes [144]. Another study focused on the chitosan-coated hernia meshes and demonstrated enhanced myofibroblast adhesion and skeletal muscle ingrowth [145]. Moreover, chitosan coating promoted the activity of M2 macrophages. Champault et al. conducted clinical study of the meshes coated with beta-glucan [146]. Reduced recurrence rate was reported for the coated implants. Moreover, post-operative chronic pain was also reduced when the modified meshes were used.

As shown above, enhancing cell adhesion and tissue integration appears to be an important objective. However, excessive tissue integration can result in an undesired visceral adhesion, which ultimately leads to a chronic pain and movement constrictions [54]. Several strategies to reduce and eliminate tissue adhesions have been developed over the past years [116]. For instance, polymeric meshes were combined with anti-adhesive layers in order to separate hernia mesh and viscera. These layers are often made of ultra-hydrophilic polymers (e.g. polyvinyl alcohol, polyethylene glycol, etc.) or hydrogels (e.g. gelatin, chitosan, etc.) [147–149]. Ultra-hydrophobic materials were also used to create a barrier and eliminate adhesions [150]. In 1996, Seprafilm® adhesion barrier was introduced, and has since become one of the best option to avoid mesh-related adhesions [116]. This layer consists of carboxymethyl cellulose cross-linked to sodium hualuronate. During the operation Seprafilm® barrier is placed around the viscera to avoid mesh contacting the organs. The adhesion barrier is then resorbed within

7 days after the surgery. Multiple clinical data confirmed the high efficacy of this approach [151]. However, there are several drawbacks of the Seprafilm® adhesion barrier, in particular its high cost and adverse side effects [152].

Another approach to reduce tissue adhesions involves incorporation of anti-adhesive therapeutic agents into hernia meshes [116]. Several animal studies were conducted with polymeric meshes coated with sirolimus and taxomifen [153,154]. The results suggested that modified meshes reduced visceral adhesions, however, additional animal and clinical studies are required to evaluate the efficacy of this approach.

A large body of research has been dedicated to hernia meshes in an attempt to prevent and treat post-operative complications. However, the translation of these studies into clinical practice is limited for a myriad of reasons. The present study aims to develop novel approaches to reduce the incidence rate of post-surgical complications, improving long-term outcomes of prosthetic hernioplasty.

CHAPTER 3*

TOWARDS ELIMINATION OF ORTHOPAEDIC INFECTIONS: NOVEL ANTIBACTERIAL COATING ON ORTHOPAEDIC WIRES

3.1. Introduction

Kirschner wires (K-wires) are extensively used in orthopaedic applications ranging from fracture fixation to deformity correction. Despite being very versatile and fairly effective, the K-wiring procedure is often associated with common pin-tract infections that can lead to even more serious issues such as osteomyelitis [155,156]. These infections arise from the use of percutaneous pinning techniques, as seen in skeletal traction, percutaneous fracture pinning, and external fixation for fracture stabilization or complex deformity reconstruction. Pin sites are niduses for infections since the skin barrier is disrupted, providing a potential passage for opportunistic bacteria to enter a previously privileged area. Multiple evidence suggests that the infection rate following a K-wiring procedure ranges from 11 to 100 %, depending on the lifetime of the implant [3,4,157]. If appropriate pin care is neglected, these infections can cause sepsis, osteomyelitis and sometimes mortality [3,158]. The economic burden of treatment for this this type of infections is expected to reach as high as $1.6B annually by 2020 [159]. Therefore, surgeons, microbiologists, and material scientists alike are scrambling to find the best possible solutions to this challenging issue.

* Results and data provided in this chapter were previously published in:
D. Gil, S. Shuvaev, A. Frank-Kamenetskii, V. Reukov, C. Gross, A. Vertegel. Novel Antibacterial Coating on Orthopedic Wires To Eliminate Pin Tract Infections. *Antimicrobial Agents and Chemotherapy*, 2017, 61(7), e00442-17, DOI:10.1128/AAC.00442-17

In attempts to prevent pin track sepsis, multiple strategies have been developed. Most of them involve coating the implants with antibiotics, antimicrobial or anti-adhesion polymers and peptides; silver or nitric ions; nanoparticles; and other antiseptics like chlorhexidine and silver-sulfadiazine [160–164]. However, a major concern associated with the implementation of antibacterial coatings is their adverse effect on adjacent tissues and bones, which inhibits fracture or fusion healing [165]. Another important issue is the *in vivo* loss of antibacterial activity resulting from the exposure of bacteria to sub-lethal concentrations of the drug, eventually leading to development of drug resistance *in situ* [166]. Hence, the development of novel coatings for reducing pin-site infections is of particular importance.

Antibacterial properties of fatty acids and their esters have been extensively studied over the past few decades. Monolaurin, also known as glycerol monolaurate, was found to be the most effective antibacterial agent among these compounds [167]. Monolaurin is currently used as a broad range antimicrobial agent in food and cosmetic industries. Multiple studies have shown that besides antibacterial properties monolaurin also possesses antiviral and antifungal activity [168–170]. In an *in vitro* studies, monolaurin prevented biofilm formation of various *Staphylococcus* species including *Staphylococcus aureus* (*S. aureus*) and *Staphylococcus epidermidis* (*S. epidermidis*), pathogens that cause approximately 80% of orthopaedic implant-associated infections [18,19, 20]. It was also shown that at sub-lethal concentrations, bacteria did not develop resistance to monolaurin

[172]. *In vivo* experiments demonstrated that oral administration of monolaurin appeared to be an effective approach to manage and treat *S. aureus* infections [171]. In a surgical site infection model [7], monolaurin exhibited antibacterial and antibiofilm activity against both gram-positive and gram-negative bacteria. Therefore, a large body of evidence suggests that monolaurin possesses profound antimicrobial properties, which make it an excellent candidate for antibacterial coating on orthopaedic devices, in particular K-wires and external fixation devices, because of high incidence rates of infections for these devices. Advantages of monolaurin as a coating include its low cost, ease of application and “Generally Recognized as Safe” (GRAS) status by the FDA; in addition, monolaurin’s low water solubility may provide for a prolonged drug release rate from the implant and improved antimicrobial performance.

In the study reported here, monolaurin is employed as a passive coating on K-wires with the long-term goal of achieving reduced incidence rate of orthopaedic implant-associated infections and decrease the burden of pin tract infections, thus improving patient outcomes. A dip-coating technique was implemented to modify stainless steel K-wires. Following physicochemical characterization of the coating, the antibacterial properties of modified wires were evaluated *in vitro* in the model experiments with *S. epidermidis,* methicillin-sensitive *S. aureus* (MSSA) and methicillin-resistant *S. aureus* (MRSA). Furthermore, the biological effect of monolaurin coating on osteoblasts was studied. The objective of this study was to

demonstrate the efficacy of monolaurin-coated K-wires *in vitro* and provide a foundation for further animal and clinical studies.

3.2. Materials and Methods

3.2.1. Materials. Stainless steel K-wires were obtained from Smith & Nephew (Andover, MA). Monolaurin, HPLC grade acetonitrile, 200 proof ethanol and phosphate buffer solution (PBS) were purchased from Sigma-Aldrich (St. Louis, MO). Difco™ Tryptic Soy Agar and BBL™ Trypticase™ Soy Broth (TSB) were obtained from BD (Franklin Lakes, NJ). Alpha Minimum Essential Medium (αMEM), fetal bovine serum (FBS), penicillin and streptomycin were purchased from Corning Inc. (Manassas, VA). MTT and LIVE/DEAD® Viability/Cytotoxicity kit were purchased from Thermo Fisher Scientific (Waltham, MA).

3.2.2. K-wire modification. Stainless steel K-wire pieces with the length of 10 mm and the diameter of 1.575 mm were used in this study. The surface area of the samples was calculated to be approximately 49.5 mm^2 assuming cylindrical geometry. Prior to the modification, the wires were cleaned in air plasma with the input power of 30 W for 15 minutes. For coating, 1 ml of monolaurin solution in ethanol (10 mg/ml) was transferred into a sterile centrifuge tube with a cleaned K-wire. After 10 min incubation, the wire was removed from the solution and air-dried for 10 minutes at room temperature under sterile conditions. Uncoated controls were prepared by incubating the wires in pure ethanol for 10 min followed by air-drying for 10 min, similarly to the coated wires.

3.2.3. Characterization of the coating

FTIR analysis of the samples. FTIR spectra were collected by averaging 16 scans obtained by the FTIR spectrometer equipped with a Thermo-SpectraTech Foundation Series Endurance Diamond ATR accessory (Thermo-Nicolet Magna 550, Waltham, MA). Scans were run at the resolution of 4 cm^{-1} and recorded in absorbance units from 500 to 4000 cm^{-1}. Baseline correction was applied to properly determine net peak heights.

Surface morphology of the samples. Monolaurin-coated K-wires were characterized using SEM (Hitachi S4800, Schaumburg, IL). Prior to imaging, samples were sputter-coated with a gold film (thickness ≈ 5-7 Å). Micrographs with a magnification of up to 50,000X were obtained using the accelerated voltage of 5 kV and the working distance of 6 mm.

Additionally, surface morphology was characterized by AFM using MFP-3D instrument (Asylum, Santa Barbara, CA) equipped with metal-coated AC240TS Olympus microcantilevers with the nominal resonance frequency of 70 kHz and a spring constant of approximately 2 nN/nm. Imaging was performed both in tapping and force-mapping modes. Samples of uncoated and coated wires were fixed on a glass slide using double sided duct tape. Topography of all samples was measured in contact mode; additionally, coated samples were scratched to measure thickness of the coating. Stickiness of the studied samples was also analyzed by force-mapping. Precise spring constant for each of the cantilevers was determined before each measurement.

The thickness of the monolaurin coating was also measured using spectroscopic reflectometry (Edmund optics, Barrington, NJ) according to the protocol adapted from the reference [173]. For this experiment, silicon wafers coated with monolaurin according to the procedure described in sec. 3.2.2 were used. Measurements were conducted with the angle of incidence of 0° for the wavelengths ranging from 400 to 900 nm. The Fresnel equation was used to fit the acquired data. A total of 3 replicates were analyzed.

Determination of monolaurin binding yield. Coated wires were prepared using a series of monolaurin solutions in ethanol with different concentrations (1, 2.5, 5, 6, 7.5, 10, 15 mg/ml). After 10 min incubation, each wire was carefully removed from the solution, air-dried for 10 min and transferred to a vial containing 1 ml of anhydrous acetonitrile, where it was sonicated for 30 minutes. The absorption spectra of the resulting monolaurin solution in acetonitrile were recorded using UV/Vis spectrophotometer (ATi UNICAM UV-2 UV/vis, Cambridge, UK) in the range of 190-300 nm. The amount of deposited monolaurin was calculated from the value of absorption at 220 nm using a calibration curve (Fig. 3.1). The latter was obtained using monolaurin solutions in acetonitrile with standard concentrations ranging from 0.1 to 10 mg/ml.

3.2.4. In vitro evaluation of antibacterial activity. The antimicrobial activity of monolaurin-coated wires was evaluated against methicillin-sensitive *S. aureus* (MSSA, ATCC® 14775), methicillin-resistant *Staphylococcus aureus* (MRSA, ATCC® 33591), and *S. epidermidis* (ATCC® 12228).

Studies of planktonic bacteria. Prior to the experiments, bacteria were cultured in soy broth until they reached the stationary phase. Afterwards, the concentration of the inocula was adjusted to 10^6 CFU/ml using fresh broth. Coated and plain wires were placed into a sterile test tube containing 1 ml of 10^6 CFU/ml bacterial suspension. Samples were incubated at 37°C under mild shaking. Aliquots of bacterial suspension were taken at the following time points: 0, 1.5, 3, 4.5, 6, 7.5, 24, 48 hours. The aliquots were analyzed by the spread-plate method according to the ISO 4833:2. Based on the data, the antibacterial efficacy was calculated as a log reduction of bacteria. A total of 4 replicates were performed to obtain planktonic bacteria viability curves.

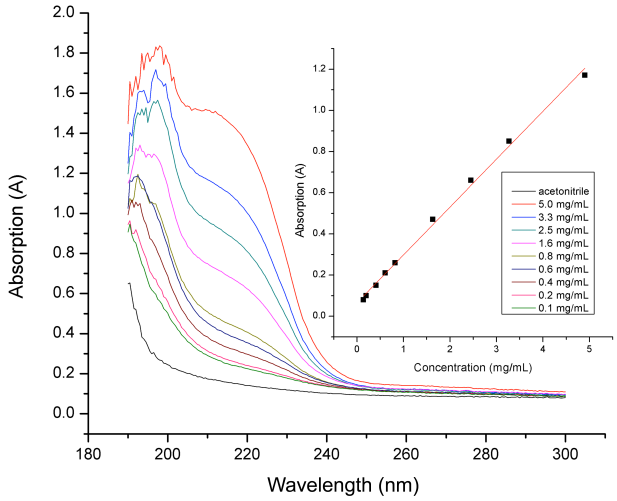

Fig. 3.1. Calibration curve measured for monolaurin

Analysis of adherent bacteria. Bacterial culture with the concentration of 10^6 CFU/ml was prepared as described in Sec. 3.2.4. Coated and plain wires were placed in a sterile 24-well plate; 1 ml of bacterial inoculum was added to the wells containing the wires. In order for bacteria to adhere and form a biofilm, the wires

were statically incubated for 48 hours at 35°C [174]. The biofilm formation was quantified using the CV assay as described by Kobayashi et al [175]. Briefly, after the 48 h biofilm growth period, coated and plain wires were transferred to a sterile 24-well plate, rinsed with PBS 3 times, and incubated with 0.1% aqueous solution of crystal violet for 10 min. After the wires were washed with PBS three times, they were placed in 33% acetic acid and incubated for 15 min under mild shaking. Optical density of the resulting solution was measured at 590 nm using a microplate reader (Bio-Tek Synergy HT, Winooski, VT). All experiments were replicated 6 times.

In addition, the number of colony forming units in the biofilm was measured according to the protocol described in the literature [176]. Briefly, after plain and monolaurin-coated wires were exposed to the bacteria inoculum for 48 hours to create a biofilm, each wire was gently rinsed with sterile PBS 3 times and placed in a test tube with 1 ml of sterile PBS. To remove the adherent bacteria, wires were vortexed for 30 s followed by sonication in an ultrasonic bath for 60 s. Colony counting was performed for the resulting bacterial suspensions using the protocol described previously (Fig. 3.2). A log reduction of adherent bacteria was then calculated. Four replicates were performed for both coated and uncoated samples.

The biofilm formation was also imaged using SEM. Sample preparation for SEM was performed using the protocol described by El Abed et al [177]. Briefly, samples were fixed with 2.5% glutaraldehyde, followed by an additional post-fixation with 1% osmium tetroxide. Then, the wires were dehydrated by successive

exposure to an ethanol gradient (50, 75, 90, 100 %), followed by the treatment with hexamethyldisilazane (HMDS). The samples were then sputter-coated with a layer of gold, and the SEM images were obtained using an accelerating voltage of up to 5 kV and a working distance of 5 mm.

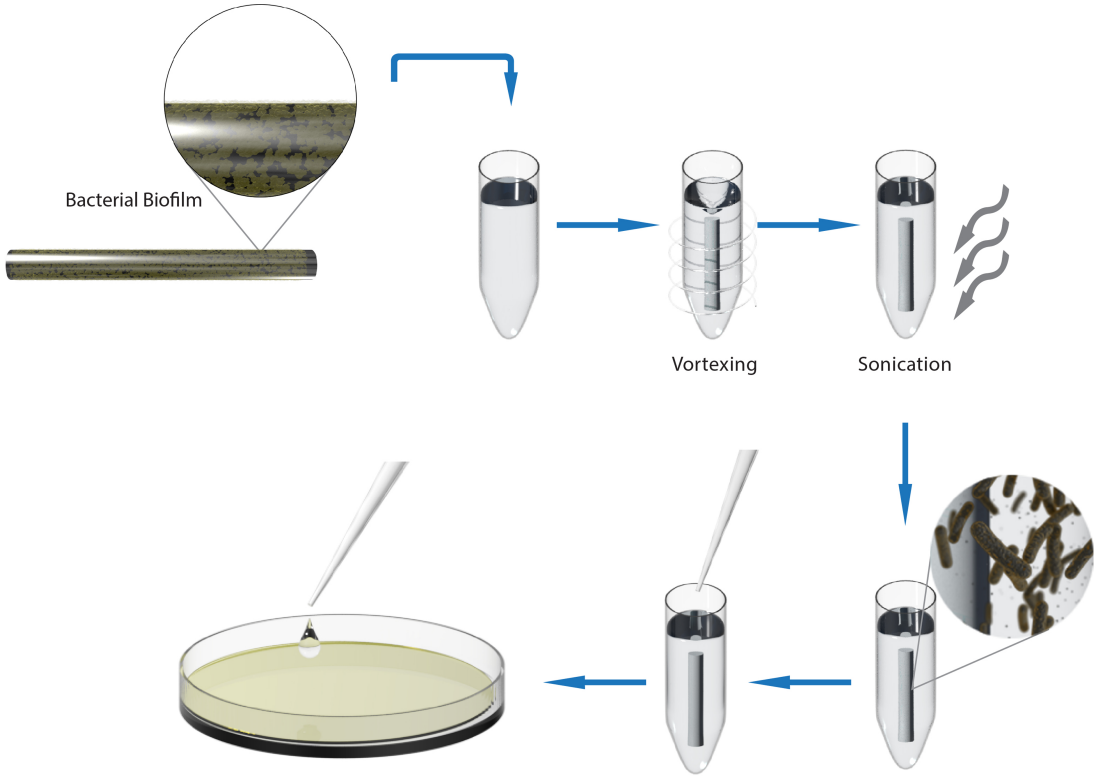

Fig. 3.2. The protocol used to dislodge bacteria from the surface of the wires.

Inhibition diameter test. Antibacterial activity of the wires was also evaluated using the zone of inhibition test. Protocol for these measurements was adapted from the literature [178]. Briefly, 10^6 CFU of bacteria were seeded on agar plates. Coated and plain wires were transferred to the center of the inoculated plates and incubated at 37°C; zone of inhibition was measured at different time points (1, 2,

3, 4 days) as described in the literature [178]. These experiments were replicated 6 times.

3.2.5. In vitro evaluation of cytotoxicity. The analysis of cytotoxicity of monolaurin-coated K-wires was performed in a model experiment with mouse 7F2 osteoblasts (ATCC® CRL-12557™). Cells were cultured in αMEM medium supplemented with 10% FBS and 1% of penicillin and streptomycin at 37°C in 5% CO_2.

MTT assay. The effect of the monolaurin coating on osteoblast proliferation was evaluated using the MTT assay. The protocol for this experiment was adapted from the literature [179]. Osteoblasts were passaged after reaching confluency, and aliquots containing ~40,000 cells were transferred into a sterile 24-well plate containing monolaurin-coated and plain wires. Samples were incubated in the presence of cells for 2, 4 and 7 days at 37°C in 5% CO_2. Following the incubation, the wires were removed from the wells, and osteoblasts were exposed to the 5 mg/ml MTT reagent for 4 hours. Then, dimethyl sulfoxide (DMSO) was added to completely dissolve formazan crystals, and the optical density of the resulting solution was measured at 570 nm using a microplate reader (Bio-Tek Synergy HT, Winooski, VT). Four replicates were performed for each of the time points.

Live/Dead® assay. The viability of osteoblasts attached to the wires was also assessed using Live/Dead® assay. To achieve cell attachment, the wires were incubated with 200 µl of osteoblast suspension (200,000 cells/ml) for 4 hours at 37°C. Then, the wires were transferred to the wells containing fresh αMEM medium

and incubated for 4 days at 37°C in 5% CO_2. After the incubation, the plain and coated wires were removed from the medium, gently rinsed with sterile PBS 3 times, and treated with calcein AM (20μM) and ethidium homodimer-1 (4μM). Following an incubation period of 30 min, wires were imaged using a fluorescent microscope (Thermo-Fisher EVOS FL Auto, Waltham, MA). The viability of cells attached to the surface of the wires was measured according to the Live/Dead® assay kit manual. Cells attached to tissue-grade polystyrene were used as the control. 4 replicates were performed for this assay.

Cell visualization. Attached osteoblasts were also imaged using SEM, and cell morphology was analyzed based on the obtained images. After cells were allowed to attach to the wires, samples were fixed and dehydrated as described previously. SEM images were obtained using an accelerating voltage of up to 5 kV and a working distance of 5 mm.

3.2.6. Table of experiments. The design of experiments conducted in this chapter are summarized in the table 3.1.

Table 3.1. Experimental design

Test samples		Micromorphology	Analysis of antibacterial activity			Cytotoxicity
SS K-wires	**Monolaurin-coated** / **Plain**	SEM & AFM	Analysis of planktonic bacteria	Analysis of antibiofilm activity	Inhibition zone test	MTT, Live/Dead, SEM

3.2.7. Statistical analysis. All numerical data is presented as the mean value ± standard deviation. One-way ANOVA was used for variance comparison. Repeated measures ANOVA was used for the analysis of the zone of inhibition experiments. Statistical difference was considered significant if P-value was less than 0.05.

3.3. Results

3.3.1. Binding yield of monolaurin. Binding yield of monolaurin was determined based on the adsorption isotherm of the drug on stainless steel K-wires (Fig. 3.3). Due to the low molar extinction coefficient of monolaurin, a large error was observed at low loading concentrations. The adsorption isotherm reached saturation at monolaurin concentration of approximately 7.5 mg/ml.

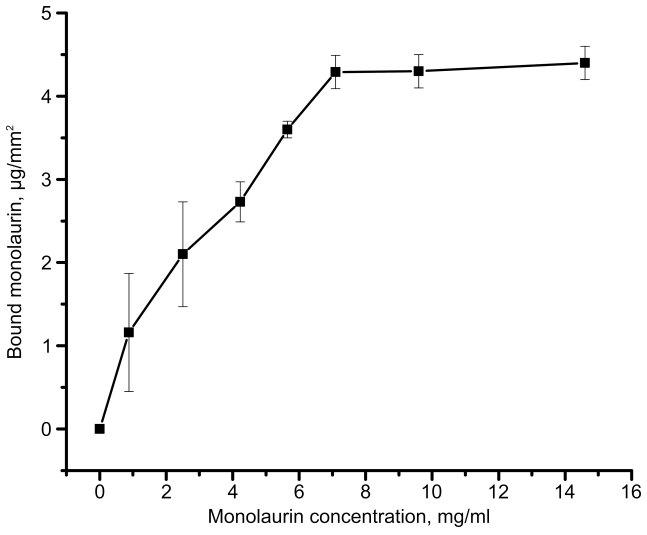

Fig. 3.3. Adsorption isotherm of monolaurin on stainless steel K-wires. Error bars were calculated based on the standard deviation values.

The saturation loading was found determined to be 84±4 μg of monolaurin per 1 cm wire, corresponding to the density of 4.3±0.2 μg/mm^2. Based on these results, 10 mg/ml monolaurin solutions were used to coat K-wires in all future experiments to ensure saturation coating.

3.3.2. Characterization of monolaurin coating. Fourier transform infrared spectroscopy (FTIR) was used to prove monolaurin adsorption on the K-wires. Fig. 3.4 shows the spectra collected from coated and pure monolaurin.

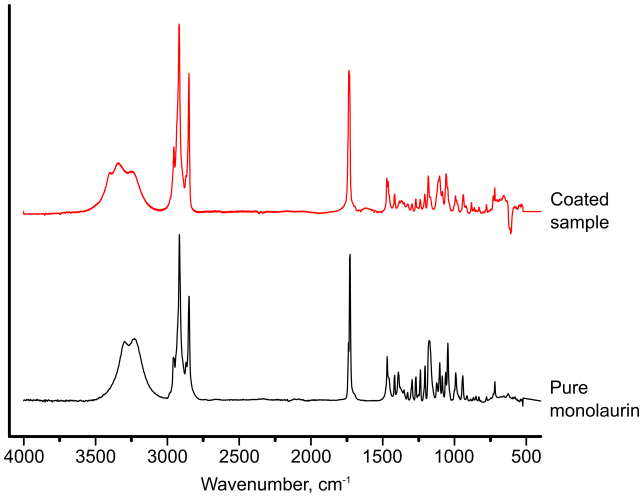

Figure 3.4. FTIR spectra of monolaurin-coated wire and pure monolaurin.

As can be seen, there is virtually no difference between the spectra of the coated sample and that of the pure monolaurin. Thus, these data confirm that the coating consists of monolaurin.

Morphological characteristics of the coating were analyzed using scanning electron microscopy (SEM), atomic force microscopy (AFM) and spectroscopic reflectometry. As shown in Fig. 3.5b, monolaurin-coated wires exhibit smooth surface with minor extrusion lines. According to the micrographs, the coating is

evenly distributed across the surface of the wire. Little to no difference can be seen when comparing surface morphology of the plain and monolaurin-coated K wires. Further analysis of micromorphological characteristics of the monolaurin coating was conducted using AFM technique.

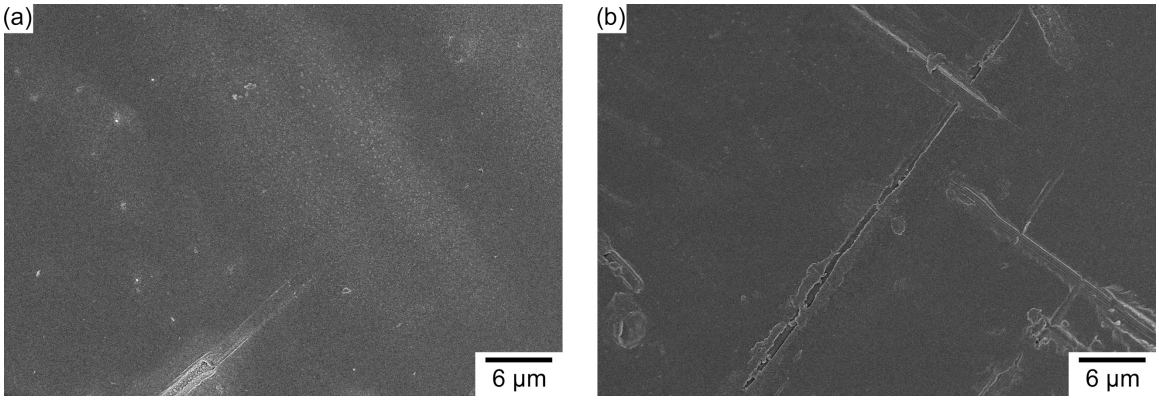

Fig. 3.5. SEM micrographs of plain (a) and monolaurin-coated (b) K-wires.

Topography images acquired by AFM (Fig. 3.6a-d) confirmed the smoothness of monolaurin coating. Using scratching technique, the thickness of the coating was determined to be 144±35 nm. These results are in good correlation with those of the spectroscopic reflectometry, which showed the thickness of the coating to be 161±57 nm. Coated samples exhibited considerably higher adhesion force between the surface and the cantilever tip compared to the uncoated samples (85.2±18.6 and 15.9±2.1 nN for coated and uncoated wires, respectively, $p<0.001$), indicating the presence of a uniform coating (Fig. 3.6e-f).

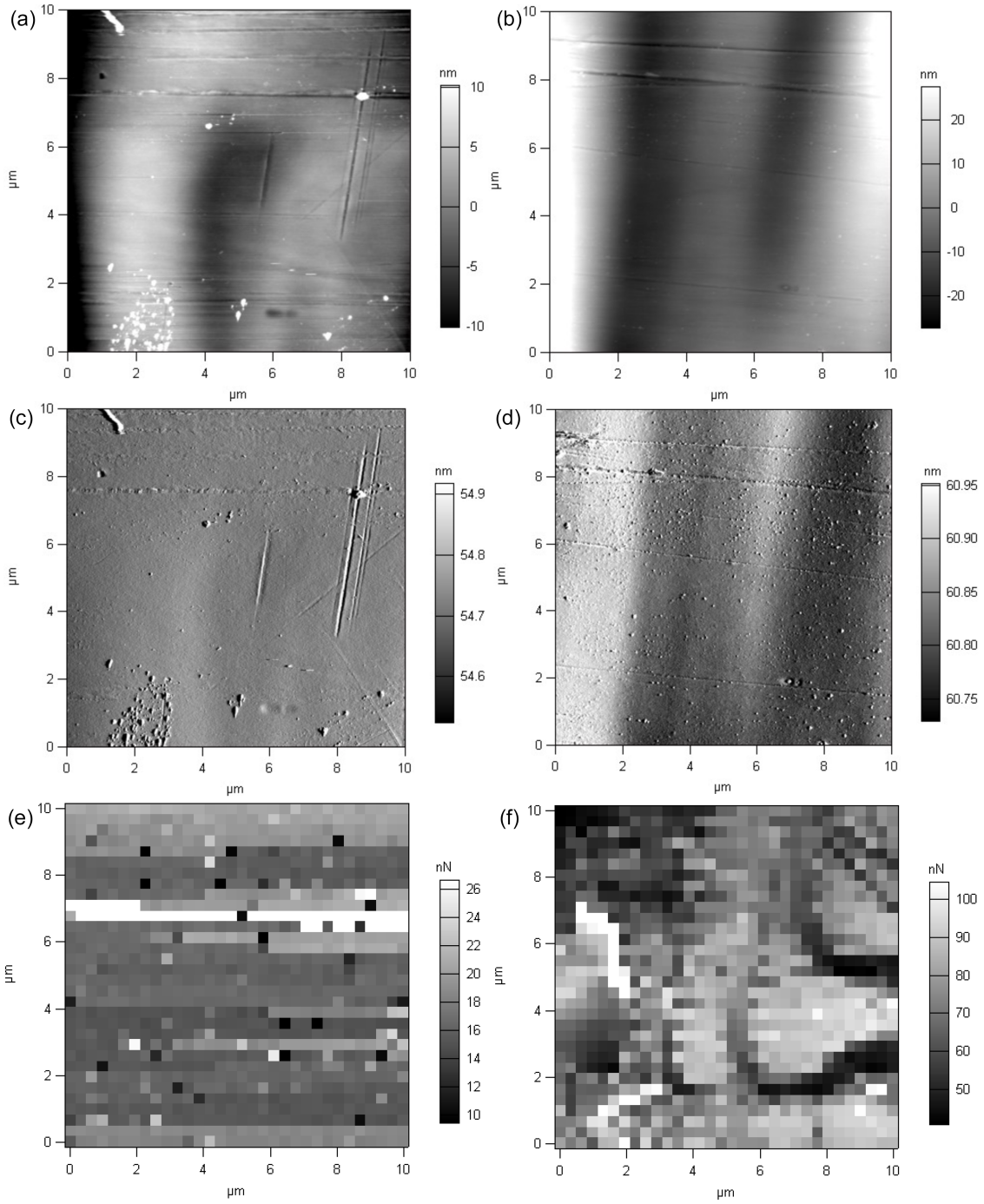

Fig. 3.6. Atomic Force Microscopy images of uncoated and coated samples. The topography (a, b), cantilever deflection (c, d) and adhesion force map (e, f) of plain (a, c, e) and monolaurin-coated (b, d, f) were acquired.

3.3.3. Evaluation of antibacterial activity

Antibacterial activity against planktonic bacteria. The antimicrobial activity of monolaurin-coated wires against planktonic bacteria was assessed based on the microbial viability curves. As shown in Figs. 3.7, 3.8, coated wires were highly efficient against MSSA, MRSA and *S. epidermidis*, completely eliminating planktonic bacteria in less than 7.5 hours.

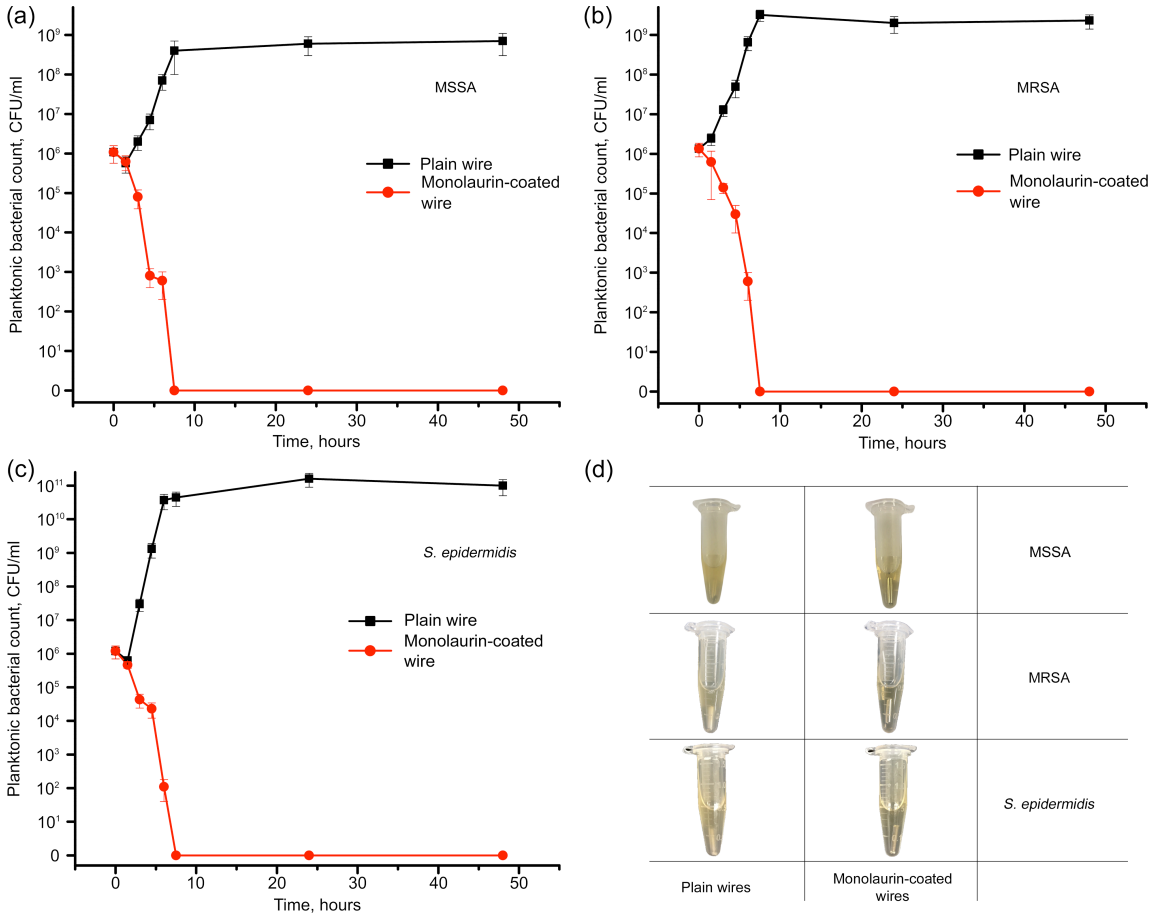

Fig. 3.7. Planktonic bacteria viability curves obtained in the presence of plain and monolaurin-coated K-wires: (a) MSSA, (b) MRSA, (c) *S. epidermidis*. (d) Representative photos of the tubes containing plain and monolaurin-coated wires incubated with the bacteria for 48 hours. Error bars were calculated based on the standard deviation values.

In the presence of the uncoated wires, the number of bacteria increased by more than two orders of magnitude over the first 7.5 hours. These data suggested that monolaurin-coated wires achieved a 6.0-log reduction of planktonic MSSA, MRSA and *S. epidermidis*. One-way ANOVA was used to compare the antimicrobial activity of monolaurin-coated and plain wires at different time points. The significant difference ($p<0.05$, $n=4$) between coated and plain samples was observed after 1.5 hours time point.

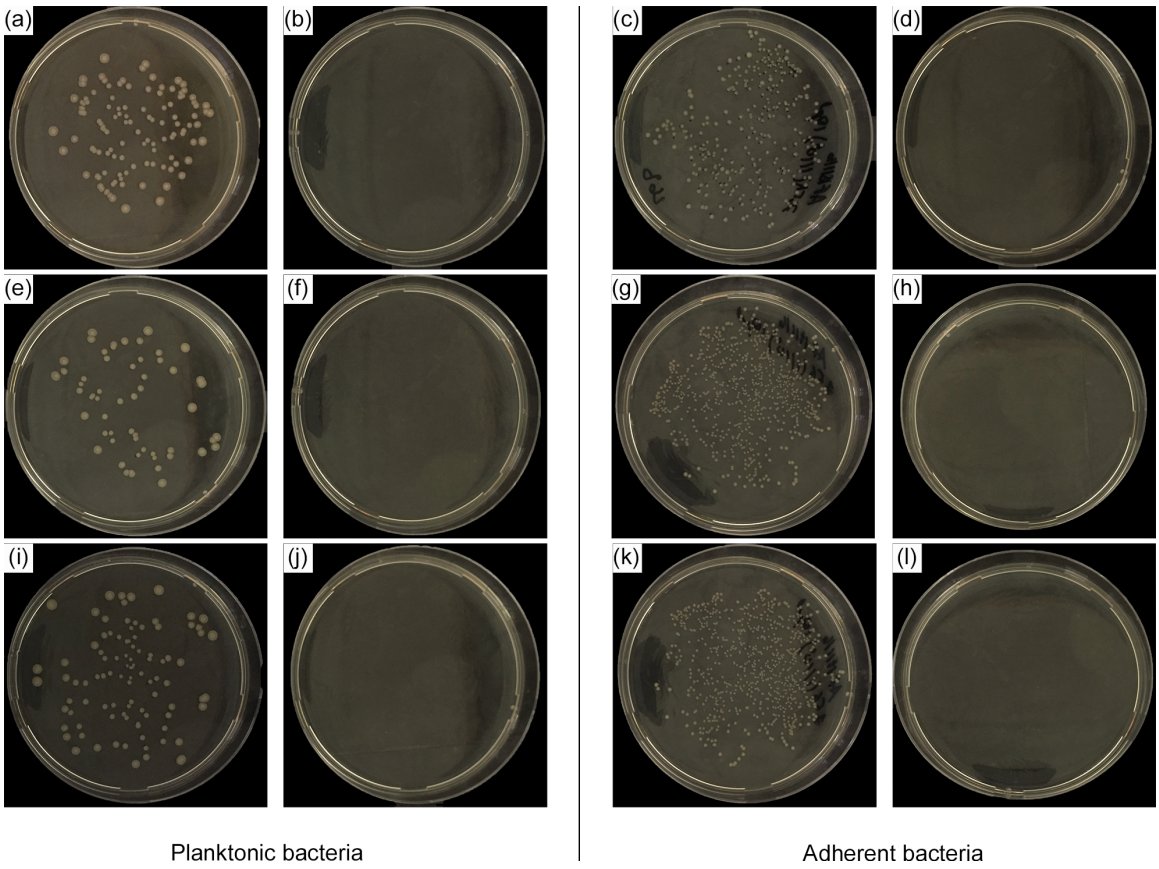

Fig. 3.8. Representative photos of recultivated bacteria incubated with the plain and monolaurin-coated K-wires. (a), (c) MSSA incubated with plain wire; (b), (d) MSSA incubated with monolaurin-coated wire; (e), (g) MRSA incubated with plain wire; (f), (h) MRSA

incubated with monolaurin-coated wire; (i), (k) *S. epidermidis* incubated with plain wire; (j), (l) *S. epidermidis* incubated with monolaurin-coated wire.

Antibacterial activity against adherent bacteria. The antibiofilm activity of monolaurin coating was evaluated by the Crystal Violet (CV) assay and quantitative analysis of adherent bacteria. The results of the CV assay are shown in Fig. 3.9a. In the case of all three bacterial strains, the absorbance values for coated wires were significantly lower when compared to those for the plain wires, indicative of antibiofilm activity of monolaurin-coated wires against MSSA, MRSA and *S. epidermidis* ($p<<0.05$, n=6).

Figs. 3.8, 3.9b show the count of adherent bacteria. Again, monolaurin-coated wires demonstrated pronounced antibiofilm properties resulting in the significant drop of the number of adherent bacteria when compared to the plain wires ($p<0.05$, n=4). Monolaurin-coated wires effected a 5.7-, 5.8- and 6.0-log reduction of adherent MSSA, MRSA and *S. epidermidis*, respectively. These results are consistent with those obtained for planktonic bacteria.

The observed antibiofilm effect was additionally confirmed by SEM imaging. As can be seen from Fig. 3.10 little or no evidence of adherent bacteria is observed on the surface of the coated wires for all three bacterial strains studied herein. On the other hand, a large number of adherent bacteria surrounded by extracellular matrix are evident on the SEM images of the uncoated wires for all three strains studied. The analysis of high magnification images (30,000X) revealed that the morphology of bacteria adherent to the plain wires is different when compared to those found on monolaurin-coated wires (Figs. 3.11).

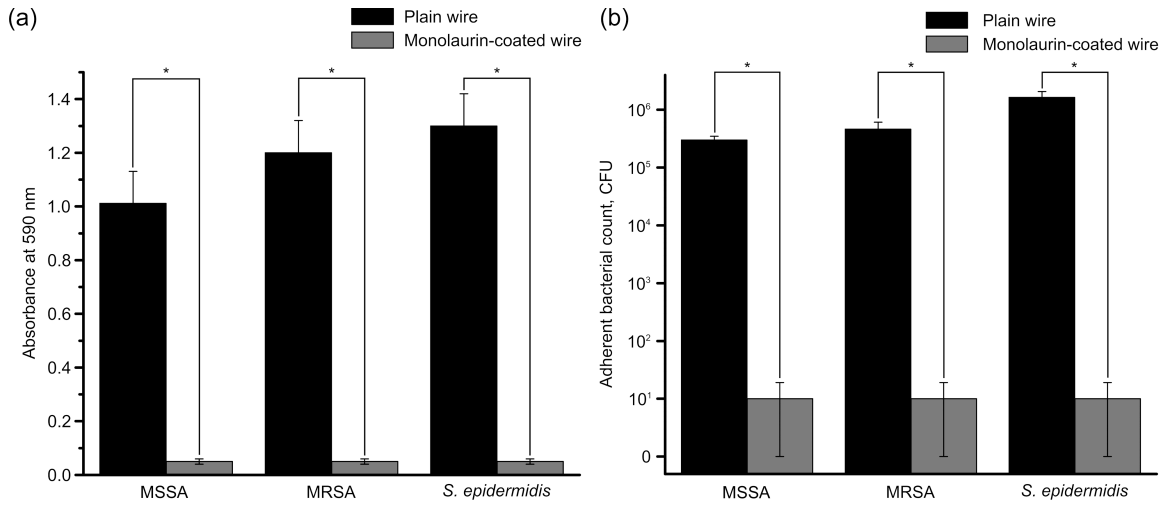

Fig. 3.9. (a) The results of crystal violet assay performed for plain and monolaurin-coated wires in the presence of MSSA, MRSA and *S. epidermidis*. (b) Adherent bacterial count for plain and monolaurin-coated wires incubated in the presence of MSSA, MRSA and *S. epidermidis* for 48 h. Asterisks represent statistically significant difference between plain and monolaurin-coated wires (*p<0.05*). Error bars were calculated based on the standard deviation values.

It is evident that in the latter case, the integrity of bacterial cell wall is disrupted, resulting in the deformation of the bacterial cell surface. In contrast, the bacteria attached to the plain wire exhibit the conventional spherical shape.

Inhibition zone test. Additional evaluation of antimicrobial activity of monolaurin-coated wires was performed by the inhibition zone assay. As shown in Fig. 3.12d, coated wires were efficient against all three bacterial strains tested.

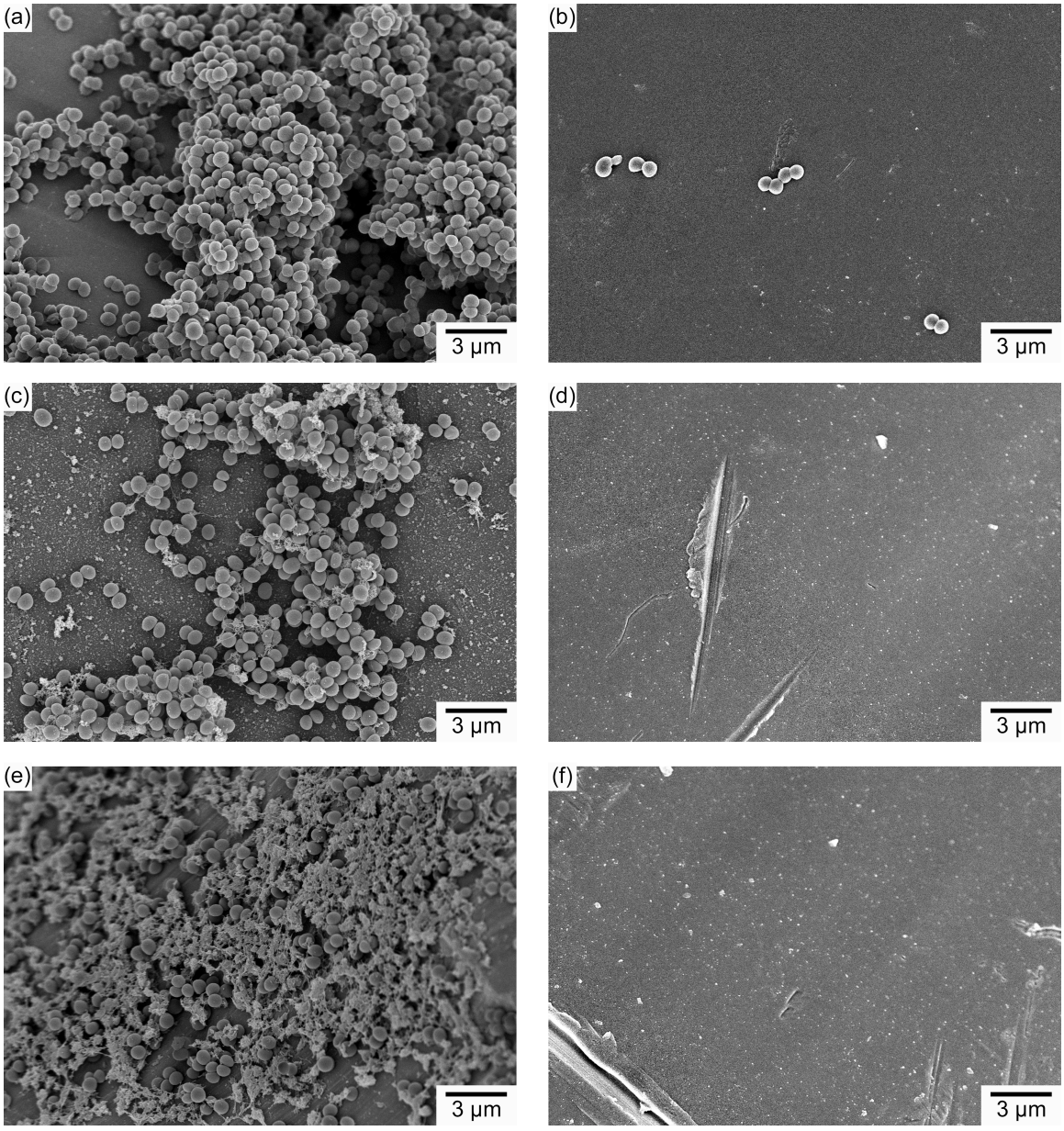

Fig. 3.10. SEM micrographs of the bacteria lodging on the surface of plain and monolaurin-coated wires. (a) *S. aureus* adherent to the plain wire; (b) *S. aureus* adherent to the monolaurin-coated wire; (c) MRSA adherent to the plain wire; (d) MRSA adherent to the monolaurin-coated wire; (e) *S. epidermidis* adherent to the plain wire; (f) *S. epidermidis* adherent to the monolaurin-coated wire.

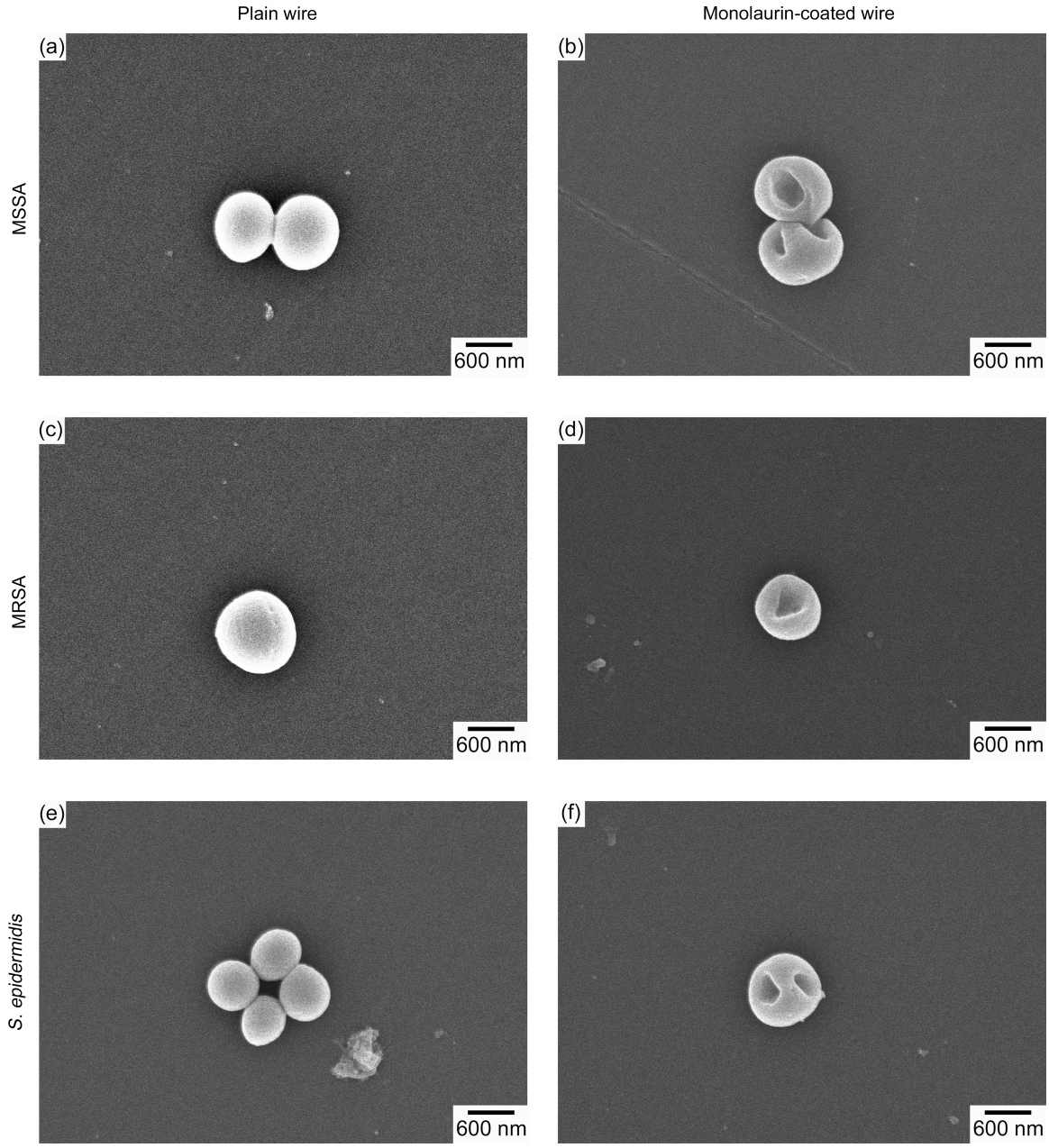

Fig. 3.11. High-resolution SEM micrographs of the bacteria adherent to plain and monolaurin-coated K-wires. (a) MSSA adherent to the plain wire; (b) MSSA adherent to the monolaurin-coated wire; (c) MRSA adherent to the plain wire; (d) MRSA adherent to the monolaurin-coated wire; (e) *S. epidermidis* adherent to the plain wire; (e) *S. epidermidis* adherent to the monolaurin-coated wire.

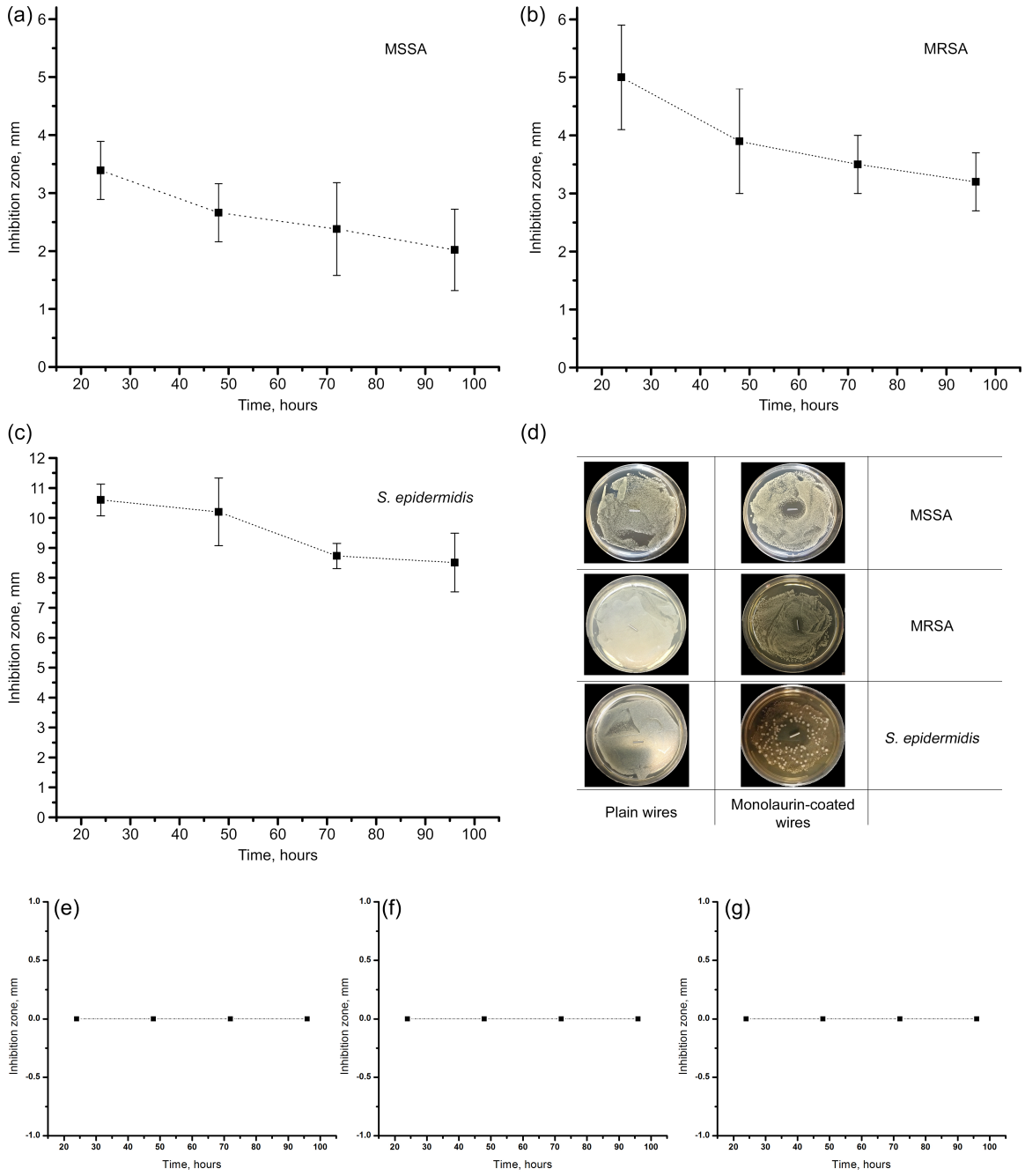

Fig. 3.12. Inhibition zone for MSSA (a), MRSA (b) and *S. epidermidis* (c) around monolaurin-coated K-wires. (d) Representative photos of inoculated agar plates containing plain and monolaurin-coated wires. Inhibition zone for MSSA (e), MRSA (f) and *S. epidermidis* (g) around plain K-wires. Error bars were calculated based on the standard deviation values.

The results of time-dependent antimicrobial efficacy test shown in Figs. 3.12a-c suggest that the inhibition diameter decreases significantly with time (p=0.028, p=0.009, p=0.035, n=6 for MSSA, MRSA and *S. epidermidis*, respectively, as determined by the repeated measures ANOVA). However, even after 96 hours of incubation, monolaurin-coated K-wires were capable of inhibiting bacterial growth for MSSA, MRSA and *S. epidermidis*.

Overall, results of the inhibition zone test are indicative of good prolonged antibacterial efficacy of monolaurin-coated wires, demonstrating their ability to inhibit growth for all three strains for at least 4 days.

3.3.4. Evaluation of cytotoxicity. The influence of monolaurin coating on cell proliferation was assessed using the methyl thiazolyl tetrazolium (MTT) assay (Fig. 3.13a). The image demonstrates that culturing osteoblasts in the presence of monolaurin-coated wires did not affect cell proliferation rate: the OD_{570}, which indirectly corresponds to the number of cells, was not significantly different for coated and uncoated wires at different time points (p=0.687, 0.781, 0.757, for day 2, 4, and 7, respectively; n=4).

Fig. 3.13b shows fluorescent images of osteoblasts stained with Live/Dead® reagents. Similarly to plain wires, monolaurin-coated wires exhibited a large number of adherent osteoblasts, vast majority of which were found to be viable (Table 3.1).

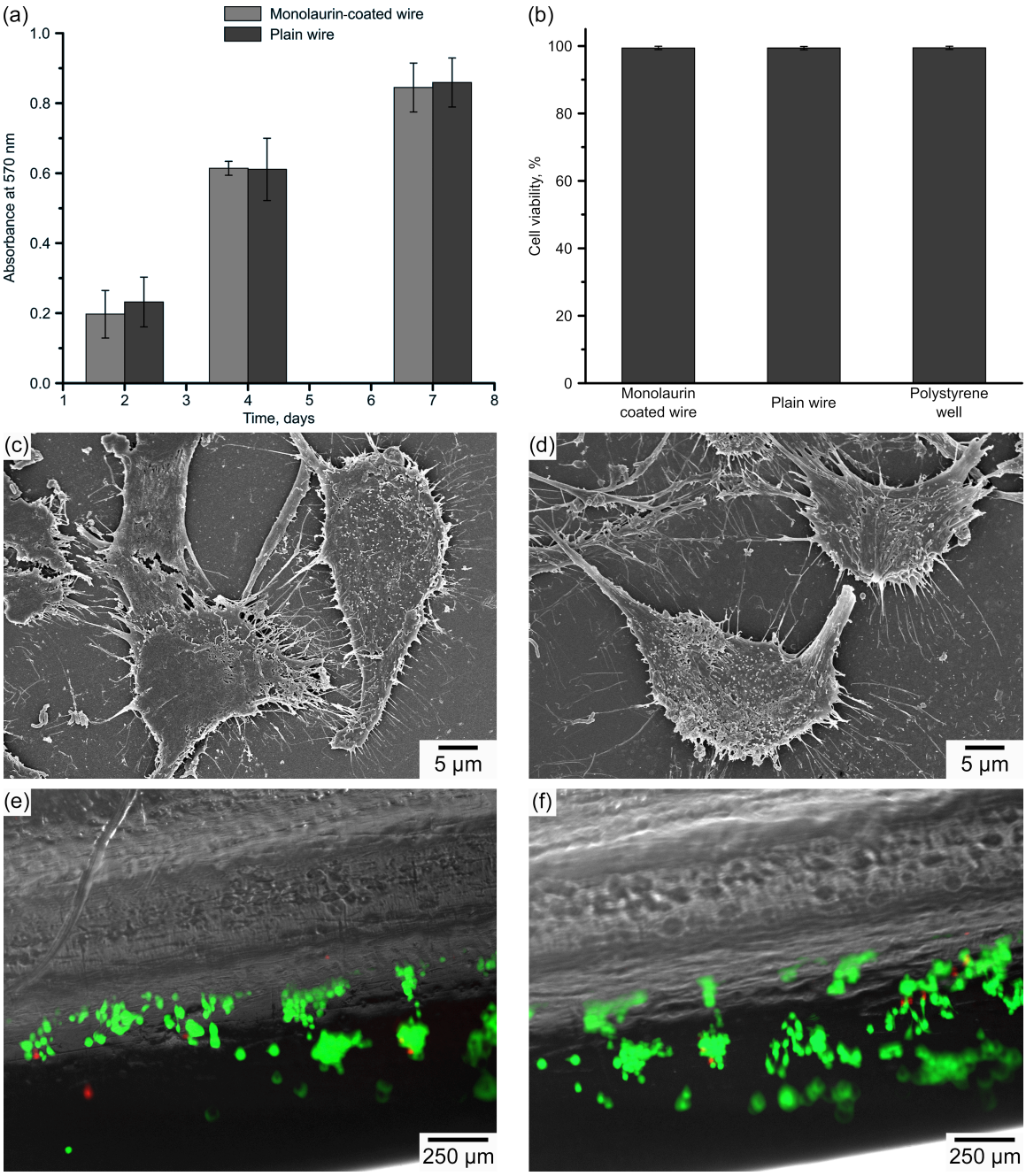

Fig. 3.13. (a) The results of the MTT assay performed on osteoblasts in the presence of plain and monolaurin-coated K-wires; (b) the viability of osteoblasts adherent to plain and monolaurin-coated samples determined by the Live/Dead® assay; SEM micrographs of osteoblasts adherent to plain (c) and monolaurin-coated (d) samples; fluorescence

microscopy images of osteoblasts lodging on plain (e) and monolaurin-coated (f) wires. Cells stained green are viable, red staining corresponds to dead cells. Error bars were calculated based on the standard deviation values.

Quantification of obtained results revealed that the percentage of viable cells was not significantly different for plain (99.4±0.1 %) and monolaurin-coated (99.4±0.1 %) wires and tissue-grade polystyrene (99.5±0.1 %), which was used as a positive control (p=0.311, n=4).

Table 3.1. Number of viable and dead osteoblasts lodging on plain and monolaurin-coated K-wires determined by Live/Dead® assay.

	Viable cells, log(cell number)	P-value	Dead cells, log(cell number)	P-value	Total number, log(cell number)	P-value
Plain wires	5.41±4.84	P=0.419, n=6	3.19±2.59	P=0.409, n=6	5.42±4.84	P=0.411, n=6
Coated wires	5.34±5.01		3.12±2.71		5.34±5.01	

The analysis of the adherent cells was performed using SEM imaging and the Live/Dead® assay. Figs. 3.13c-f display micrographs of the osteoblasts adherent to the surface of plain and monolaurin-coated wires. Good cell attachment and spread across the surface is evident from these images; osteoblasts exhibited normal polygonal morphology with extended filopodia. Little to no difference can be noticed when comparing plain and modified samples.

Thus, the results of SEM imaging and the Live/Dead® assay are in good agreement with the results of the MTT assay, and suggest good biocompatibility and no cytotoxicity of monolaurin-coated K-wires.

3.4. Discussion

The present work focusses on potential benefits of using monolaurin as an antibacterial coating on orthopaedic K-wires in attempt to reduce the burden of pin-tract infections, in particular those caused by *S. aureus* (including MRSA) and *S. epidermidis.*

In this study, stainless steel K-wires were coated with monolaurin using a simple yet effective dip-coating method. The proposed methodology appears to be fairly inexpensive and simple, and does not require the use of toxic chemical compounds or thermal/mechanical treatment that may cause structural, chemical or physical alterations in the implants. The “GRAS” status of ethanol and monolaurin, the only compounds used for the manufacturing of the coated K-wires, can facilitate the translation of modified wires into clinical practice.

Given that binding yield of monolaurin at saturation was found to be ca. 4.3 $\mu g/mm^2$, the total dose of monolaurin absorbed on a 1 cm K-wire is 84 µg. Although the antibacterial activity of monolaurin has been studied previously, there are still debates regarding the therapeutic dose and the minimally inhibitory concentration (MIC) of this compound. Having analyzed the antibacterial activity of monolaurin against 29 strains of *S. aureus*, including MRSA, K. Holland et al. [180] determined

that its MIC is in the range from 10 to 20 μg/ml. However, H. Preuss et al. [181] calculated the MIC of monolaurin against *S. aureus* to be 62.5 μg/ml. Another study suggests that the MIC of monolaurin against *S. aureus* is in the range from 25 to 50 μg/ml [182]. At the same time, we were unable to find the MIC of monolaurin against *S. epidermidis* in the literature. However, the antimicrobial activity of lauric acid against *S. epidermidis* is well studied: the MIC was determined to be 3.9 μg/ml [183]. Multiple studies suggest that monolaurin has better antimicrobial properties than lauric acid [172,182,184]. Therefore, the MIC of monolaurin against *S. epidermidis* can be expected to be lower than 3.9 μg/ml. Overall, even if it is difficult to estimate the volume of liquid to which a K-wire is exposed *in vivo* after the implantation, the dose of monolaurin introduced with K-wires in this study (84 μg per one cm of wire) is expected to provide antibacterial properties to the implants at least during the first days after the implantation. Results of our inhibition zone tests support this conclusion. Nonetheless, further animal studies are required to determine if the current dose is sufficient to provide a therapeutic effect *in vivo*.

There is a general consensus that increased surface roughness leads to the enhanced osteointegration, primarily due to the more developed bone-to-implant contact [42,185]. However, in certain cases improved osteointegration can be undesirable [186]. The use of external fixators and K-wires implies the subsequent removal of the implants, and a more developed bone-to-implant contact would increase frictional forces between the implant and bone upon removal, causing severe discomfort for patients. Therefore, alterations of surface characteristics, in

particular roughness, of external fixators and K-wires should be avoided. The results of SEM and AFM imaging conducted herein showed that topography of the monolaurin-coated wires was similar to that of the plain wires (Figs. 3.5, 3.6). The only parameter that was affected by the presence of monolaurin coating is the surface stickiness, as measured by AFM. However, an observed increase of stickiness is not expected to affect cell adhesion and osteointegration in any way, since those responses are guided biochemically (through adhesion proteins), not physically. Hence, the modification of K-wires with monolaurin coating is not anticipated to influence osteointegrative properties of the implants. One possible issue that can be caused by the altered stickiness of the wires is their handling by the surgeon during the implantation and removal. Here, we qualitatively tested handling of the coated wires in a pilot experiment by using a wire to pierce a silicon rubber Septa flask cork, and did not see any difference between handling coated and uncoated wires. However, handling can still be an issue during the actual surgery and will be assessed in detail during future animal studies.

The present study was primarily focused on the *in vitro* analysis of antibacterial activity of monolaurin-coated K-wires. *S. aureus* (MSSA and MRSA) and *S. epidermidis* were tested here mainly because these pathogens cause majority of implant-associated infections. It was estimated that all existing pathogens except for staphylococci account for only 22% of orthopaedic infections [187]. Hence, the importance of fighting staphylococcal infection cannot be overestimated. High activity against MRSA noticed here for monolaurin-coated

wires is of special interest because these antibiotic resistant strains cause the highest morbidity and mortality.

Since most pin-site infections are caused by the formation of bacterial biofilm on the implant surface, the modified wires are required to possess pronounced antibiofilm activity. However, the efficacy against planktonic pathogens should also not be underestimated. In 1987, Anthony Gristina introduced the concept called “race to the surface” [188]. During the initial post-operative period, the host defense system is impaired and vulnerable to the bacteria introduced during surgery. Gristina suggested that there is a “race” to the surface of the implant between host cells and bacteria from adjacent tissues; if the race is won by bacteria, the risk of the implant infection increases considerably. Therefore, treatment needs to be also directed against nearby planktonic bacteria. Given monolaurin’s low water solubility, it is expected that coated K-wires can potentially provide prolonged drug release upon implantation. Thus, monolaurin coating is anticipated to be effective against planktonic bacteria.

As predicted, monolaurin-coated K-wires exhibited excellent antimicrobial properties against planktonic MSSA, MRSA and *S. epidermidis*, completely eliminating of up to 10^6 CFU in the case of each of these strains (Figs. 3.7, 3.8). Monolaurin-coated wires also prevented biofilm formation, as indicated by the results of the crystal violet staining and SEM imaging (Figs. 3.8 - 3.11). It is important to emphasize that those few bacteria found on the surface of the modified wires had disrupted cell walls suggesting that these microorganisms were

not viable. Although the consensus regarding monolaurin's mechanism of antibacterial action has not been reached, alteration of the plasma membrane and disruption of the bacterial cell wall is considered to be one of the two most likely mechanisms of action [172,182]. An alternative mechanism assumes that monolaurin is able to interfere with bacterial two-component regulatory systems. Monolaurin was found to inhibit WalK/R, one of the 16 two-component regulatory systems in *S. aureus*, leading to the death of the bacteria [189]. In this study, we observed direct confirmation of the disruption of bacterial cell walls; however, the second mechanism could also play a role as it was not studied here.

Since the cytotoxicity of antibacterial agents is an important issue [5], the cytocompatibility of monolaurin-coated K-wires has been extensively studied herein (Fig. 3.13). According to the ISO 10993, a material is considered to be cytotoxic if cell viability in its presence drops below 70% [178]. In this study, we did not observe evidence of any adverse effects of monolaurin on osteoblast viability; cell viability was found to exceed 99%. The size, shape, morphology and number of osteoblasts adherent to the surface of modified wires suggest good biocompatibility and lack of cytotoxicity of the monolaurin coated wires. These results were not unexpected considering known safety record of monolaurin [172,182,190].

3.5. Conclusions

In conclusion, monolaurin-coated Kirschner wires were manufactured, and their performance was evaluated *in vitro*. Prepared wires showed pronounced antibacterial and antibiofilm activity against *methicillin-sensitive and methicillin-resistant S. aureus*, and *S. epidermidis*. Excellent biocompatibility of monolaurin-coated implants was demonstrated in a mice osteoblast model. Data obtained here serve as the foundation for further animal and clinical studies of monolaurin-coated K-wires. Taking into account the advantages of monolaurin as an antibacterial coating, the approach proposed in this work can have a huge potential in orthopaedic applications.

CHAPTER 4*

IN VITRO STUDY ON THE DETERIORATION OF POLYPROPYLENE HERNIA REPAIR MESHES

4.1. Introduction

According to the National Center for Health Statistics nearly five million people in the US suffer from some form of hernia, and this number is expected to increase due to the growing prevalence of obesity [191]. Due to this, hernia repair surgeries are among the most common operations, with over a million procedures performed in the US annually [192].

After the introduction of polypropylene (PP) hernia repair meshes in 1958, mesh hernioplasty became the gold standard for surgical hernia repair. Today, hernia repair meshes are the most widely used medical implants [52]. Such resounding success glutted and rapidly expanded the hernia repair mesh market. However, manufacturers are often reluctant to discuss product disadvantages, some of which lead to complications after hernia repair surgery. Chronic postoperative pain appears to be one of the most adverse and common complications [193]. Evidence from several sources suggests that almost 20% of patients who undergo the surgery experience chronic postoperative pain, and the quality of life for more than half of these patients is compromised to such an extent that they cannot participate in daily activities [84]. Recently, the complaints became so numerous that the FDA issued a warning about the complications associated

* Results and data provided in this chapter were previously published in:
D. Gil, J. Rex, V. Reukov, A. Vertegel. In vitro study on the deterioration of polypropylene hernia repair meshes. *Journal of Biomedical Materials Research B*, Accepted manuscript.
As of 9/26/2017 DOI was not provided

with the implantation of the prosthetic meshes [194]. Moreover, the FDA is considering reclassifying surgical meshes from Class II to Class III products [195].

Although the mechanism of development of post-hernioplasty chronic pain is still the subject of debate, much of the evidence points towards oxidative stress as the key factor causing the complication [196–198]. Despite recent improvements to the structure and design of hernia repair meshes, these implants remain a foreign body that triggers an inflammatory response after the implantation. Macrophages and neutrophils, which are in the vanguard of the foreign body response, release a milieu of oxidants and enzymes that interact with the implanted material and may cause its deterioration. A large body of evidence suggests that reactive oxygen species (ROS), in particular superoxide and hydroxide radicals, are capable of oxidizing the materials of the mesh [9,198,199]. It was also reported that myeloperoxidase (MPO) – the enzyme released by neutrophils – can also facilitate mesh deterioration [200]. MPO catalyzes the conversion of hydrogen peroxide and chloride anions to hypochlorous acid (HOCl), a strong oxidative agent. Overall, oxidative stress at the site of implantation causes polymeric implants to lose their structural and mechanical integrity; crystallinity and molecular weight may also change [198]. This can result in the mechanical stiffening and/or shrinkage of the mesh, which may ultimately lead to the development of post-operative chronic pain [64,193,201].

It goes without saying that, depending on the material, surgical meshes may have varying susceptibility to either MPO or ROS. Even mesh design may play a

role in the susceptibility of a mesh to deterioration [85]. A number of recent studies showed that effect of the oxidative stress on hernia repair meshes made of the same material can be different, resulting in different complication rates [84,201]. Thus, in order to improve the performance of hernia repair meshes, it is of particular importance to reveal the mechanism of their deterioration.

The vast majority of the current mechanistic studies involve analysis of the explanted meshes [9,194,202]. However, this approach has several vital drawbacks. In particular, since only failed meshes are subjected to analysis, there is no positive control that can be used as a reference. Moreover, analysis of the explanted materials implies the use of procedures to remove residual tissue, which involve treatment in an oxidative environment [8,9,202]. This can lead to additional physical, chemical and structural alterations, making it difficult to reveal the actual mechanism of mesh deterioration.

In an attempt to address these limitations and provide better understanding of the mechanism of mesh deterioration we developed in vitro methodology that mimics aspects of the oxidative environment at the tissue-implant interface after surgery. Based on a set of physicochemical analyses, a protocol for characterizing the degree of oxidative damage to the meshes was developed. Such an approach may lead to an improved understanding of the processes resulting in the structural, physical and chemical alterations in hernia repair meshes under oxidative stress.

4.2. Materials and Methods

4.2.1. Hernia repair meshes. In the present work, two types of hernia repair mesh were studied: UltraPro® (Ethicon, Somerville, NJ) and Composix™ EX (Bard Davol, Warwick, RI), which were kindly donated by the Carolinas Medical Center (Charlotte, NC). These meshes are among the most widely used for hernia repair and have proven their reliability and efficiency over the past years. When compared with UltraPro®, Composix™ meshes are known to be more susceptible to oxidative stress and more often lead to complications. This fact will be used to evaluate the predictive power of the proposed *in vitro* models.

UltraPro® lightweight meshes consists of non-absorbable polypropylene monofilament fibers and an absorbable poliglecaprone-25 monofilament portion. Composix EX heavyweight meshes also consist of two parts: Polypropylene BARD® Mesh on the one side to promote tissue ingrowth and submicronic expanded polytetrafluoroethylene (ePTFE) sheet on the other side to prevent bowel-cell adhesion to the prosthesis. As stated in the literature [9,203], Teflon™ shows outstanding biocompatibility and undergoes only minute degradation after being implanted. Therefore, only the polypropylene portion of Composix™ meshes was analyzed in the course of this work.

4.2.2. Oxidative deterioration of the meshes. In the present work, the effect of reactive oxygen species (ROS) and hypochlorite (OCl^-) was mimicked.

To simulate the activity of ROS towards hernia repair meshes, a previously developed model system was utilized [204]. UltraPro® and Composix™ meshes

were exposed to 100 ml of 1.63M H_2O_2 and 0.05M $CoCl_2$ solution (Sigma-Aldrich, St. Louis, MO). The 1.63M H_2O_2 solution was prepared from 35% w/w H_2O_2 solution (Alfa Aesar, Haverhill, MA) stabilized by 0.05% $Na_4P_2O_7 \bullet 10H_2O$. Additionally, glass wool (Sigma-Aldrich, St. Louis, MO) was added to the solution to provide an additional surface for free radical generation. Samples were treated in the oxidative medium for 40 days at 37°C. The $H_2O_2/CoCl_2$ solution was replaced every 3 days to eliminate the effect of H_2O_2 degradation. After the treatment, the meshes were rinsed with 500 ml of distilled water and air-dried at room temperature.

The effect of hypochlorite on the prosthetic mesh materials was tested according to the protocol described elsewhere [205]. Briefly, the meshes were treated in 100 ml of 1 mM NaOCl solution (Sigma-Aldrich, St. Louis, MO) for 40 days at 37°C. After the treatment, the meshes were rinsed with 500 ml of distilled water and air-dried at room temperature.

4.2.3. Characterization of the meshes

Scanning electron microscopy. Micromorphological characteristics of the treated and plain meshes were analyzed by means of a variable pressure scanning electron microscope (Hitachi S3400, Tarrytown, NY). Samples were not coated with a conductive material prior to the imaging. Images with a magnification of up to 2,000X were obtained using an accelerating voltage of 20 kV and a working distance of 7.0 – 11.3 mm. Chamber pressure was in the range of 25-50 Pa.

Fourier transform infrared spectroscopy. Chemical alterations to the meshes were analyzed using Fourier transform infrared spectroscopy (FTIR). Samples were not subjected to any form of special treatment prior to the experiments and were analyzed *in toto*. The spectra were obtained using a Thermo-Nicolet Magna 550 FTIR spectrometer with a Thermo-SpectraTech Foundation Series Endurance Diamond ATR accessory (Thermo Fisher Scientific, Waltham, MA). Scans were recorded in the range from 500 to 4000 cm^{-1} with a resolution of 4 cm^{-1}. A total number of 5 replicates were performed.

X-ray photoelectron spectroscopy. Surface composition of the meshes was analyzed using X-ray photoelectron spectroscopy (XPS). The measurements were conducted on a Kratos AXIS Ultra DLD spectrometer (Shimadzu, Columbia, MD) using non-monochromatic AlKα X-radiation (1253.6 eV). Binding energy of the C-C component of C1s peak was set at 285 eV and used thereafter as a standard for the binding energy calibration. The measurements were carried out at a pressure of 10^{-8} torr. Surface composition was assessed by analyzing the peaks that correspond to C1s and O1s emissions.

Differential scanning colorimetry. The effect of oxidative stress on the physical properties of the meshes was analyzed by means of differential scanning calorimetry (DSC). The analysis was performed on a Q1000 DSC instrument (TA Instruments, New Castle, DE). The samples were heated up to 200°C with a heat rate of 20°C/min and then kept at a target temperature for 5 min. All measurements

were performed in a nitrogen atmosphere. Onset melting temperature (T_m) and heat of fusion (H_f) were calculated for each sample from the melting endotherms.

The degree of crystallinity (X_c) of the meshes was calculated according to the following formula [206]:

$$X_c = \frac{H_f}{H_{f,100}} \times 100\%$$

where $H_{f,100}$ is the heat of fusion of 100% crystalline polypropylene and was considered to be 209 J/g [206]. A total number of 4 replicates were performed for the analysis.

Water uptake experiments. The protocol for water uptake experiments was adapted from elsewhere [207]. The meshes were cut into small pieces (≈ 20 mg) and kept in a desiccator for 48 hours at room temperature. Then the samples were weighted to the nearest 0.1 mg using an AE 200 Balance (Mettler Toledo, Columbus, OH). The meshes were then transferred to centrifuge tubes filled with distilled water and maintained for 10 days at room temperature to reach saturation. Following incubation, the samples were removed from water, wiped free of surface moisture and weighed. Water uptake (*WU*) was calculated using the following formula [208]:

$$WU\ (\%) = 100\% \times \frac{M_f - M_0}{M_0}$$

where M_0 represents the original dry weight of the sample and M_f - the weight of the sample after being kept in water. Five replicates were performed for each of the mesh samples.

Tensile testing. Mechanical properties of the meshes were evaluated by means of uniaxial tensile testing. The experiments were performed using a Synergie 100 (MTS, Eden Prairie, MN). Pieces of the meshes (1×4 cm) were fixed in the machine and stretched with a 5 cm/min crosshead rate until the mesh was loaded to failure. Afterwards, stress-strain curves were plotted, and the elastic moduli were calculated for each sample. A total number of 7 replicates were analyzed.

4.2.4. Table of experiments. The design of experiments conducted in this chapter are summarized in the table 4.1.

Table 4.1. Experimental design

Meshes	Treatment	Micro-morphology	Surface oxidation	Structural properties	Mechanical properties	Swelling
UltraPro®	**-** **ROS** **OCl^-**	SEM	FTIR & XPS	DSC	Tensile testing	Water uptake
Composix™	**-** **ROS** **OCl^-**	SEM	FTIR & XPS	DSC	Tensile testing	Water uptake

4.2.5. Statistical analysis. Numerical data is shown as the mean value ± standard deviation. One-way ANOVA was used for data comparison. Statistical difference was considered significant if P-value was less than 0.05.

4.3. Results

4.3.1. Scanning electron microscopy. SEM images provided essential information regarding morphology of the meshes. The micrographs of untreated UltraPro® and Composix™ meshes demonstrated that these samples exhibited a relatively smooth surface with evidence of parallel extrusion lines, which are introduced to the mesh fibers during the manufacturing process (Figs. 4.1a-b). In the micrographs of the meshes treated in $H_2O_2/CoCl_2$ solution, the surface of the UltraPro® meshes remained relatively smooth, although several minor defects and cracks were noticeable as indicated by red arrows (Fig. 4.1c). The Composix™ meshes displayed stronger evidence of deterioration: the surface exhibited a plethora of defects in the form of deep and wide cracks that formed along the extrusion lines (red arrows), and small holes (yellow arrows), indicative of material degradation (Fig. 4.1d).

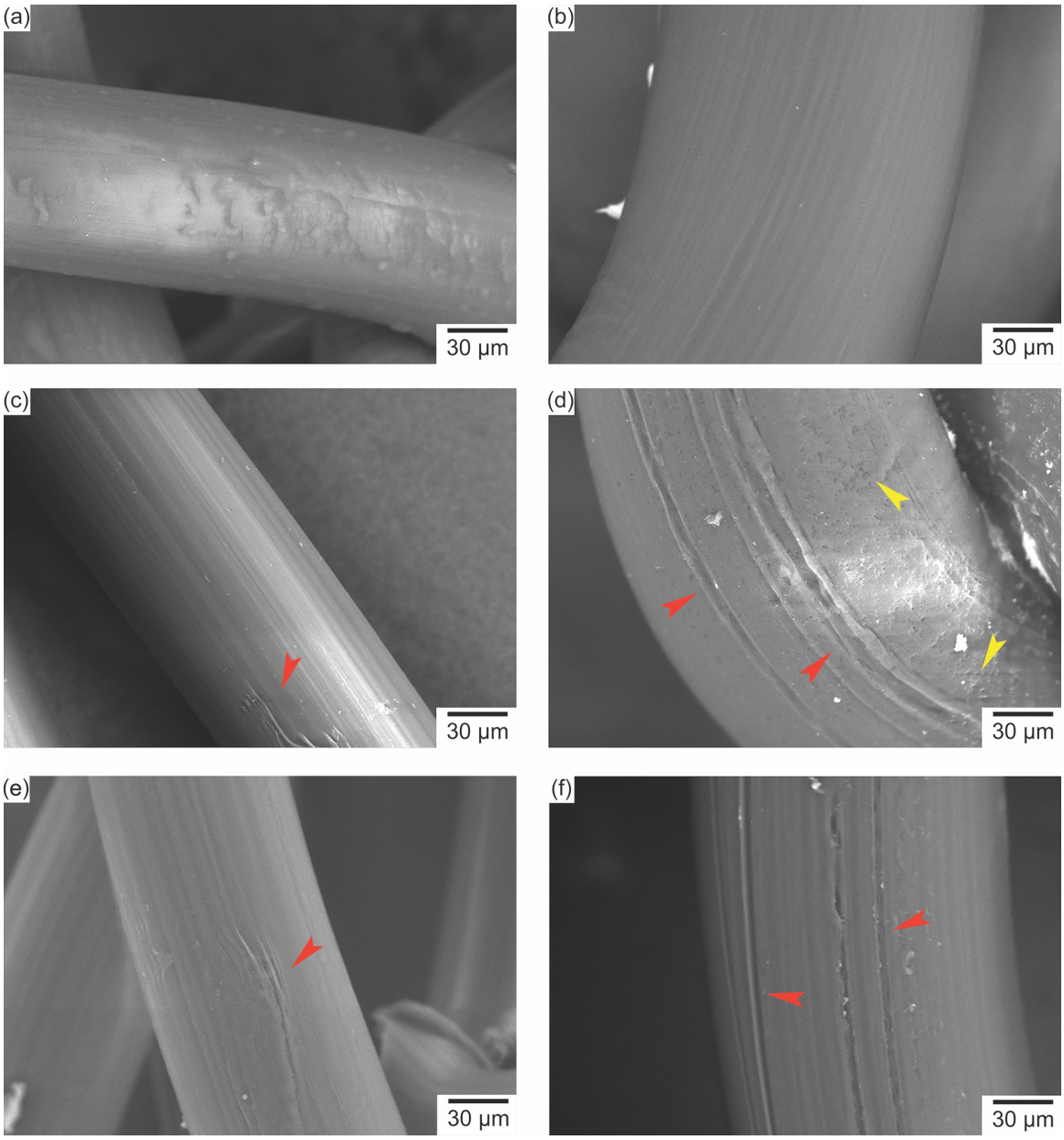

Fig. 4.1. Microphotographs of the UltraPro® and Composix™ meshes treated in $H_2O_2/CoCl_2$ and NaOCl solutions: (a) – plain UltraPro® mesh; (b) – plain Composix™ mesh; (c) – UltraPro® mesh treated in $H_2O_2/CoCl_2$ solution; (d) – Composix™ mesh treated in NaOCl solution; (e) – UltraPro® mesh treated in $H_2O_2/CoCl_2$ solution; (f) – Composix™ mesh treated in NaOCl solution

When treated in NaOCl, the UltraPro® samples again showed a smooth surface with few signs of deterioration, while the Composix™ meshes exhibited major cracks and fissures, indicated with red arrows (Figs. 4.1e-f).

4.3.2. Fourier transform infrared spectroscopy. FTIR spectroscopy was used to assess chemical alterations introduced during the treatments. The spectra collected from the treated and plain meshes are displayed in Fig. 4.2. Peaks at 2946 - 2836, 1456 and 1375 cm^{-1} correspond to pristine polypropylene and can be ascribed to the various types of C-H and C-C vibrations. Hence, these bands can be observed on every spectrum and weren't analyzed thereafter.

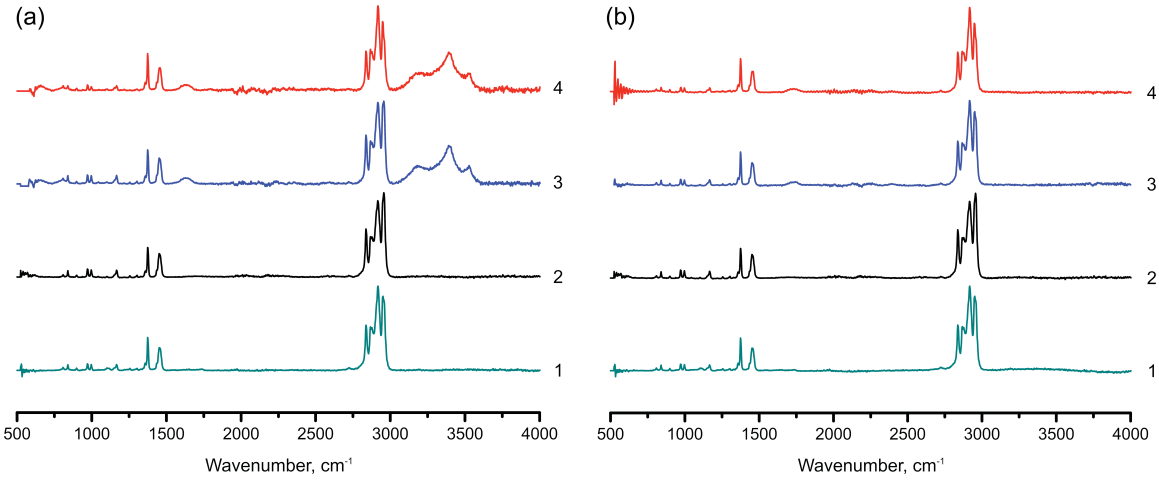

Fig. 4.2. FTIR spectra of UltraPro® and Composix™ meshes treated in $H_2O_2/CoCl_2$ (a) and NaOCl (b) solutions: 1 - plain UltraPro®, 2 – plain Composix™, 3 – treated UltraPro®, 4 – treated Composix™

Spectra of the meshes treated in $H_2O_2/CoCl_2$ solution show the emergence of several additional peaks (Fig. 4.2a). Of particular interest are bands at 1720 cm^{-1}; indicative of the presence of carbonyl groups (C=O); these can be observed only in the spectra of the treated samples. The intensity of these signals was not

significantly different for treated UltraPro® and Composix™ meshes. Broad bands at 3100-3600 cm^{-1} correspond to the intra- and intermolecular H-bonded hydroxyl groups.

Fig. 4.2b shows FTIR spectra of the meshes treated in NaOCl solution. The bands corresponding to the carbonyl groups (C=O) can also be observed on the spectra of the treated UltraPro® and Composix™ meshes. The intensity of these peaks was again not significantly different for treated UltraPro® and Composix™ meshes. Concurrently, no signs of hydroxyl groups were found on the spectra of the treated samples.

4.3.3. X-ray photoelectron spectroscopy. XPS spectra were obtained to analyze mesh surface composition before and after the treatments.

As expected, the two major elements detected by the XPS method were carbon and oxygen (hydrogen is undetectable by XPS). Traces of silicon and chlorine, which appear to be impurities, were also found. The obtained results allowed for evaluation of the surface composition of the meshes by analyzing the intensity of the peaks at 285 and 532 eV, corresponding to C1s and O1s emissions, respectively. Fig. 4.3 displays typical low-resolution XPS spectra of plain and treated UltraPro® and Composix™ meshes. Of particular interest were the bands corresponding to the O1s emission. It is evident that the relative intensity of these signals increases after both treatments. These results are indicative of surface oxidation caused by ROS and hypochlorite.

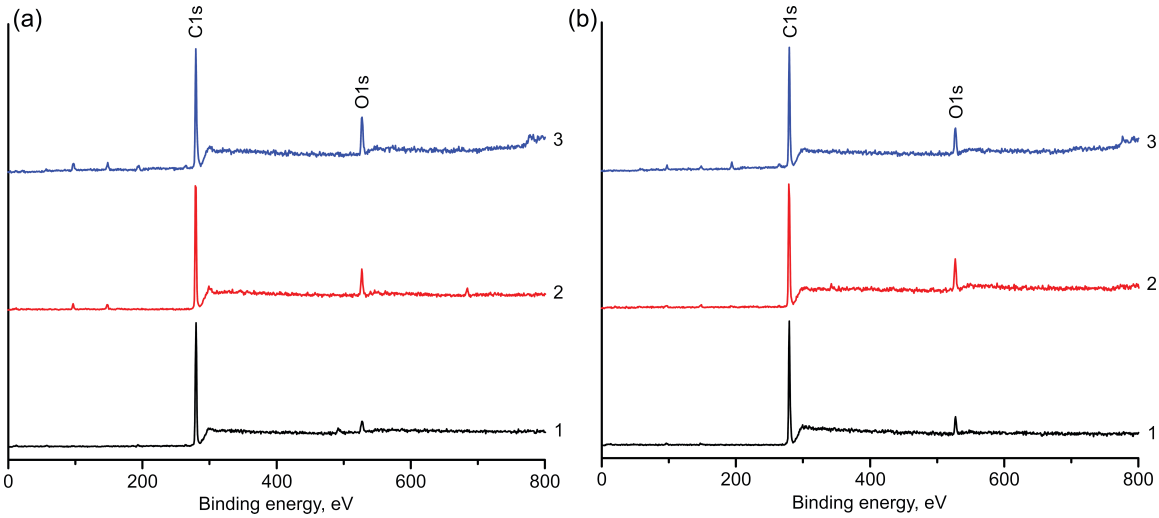

Fig. 4.3. Typical low-resolution XPS spectrum obtained for UltraPro®(a) and Composix™(b) meshes. 1 – plain mesh, 2 – mesh treated in in $H_2O_2/CoCl_2$, 3 – mesh treated in NaOCl

4.3.4. Differential scanning calorimetry. DSC was used to study structural properties of the meshes. Single cycle experiments were conducted for all samples. Figs. 4.4a-b show the DSC thermograms collected from the pristine UltraPro® and Composix™ meshes compared to those treated in $H_2O_2/CoCl_2$ solution. The onset temperature for UltraPro® did not change significantly after the treatment, and was 163.0±1.3°C and 161.2±1.3°C for untreated and treated mesh, respectively (p = 0.09, n = 4). The calculated heat of fusion (Fig. 4.5a) for the treated UltraPro® sample was found to be 84.7±5.4 J/g, whereas the value for the pristine UltraPro® sample was calculated to be 87.9±8.2 J/g. These two values were not significantly different (p = 0.54, n = 4). In the case of Composix™ meshes, the onset temperature was found to be 157.2±1.1°C and 151.3±1.2°C for the pristine and treated mesh, respectively. These temperatures were found to be significantly different ($p << 0.001$, n = 4). Furthermore, the treated meshes had a

significantly lower heat of fusion of 84.8±6.8 J/g as compared to 98.3±2.6 J/g for the plain Composix™ mesh (p = 0.010, n = 4).

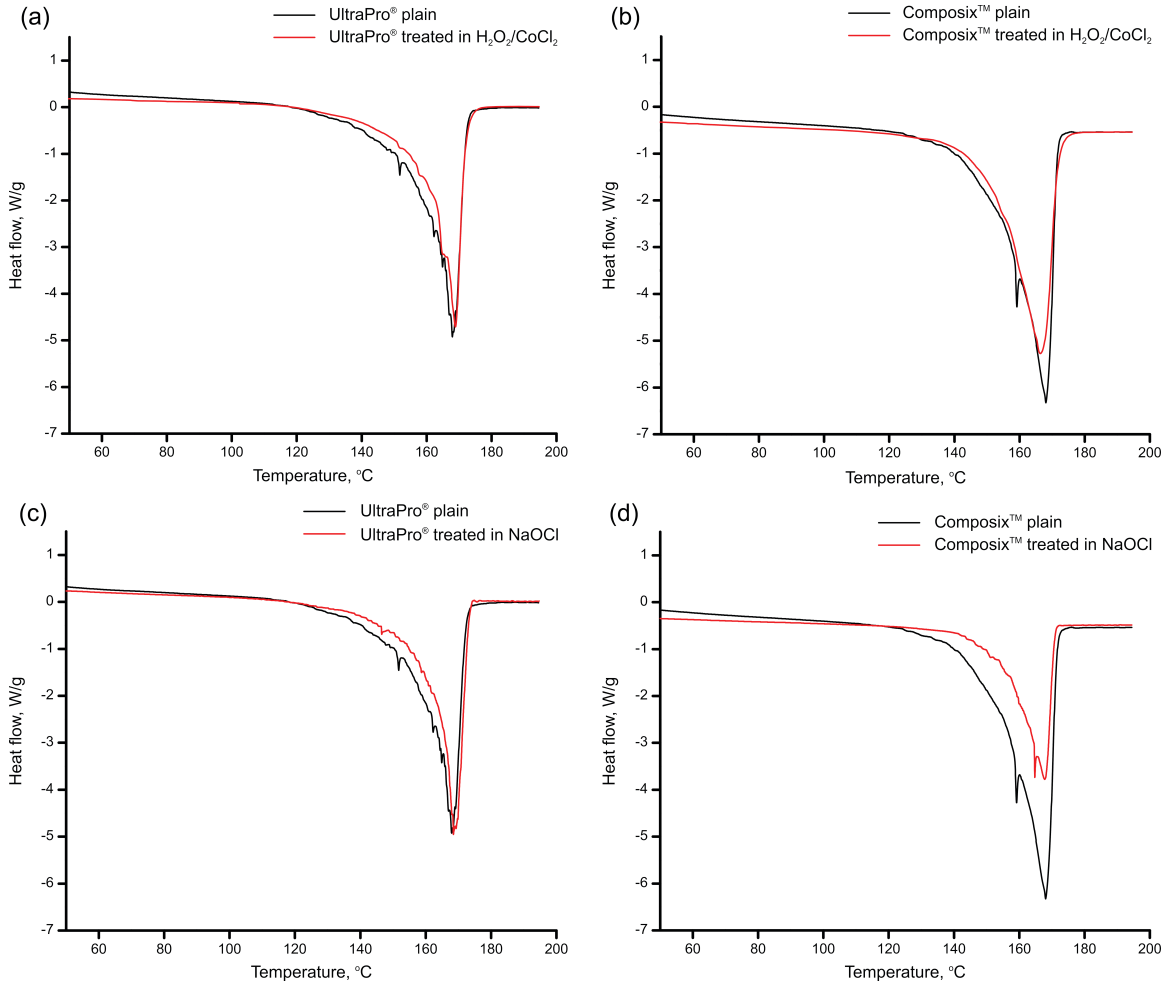

Fig. 4.4. DSC curves for the UltraPro® (a, c) and Composix™ (b, d) meshes treated in $H_2O_2/CoCl_2$ (a, b) and NaOCl (c, d) solutions.

Figs. 4.4c-d display the results of the DSC measurements for the meshes treated by hypochlorite compared to those for the untreated meshes. For the UltraPro® mesh, the onset temperatures for the plain and treated mesh were found to be 163.1±1.3°C and 162.0±1.2°C, respectively. The difference between these temperatures was not statistically significant (p = 0.2, n = 4). The heat of fusion for

the plain UltraPro® mesh was 87.9±8.2 J/g, whereas the heat of fusion for the treated UltraPro® mesh, was 84.4±4.3 J/g (Fig. 4.5b). These values were also not found to be significantly different (p = 0.48, n = 4). In the case of the Composix™ meshes treated by hypochlorite, the onset temperatures were 157.2±1.1°C and 152.1±1.2°C for the plain and treated samples, respectively, and these values were found to be significantly different (p = 0.001, n = 4). Similarly, the heat of fusion for the treated Composix™ meshes (85.9±1.8 J/g) was ca 13% lower compared to the heat of fusion for the untreated Composix™ meshes (98.3±2.6 J/g), and these two values were significantly different (p = 0.0002, n = 4).

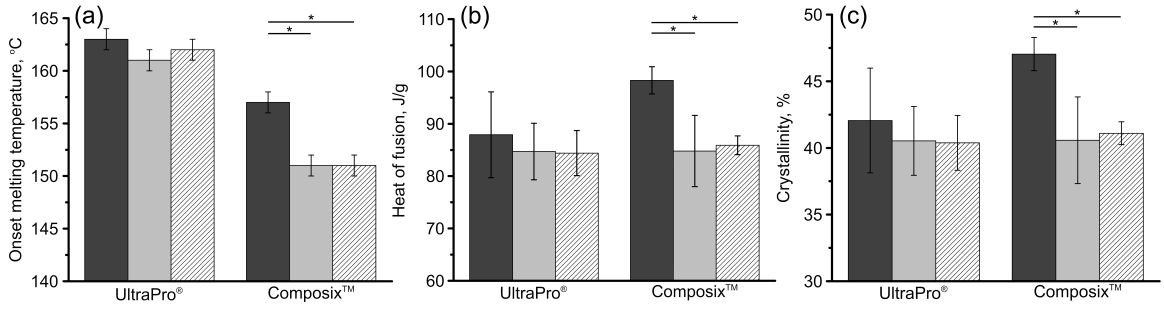

Fig. 4.5. The onset melting temperature (a), heat of fusion (b) and crystallinity (c) of the UltraPro® and Composix™ meshes treated in $H_2O_2/CoCl_2$ and NaOCl solutions. Dark grey bars – plain mesh, light gray bars – mesh treated in $H_2O_2/CoCl_2$; white bars – mesh treated in hypochlorite. Asterisks demonstrate significance difference (p < 0.05, n = 4). Error bars were calculated based on the standard deviation values.

Fig. 4.5c compares the crystallinity of the pristine and treated meshes. As could be expected based on the observations for the onset temperatures and heat of fusion, a significant drop in crystallinity after the exposure to ROS and hypochlorite anions was only observed for Composix™ meshes (p = 0.009 for ROS

treatment and $p = 3*10^{-4}$ for NaOCl treatment, respectively, n = 4), but not for the UltraPro® meshes ($p = 0.53$ for ROS treatment and $p = 0.48$ for NaOCl treatment, respectively, n=4).

4.3.5. Water uptake experiments. Water uptake experiments were conducted to compare the swellability of UltraPro® and Composix™ meshes. After immersion in water for 10 days, both types of mesh reached a constant water absorption level. The weight of the UltraPro® meshes increased by 2±1%, while the weight of the Composix™ increased by 6±3%. Therefore, it was shown that Composix™ hernia repair meshes absorb significantly more water when compared to UltraPro® meshes ($p = 0.022$, n = 5).

4.3.6. Mechanical testing. The plain and treated meshes underwent tensile testing to evaluate alterations in mechanical properties following the oxidative treatments.

Typical tensile force-displacement relationships for plain and treated polypropylene meshes are presented in Fig 4.6a. It can be noted that the force-displacement curves consist of two distinct regions. The first region (E_I) corresponds to the initial elastic deformations caused by the stretch of the mesh weft. The second region (E_{II}) corresponds to the elastic behavior of the mesh fibers and appears to be the stiffness of the material [78]. Only these parameters were analyzed in this work since they are relevant to the properties of the mesh material. The stiffness values are presented in Fig 4.6b.

Generally, oxidative treatments led to an increase in the stiffness. However, it can be seen that the parameter for the UltraPro® meshes increased significantly ($p << 0.001$, n = 7) only after the treatment in $H_2O_2/CoCl_2$ solution.

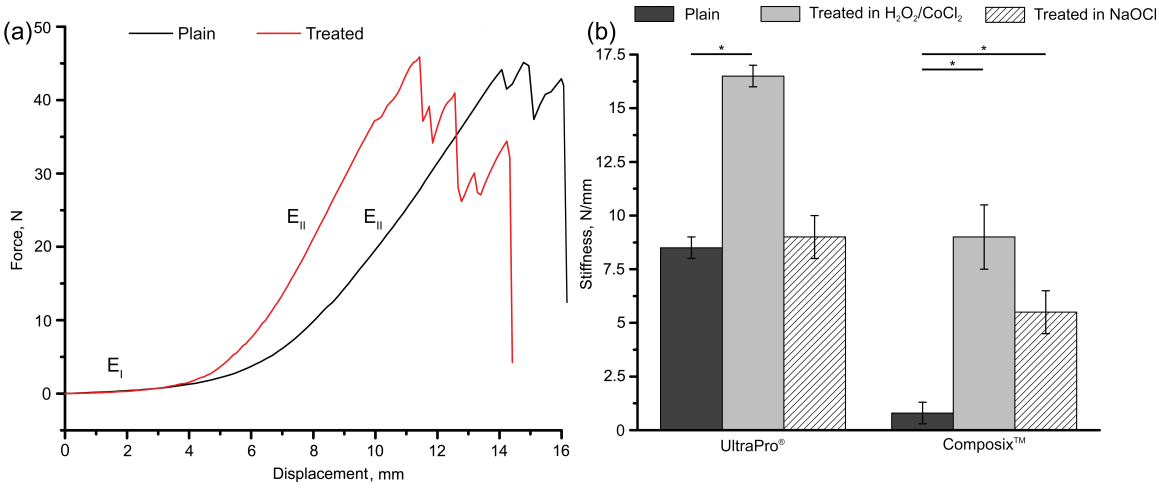

Fig. 4.6. (a) Typical force-displacement curve obtained for plain and treated in $H_2O_2/CoCl_2$ Composix™ mesh. (b) Stiffness of the UltraPro® and Composix™ meshes treated in $H_2O_2/CoCl_2$ and NaOCl solutions. Asterisks demonstrate significance difference ($p < 0.05$, n = 7). Error bars were calculated based on the standard deviation values.

The Composix™ meshes showed a significant ($p = 0.0001$, n = 7) increase in the stiffness in the case of both treatments. Furthermore, the parameter for Composix™ meshes increased by more than 10-fold in the case of both treatments, while the stiffness for the UltraPro® meshes only increased by ca 2-fold.

4.4. Discussion

Modern macroporous monofilament polypropylene (PP) meshes, such as UltraPro® and Composix™, are widely used for hernia repair surgeries. The use of

PP prosthetic meshes in hernioplasty has become so common as a result of general confidence in the high biocompatibility and reliability of the implants [107]. Moreover, according to multiple references, implantation of PP meshes is also associated with a relatively low recurrence rate [209]. All these characteristics make PP meshes the gold standard for hernia defect closure. At the same time, it was reported that nearly 20% of patients who have undergone hernioplasty experience chronic pain 1 year after the surgery [202,210]. The only treatment option for those patients appears to be a revision surgery, which places an additional burden on the patient and the healthcare system.

A growing body of evidence points to oxidative stress as a key factor in the development of the complications associated with post-hernioplasty chronic pain [198,211–213]. When exposed to the myriad of oxidants and enzymes after the implantation, hernia repair meshes may undergo various structural, chemical and mechanical changes. This can cause alterations in the mesh's linear dimensions [54]. It was shown that mesh shrinkage or expansion is associated with the development of chronic pain and increased chance of the recurrent herniation [214,215]. Moreover, mesh stiffening can lead to mechanical irritation of the surrounding tissues, thus provoking further excessive inflammatory response [54].

However, there is a lack of consensus regarding the mechanism of hernia repair mesh deterioration caused by oxidative stress. Analysis of failed explanted meshes cannot fully reveal the mechanism of implant failure; this is mainly due to the absence of a positive control and the necessity of removing tissue residues.

One possible solution could be an *in vitro* model that mimics oxidative stress at the mesh-tissue interface.

The present work focused on the influence of ROS and hypochlorite anions on the physical, chemical and structural integrity of hernia repair meshes. The *in vitro* system developed by Zhao, et al. was used herein to simulate the effect of ROS on prosthetic meshes [216]. In a model experiment to mimic environmental stress cracking of polyurethane elastomers, it was shown that the oxidative medium consisting of hydrogen peroxide and cobalt (II) chloride is a reasonable model to mimic *in vivo* oxidative stress conditions. In this system cobalt chloride is added to facilitate the production of ROS according to the Haber-Weiss reaction [217]:

$$H_2O_2 + CoCl_2 \rightarrow Co^{3+} + OH^- + OH^{\cdot}$$

Later, Zhao et al. modified the oxidative system by adding glass wool to enhance interactions between ROS and studied materials [204]. It was stated that the *in vitro* approach precisely mimicked the *in vivo* oxidative environment at the tissue-biomaterial interface [204].

In an attempt to simulate the effect of hypochlorite anions produced by myeloperoxidase, the meshes were treated in a sodium hypochlorite solution with a concentration of 1 mM. It is believed that this *in vitro* system provides a sufficient correlation with the *in vivo* oxidative stress [205,218]. The hypochlorite concentration used in the present study is somewhat similar to the local concentration observed in natural systems at the inflammatory site [219,220]. It is

important to emphasize that both approaches used herein to mimic the *in vivo* oxidative environment at the tissue-biomaterial interface have never been applied to study hernia repair meshes.

Better understanding of the effect of oxidative stress requires identification of the structural, physical and chemical alterations in the meshes upon exposure to oxidative insult. Previous experiments with gamma irradiation of polymers revealed that three important molecular effects may occur in polyolefins in the presence of free radicals: 1) chain branching, followed by cross-link formation; 2) chain scissions, which can also be followed by chain cross-linking; and 3) chemical oxidation, also resulting in cross-linking due to the formation of hydrogen bonds between the polymer chains (Fig. 4.7) [221,222]. Our results suggest that all meshes exposed to the oxidative media underwent these transformations. However, the extent of the alterations was different when comparing UltraPro® and Composix™ meshes.

The analysis of chemical oxidation of the meshes was performed using FTIR and XPS techniques. Since both mesh types were exposed to oxidative stress, the formation of oxygen-containing groups, particularly carboxyl groups, was likely to occur. This assumption was supported by the data. The FTIR spectra of both UltraPro® and Composix™ meshes, treated in either $H_2O_2/CoCl_2$ or NaOCl solutions, revealed the emergence of bands that can be ascribed to carboxyl groups. However, signal-to-noise ratio for these bands was calculated to be ca. 2.5:1, which did not allow accurate comparison of the peak intensities. Therefore,

XPS was used for an additional surface characterization. The results were in good agreement with the FTIR studies, and demonstrated an increase of the oxygen content on the surface of treated meshes, suggestive of the formation of oxygen-containing functional groups on the surface. The signal-to-noise ratio for the O1s bands in the XPS studies was ca. 8:1. This allowed for accurate comparison of the intensities of the peaks for different samples, and brought us to the conclusion about a similar degree of surface oxidation for Ultrapro® and ComposixTM meshes after the treatments. Thus, taken together, results of FTIR and XPS studies showed the evidence of surface oxidation following oxidative treatments for both Ultrapro® and ComposixTM meshes, and indicated that the degree of surface oxidation was similar for both types of meshes. Therefore, we should expect similar degree of cross-linking due to the formation of hydrogen bonds for these two meshes.

Information about chain branching and scissions can be obtained from DSC experiments. Our results suggest that these alterations were far more likely to occur in the case of Composix™ meshes since the degree of crystallinity and onset melting temperature for these meshes changed significantly after exposure to oxidation (Fig. 4.5) [197]. At the same time, the difference between the treated and plain UltraPro® meshes was not found to be significant. It should be noted that onset temperature corresponds to the beginning of the phase transition, and is not the same as the position of the peak on DSC. Typically, onset temperatures are reported in the literature for characterization of functional polymeric materials,

including hernia meshes, since these parameters correlate better with the degree of crystallinity [197].

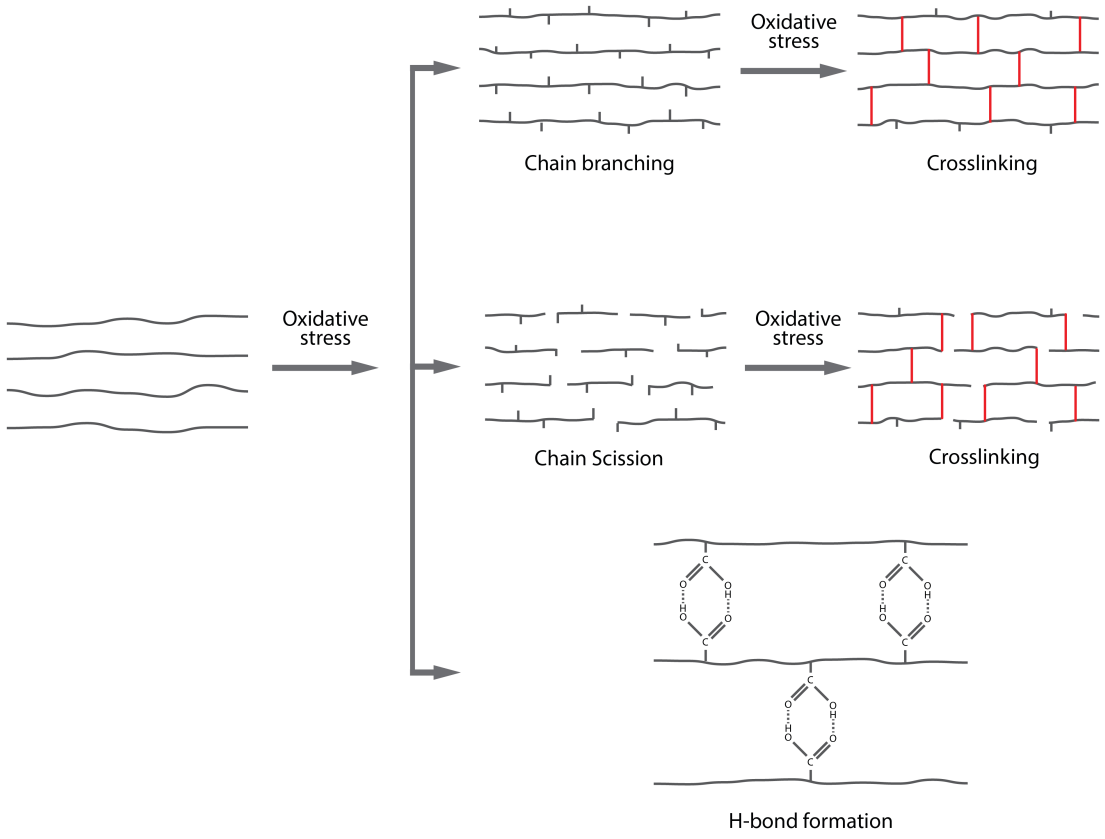

Fig. 4.7. Molecular effects occurring in polyolefins when exposed to oxidative insult

It is known that under oxidative conditions, chain branching and chain scissions may lead to the formation of cross-links between the polymer chains [9,194]. In addition, these processes may lead to the increase of the number of polymer chain entanglements [223]. These structural alterations often result in an increased stiffness of the material [9,194]. The results of the mechanical testing conducted in the present work indirectly confirmed the formation of cross-links and chain entanglements in the studied meshes. The tensile testing experiments

demonstrated a significant increase of the stiffness of the Composix™ meshes that have undergone the treatment in $H_2O_2/CoCl_2$ and NaOCl solutions. At the same time, mechanical properties of the UltraPro® meshes changed only after being exposed to ROS, though the extent was much lower than with Composix™ meshes. Concurrently with increase of the stiffness of the treated meshes, the E_I region of the samples decreased substantially following exposure to the oxidative insult. Apparently, this effect is due to excessive deterioration of the regions of mesh filament entanglements, which largely determine the E_I region of the force-displacement curves. High degradation of these regions of hernia meshes was demonstrated for the implants exposed to the oxidative insult [197]. Although, this effect was not assessed in this work, future studies should involve analysis of the degradation of mesh entanglement regions.

In combination, the results of our studies indicate that mesh stiffening upon oxidation is unlikely to be caused by cross-linking due to the formation of new hydrogen bonds, but rather is caused by polymer branching and/or chain scissions leading to polymer chain cross-linking. Future studies of molecular weight distributions of polypropylene before and after oxidative treatment may help to elucidate the exact mechanism of the oxidative mesh stiffening.

All the molecular effects described above may lead to micromorphological alterations of the mesh surface. Scanning electron microscopy was used herein to evaluate these changes. In good agreement with the previous results, Composix™ meshes exposed to ROS or NaOCl exhibited more pronounced

micromorphological alterations. These results are also in agreement with those obtained for the explanted polypropylene hernia repair meshes that also demonstrated cracks, extrusion lines and holes on the surface [9,194,196,202,224]. The surface of treated UltraPro® meshes remained smooth with barely noticeable signs of deterioration.

Thus, the obtained results suggest that Composix™ meshes are more susceptible to oxidative stress when compared with UltraPro® meshes. This effect can be explained by the results of water uptake experiments. We have shown that Composix™ meshes are capable of absorbing significantly (p = 0.022, n = 5) more water than UltraPro® meshes. The increased absorption of water during swelling provides a passage for water soluble oxidants, thus enhancing oxidation and the formation of chain scission and cross-link domains in the Composix™ hernia repair meshes.

4.5. Conclusions

In the present work, we compared the susceptibility of Composix™ and UltraPro® meshes to *in vitro* oxidative challenge. The meshes were subject to two model treatments that mimic *in vivo* effects of reactive oxygen species and hypochlorite anions. It was found that both treatments increased the stiffness of the meshes. We speculate that such changes in mechanical properties are caused by formation of cross-links between the polymer chains, chain scissions, and hydrogen bonds between the carboxyl groups introduced to the materials. We

have demonstrated that Composix™ meshes, when compared with UltraPro® meshes, were more vulnerable to the oxidative stress caused by either reactive oxygen species or hypochlorite anions. This is in agreement with clinical observations of lower incidence of chronic postoperative pain in the case of the UltraPro® meshes.

CHAPTER 5*

ANTI-INFLAMMATORY COATINGS ON HERNIA REPAIR MESHES

5.1. Introduction

Hernia repair surgeries are among the most common operations with over 20 million procedures performed worldwide each year [192]. The use of polymeric mesh in incisional hernioplasty was first proposed in 1958 by Dr. Usher [52]. Since then, insertion of prosthetic implants became a well-established procedure for reinforcing the closure of hernia defects. Polypropylene is commonly used in the construction of these meshes as it possesses several vital characteristics such as high chemical inertness and strong ability to integrate with surrounding tissues, resulting in relatively low inflammatory response. Because of these properties, polypropylene has become the most commonly used mesh for hernioplasty worldwide. Nevertheless, mesh-related complications continue to be observed after hernia repair surgeries. Recurrences, seroma formation, adhesions, infections and bowel obstruction have been observed [225]. Post-operative chronic pain is of particular importance since nearly 30% of the patients have to deal with this problem [84].

While exact mechanism of development of chronic pain still remains a subject of debate, a growing body of evidence points towards oxidative stress as one of the major factors leading to the implant deterioration and chronic postoperative pain in hernioplasty [194,197,226]. It was reported [227,228] that

* Results and data provided in this chapter were previously published in:
D. Gil, J. Rex, W. Cobb, V. Reukov, A. Vertegel. Anti-inflammatory coatings of hernia repair meshes: a pilot study. *Journal of Biomedical Materials Research B,* 2017, 00B:000–000, DOI:10.1002/jbm.b.33834

reactive oxygen species (ROS), in particular superoxide and hydroxide radicals, cause the most harm to the material of the mesh. It was also shown [196,226] that hypochlorite ions (OCl^-) produced by enzyme myeloperoxidase present in neutrophils can contribute to the process of oxidative degradation of the implant. This suggests that oxidative stress plays a crucial role in the development of complications following hernia repair surgeries.

Within the past few years, several strategies aiming to reduce the prevalence of complications were developed. For instance, clinical studies showed that host-site integration can be drastically enhanced by using hernia repair meshes with large hexagonal pores [85]. Other works demonstrated that altering mesh density affects the healing process after the surgery: lightweight hernia repair meshes were shown to reduce tissue adhesion and improve tissue integration compared to heavyweight meshes [84,201]. However, these approaches yielded only incremental improvements in long term outcomes of hernioplasty. Moreover, reducing the polypropylene content of meshes has weakened their structure and led to cases of central mesh fracture [229].

One promising strategy to reduce complications could be the use of surface coatings on hernia repair meshes. Expanded polytetraflouroethylene mesh has been coated with silver chlorhexidine in an effort to provide bactericidal activity. This coating has shown to kill species of *Staphylococcus aureus* and methicillin-resistant *S. aureus* out to 14 days [230]. Omega-3 fatty acid has been used on polypropylene mesh to reduce inflammation and tissue adhesions when compared

to a reference mesh [136]. The use of coatings was found to be highly efficient, being hailed as one of the “the most important incremental advances for mesh design” [136]. However, omega-3 fatty acid can alter the handling characteristics of the mesh, which poses a problem for laparoscopic repairs where the mesh is introduced through a trocar. Additionally, there are concerns with a higher incidence of postoperative infections [231]. As such, the search for a safe and efficient anti-inflammatory coating is of a great importance for the field.

Vitamin E, which refers to a family of tocopherols and tocotrienols, is a well-known and potent anti-oxidant. Vitamin E was tested as a drug candidate for treatment of a number of conditions, in which oxidative stress plays important pathophysiological role, such as Amyotropic Lateral Sclerosis, Alzheimer’s syndrome, arthritis, asthma, kidney and liver diseases, and stroke [232]. It showed efficacy in a number of animal models for these conditions, and in clinical trials as a supplemental treatment of rheumatoid arthritis [233] and asthma [234]. While use of vitamin E has not been studied extensively in hernia repair, one study found that intraperitoneal injection of vitamin E following implantation of a hernia mesh reduced the number of peritoneal adhesions in a rat model [235]. Furthermore, poor solubility of vitamin E in water can be expected to result in an enhanced adsorption onto hydrophobic meshes and provide a sustained release rate for a prolonged period of time. Additionally, Vitamin E is generally recognized as safe (GRAS) by the FDA, which can facilitate translation of vitamin E-coated meshes into clinical practice.

Herein, we have hypothesized that coating hernia repair meshes with Vitamin E will lead to a reduced inflammatory response and reduced formation of connective tissue in the vicinity of the mesh, improving the long-term outcomes of the hernia repair surgery. Hence, the goal of this work was to evaluate *in vivo* anti-inflammatory and anti-adhesive properties of Vitamin E-coated polypropylene hernia repair meshes. We also endeavored to replicate the retromuscular repair which is becoming increasingly popular in humans for ventral hernia repair with mesh.

5.2. Materials and Methods

5.2.1. Hernia repair meshes. Prolene® polypropylene mesh (Ethicon Inc., a Johnson & Johnson company, Langhorne, PA) was kindly donated by the Carolinas Medical Center (Charlotte, NC) and used in the course of this study. This type of implant is a heavyweight non-absorbable mesh with a density of 80 g/m^2. The specific surface area of the meshes was determined by low-temperature nitrogen adsorption using Brunauer–Emmett–Teller (BET) analysis and was calculated to be 3.4 m^2/g. Heavyweight polypropylene mesh was chosen because this implant exhibits a noticeable inflammatory response. For *in vitro* experiments 1 x 1 in. square samples were cut using sterile metal scissors. For animal studies 3 x 3 cm square pieces were cut and re-sterilized under UV radiation for 60 minutes prior to implantation.

5.2.2. Preparation of vitamin E-coated meshes. Vitamin E (Sigma-Aldrich, St. Louis, MO) was dissolved in 95% medical grade ethanol (Sigma-Aldrich, St. Louis, MO). 10 ml of the solutions with different vitamin E concentrations were transferred into a 6-well plate containing pieces of surgical mesh in each well. Samples were incubated overnight in the dark at 8^{o}C. Meshes were then retrieved and air-dried overnight in the dark at room temperature.

In order to determine binding yield of vitamin E, its solutions with concentrations of 5, 10, 50, 100 and 200 mg/ml were prepared and used to coat the meshes. After the samples were coated with vitamin E and air-dried, they were transferred to pure 95% ethanol and incubated overnight in the dark at 8^{o}C in order to reach adsorption-desorption equilibrium. 100 μl aliquots of wash solutions were collected and analyzed by measuring optical density at 292 nm using a microplate reader (Bio-Tek® Synergy™ III). Concentrations of vitamin E in wash solutions were determined using a standard curve, and the amount of vitamin E absorbed on the meshes was calculated from these concentrations assuming complete removal of vitamin E from the surface. In order to validate this assumption, the amount of absorbed vitamin E was measured after the mesh was removed from wash solution. It was shown that only negligible amount of α-tocopherol remained on the mesh. Adsorption experiments were replicated 4 times.

5.2.3. Mechanical testing. Mechanical testing of plain and modified meshes was performed using an MTS® Synergie™ 100 machine with a 100 N load cell. 4 pieces of plain and modified mesh, 2 x 4 cm each, were clamped to the machine

and stretched with the rate of 50 mm/min until the sample failed. Following testing, fore-displacement curves curves were plotted; tensile strength and structural stiffness were calculated.

5.2.4. In vitro determination of vitamin E release profile. After adsorption experiments were carried out, 100 mg/ml vitamin E solution was used to coat the implants, as this concentration was considered to be optimal for further studies. For drug release experiments, vitamin E-coated meshes were incubated in 10 ml of 10% bovine serum albumin (BSA) solution in PBS buffer at 37^{o}C. To determine release kinetics, samples were taken from the BSA solution at different time points (1, 2, 4, 7, 10 days). Concentration of remaining vitamin E was determined by measuring optical density at 292 nm, as described in sec. 5.2.2. All experiments were replicated 4 times.

5.2.5. Animal study. One 13-week old male New Zealand white rabbit was used in this study. For the pilot animal experiment, a rabbit model was chosen, since rabbits are large enough to accommodate 2 pieces of mesh sufficiently separated. The weight of the animal was approximately 3200 g. All animal experiments were conducted according to the protocol approved by institutional animal care and use committee of Clemson University (AUP-2015-019). The rabbit was hosted in Godley-Snell Animal Facility at Clemson University and treated according to the established standards. Prior to the surgery, the animal was anesthetized using acepromazine 1 mg/kg, ketamine HCL 33 mg/kg, atropine 0.02-0.05 mg/kg, and buprenorphine 0.05 mg/kg.

After skin asepsis, a 5-cm incision was made in the midline of the animal's ventral abdominal wall. The abdominal cavity was carefully entered along the *linea alba*. Just lateral to the *linea alba*, the posterior fascia was incised to the level of the rectus muscle. The posterior sheath was then carefully peeled off of the rectus muscle laterally. At the semilunar line, the dissection transitioned to the plane between the transversus abdominis and internal oblique muscles laterally. An intermuscular plane was created to accommodate a 3x3 cm piece of mesh (Fig. 5.1).

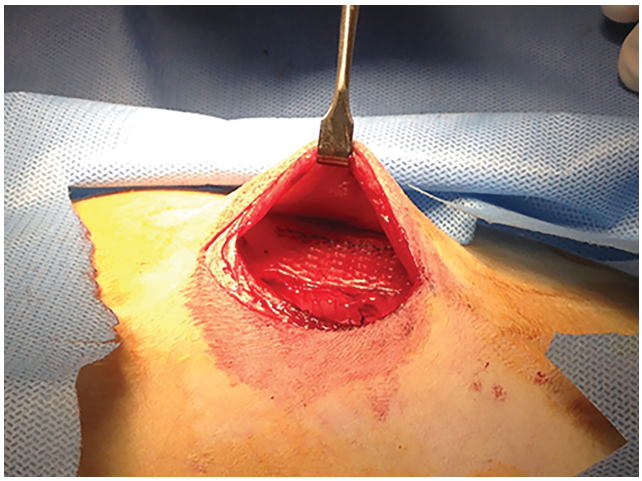

Fig. 5.1. Mesh implantation procedure.

The posterior sheath was then re-approximated in the midline with 4-0 polydioxanone suture in a running fashion. One sample of a Vitamin E-coated and an uncoated Prolene® mesh were implanted into the rabbit on either side, symmetrically with respect to the *linea alba*. Of note, coated meshes were not sticky and their handling was not different from uncoated meshes. The mesh pieces were secured to the muscle inferiorly at the four corners with 4-0 polydioxanone suture. The anterior fascia was then closed in the midline with 4-0

polydioxanone suture in a running fashion. Skin was sutured with 3-0 polydioxanone sutures.

5.2.6. Mesh explanation and histological evaluation. 5 weeks following the surgery, the rabbit was euthanized and tissue-mesh explants were excised *in toto*. Explanted specimens contained fascia, mesh, abdominal muscles and skin. After being processed, each sample was embedded in paraffin and 10 μm sections were cut using a microtome.

Both foreign body granuloma and intra-pore spaces were subjected to histological analysis. For this purpose, slides were stained with hematoxylin and eosin (H&E), picrosirius red, Masson's trichrome and Movat's pentachrome, followed by observation under light microscope. A modified histological scale was created based on [193] and ISO 10993-6 (table 5.1). Inflammatory response was assessed by counting the number of macrophages and Foreign Body Giant Cells (FBGCs) surrounding the meshes. Collagen organization, fibrosis, neovascularization and fatty infiltrates were examined and graded by an independent experienced histologist in a blinded manner. Slides stained with picrosirius red were observed through crossed polars in order to analyze the structure of collagen frameworks. Selected areas were examined using ImageJ software (NIH, Bethesda, MD). Hue analysis was performed based on the methodology described in [236]. Briefly, 256 hues were divided into 2 groups. The first group (hue range 0 – 49) was ascribed to mature collagen bundles; the second group with a range of 50 – 100 was attributed to immature collagen fibrils. Using

the software, the number of pixels in each group was computed and percent volume fraction of each type of collagen was calculated.

Table 5.1. Histological scoring system

Response	Score				
	0	1	2	3	4
Collagen organization	None	Minimal organization	Mild organization	Moderate organization	Well-organized
Fibrosis	None	Narrow band	Moderately thick bands	Thick bands	Extensive bands
Neovascularization	None	Minimal capillary proliferation	Mild amount of capillaries	Moderate bands of capillaries	Abundant vascularity
Fatty infiltrate	None	Minimal amount of fat	Mild amount of fat	Broad/elongated fatty infiltrates	Severe fatty infiltrates

5.2.7. Table of experiments. The design of experiments conducted in this chapter are summarized in the table 5.2.

Table 5.2. Experimental design

Mesh	Type	In vitro experiments	Animal experiments		
		Sample characterization	Cellular response	Tissue characterization	Collagen characterization
Prolene™	Plain Vitamin E-coated	Drug yield, drug release, mechanical testing, ORAC	H&E	H&E, Masson's, Movat's stainings	Picrosirius red

5.2.8. Statistical analysis. All numerical data is presented as mean value ± standard deviation. Student's t-test and one-way ANOVA was used for variance comparison. Statistical difference was considered significant if P-value was less than 0.05. Statistical analysis was performed using Excel (Microsoft, Redmont, WA).

5.3. Results

5.3.1. Mechanical properties of the meshes. Results of mechanical testing are presented in table 5.3. Structural stiffness and tensile strength of the coated and plain meshes were determined for five replicates and were not found to be significantly different (p = 0.18 and 0.38, respectively).

Table 5.3. Mechanical properties of plain and vitamin E coated meshes

	Plain mesh	Vitamin E-coated mesh	P-value
Stiffness, N/mm	5.5 ± 0.4	4.6 ± 1.1	0.18
Tensile strength, N	1.1 ± 0.1	1.2 ± 0.3	0.38

5.3.2. Binding yield of vitamin E. Fig. 5.2 shows binding yield for vitamin E on a 1x1 in. piece of Prolene® mesh from ethanol solutions with different initial drug concentrations. The amount of Vitamin E loaded on the mesh increases with the concentration of the initial solution for concentrations up to 100 mg/ml (p<0.0001, n=4). For higher initial concentrations the coating was sticky, and some vitamin E was draining from the mesh upon storage. This made controlled loading difficult for initial concentrations higher than 100 mg/ml. Thus, loading for all further experiments was performed using initial vitamin E concentration of 100 mg/ml.

5.3.3. Vitamin E release profile. A vitamin E release profile was evaluated in the presence of BSA, to model presence of protein solution in the vicinity of the implant *in vivo*. Fig. 5.3 shows the release profile for a coated mesh incubated in 10% protein solution.

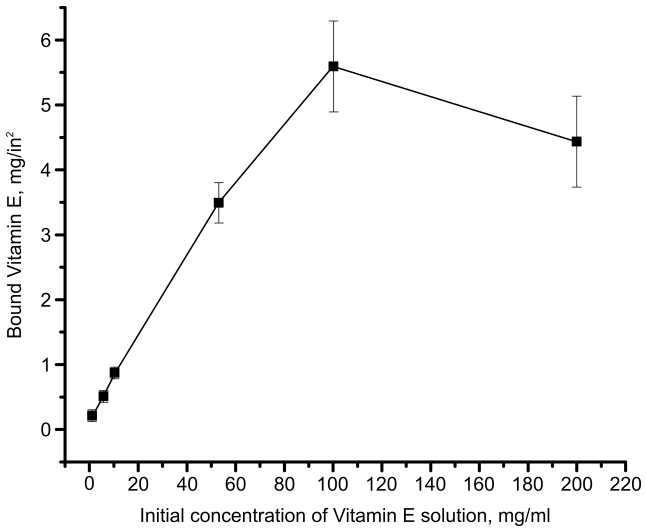

Fig. 5.2. Binding yield of vitamin E on polypropylene hernia repair mesh (*n = 4*). Error bars were calculated based on the standard deviation values.

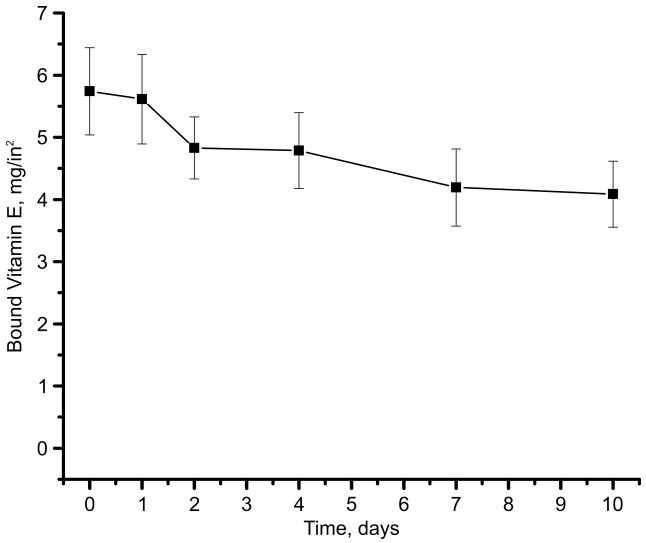

Fig. 5.3. *In vitro* release profile of vitamin E from coated meshes after the exposure to 10% BSA solution (*n = 4*). Error bars were calculated based on the standard deviation values.

A significant drop of bound Vitamin E was measured after 10 days of incubation in BSA (p = 0.1, n=4). However, it was shown that approximately 70%

of Vitamin E still remained on the mesh. These results indicate that α-tocopherol adsorbed on the implant can potentially provide a prolonged release profile *in vivo*.

5.3.4. Wound healing. The rabbit successfully survived until the end of the experiment. The *linea alba* healed well; no indications of wound dehiscence, infections, or any other complications were observed.

5.3.5. Histological evaluation. Histopathological examination was performed to assess inflammation, capsule formation, neovascularization, fatty infiltration and collagen composition. Plain and vitamin E - coated meshes showed different levels of host tissue response.

First, H&E staining was used to assess inflammatory and FBGC response, as well as the presence of fatty infiltrates and neovascularization in the vicinity of the implants (Fig. 5.4).

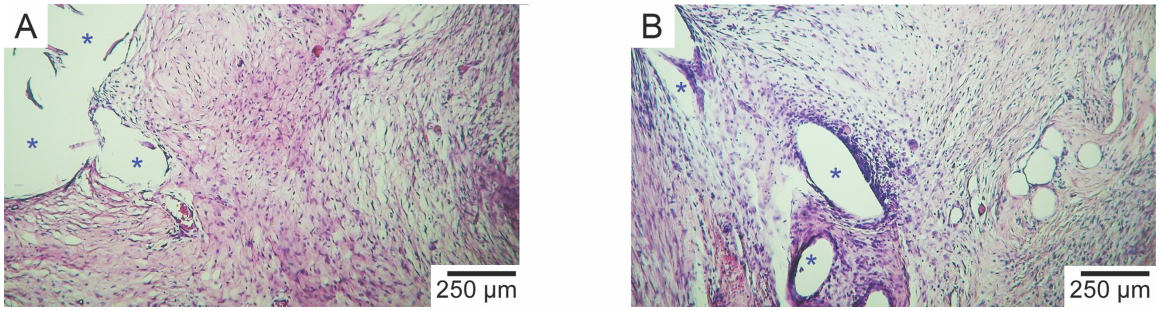

Fig. 5.4. Representative photomicrographs of histological slides stained with H&E at 40x. Asterisks show the area where mesh fibers were originally present. (A) Polypropylene mesh coated with vitamin E. (B) Plain polypropylene mesh.

The number of macrophages infiltrated in the tissue surrounding the implants is shown in table 5.4. It can be seen that the number of macrophages in the case of the plain sample was significantly larger compared to the drug-coated implant

(p<0.0001, n=11). Concurrently, little evidence of foreign body giant cells was found in either of the implants. Compared to vitamin E-coated mesh, plain mesh displayed a significantly larger amount of fatty infiltrates. Moreover, a significantly higher level of neovascularization was found around the plain mesh when compared to vitamin E-coated implant.

Table 5.4. Number of macrophages infiltrating mesh-tissue interface

Cell type	Number of cells per high powered (400 x) field	
	Plain mesh	Vitamin E – coated mesh
Macrophages	23 ± 4	13 ± 4

Movat's staining was used to visualize host fibrotic response to the implants. As predicted, both meshes induced the formation of fibrin bundles (Fig. 5.5), which are very densely packed and are found surrounding the implants (peri-filamentous) rather than within intra-pore space. At the same time, there was a noticeably smaller amount and density of fibrin bands surrounding vitamin E-coated mesh.

Masson's trichrome staining was used to assess tissue ingrowth in terms of collagen deposition and organization. Fig. 5.6 depicts microscopic evaluation of stained tissues around both of the implants. Collagen bundles were deposited in both peri-filamentous and intra-pore spaces. Furthermore, collagen surrounding both of the meshes appears to be loosely packed with empty inter-fiber spaces. At the same time, it can be seen that each mesh displays different level of collagen content as well as organization. Plain mesh is encompassed by much thicker collagen capsule. Fibrotic response to the uncoated mesh possesses a significantly higher level of organization—collagen fibers appear more aligned

when compared with the coated implant. Moreover, Vitamin E-coated mesh is surrounded by a higher content of elastin fibers (red/pink areas) when compared with the plain implant.

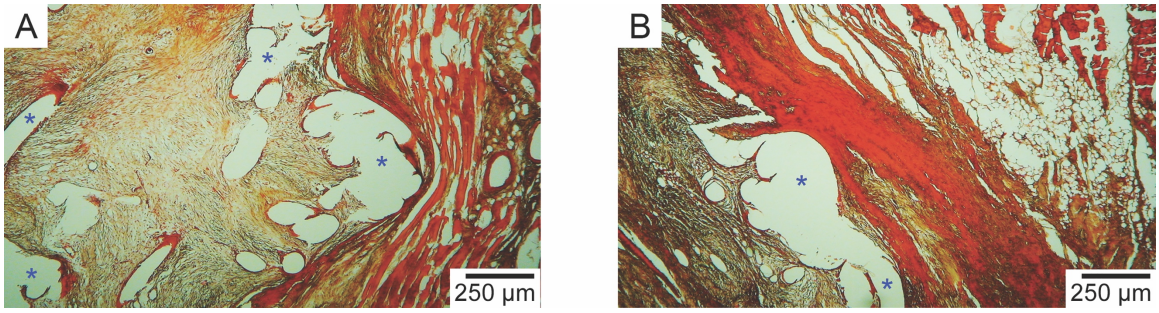

Fig. 5.5. Photomicrographs of histological slides stained with Movat's trichrome at 40x. Asterisks show the area where mesh fibers were originally. Broad bands stained bright red represent fibrin. Dark areas represent elastin fibers and nuclei. (A) Polypropylene mesh coated with vitamin E. (B) Plain polypropylene mesh.

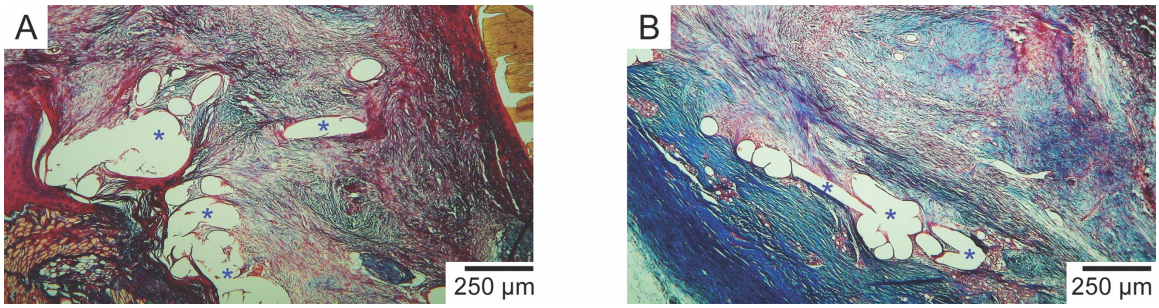

Fig. 5.6. Photomicrographs of histological slides stained with Masson's trichrome at 40x. Asterisks show the area where mesh fibers were originally. Bands stained blue represent collagen. Red areas represent elastin and muscle tissues. (A) Polypropylene mesh coated with vitamin E. (B) Plain polypropylene mesh.

In order to perform semi-quantitative histological evaluation, the modified histological grading scale shown in table 1 was used. Stained slides were

examined and graded by an experienced independent histologist in a blinded manner. The qualitative observations described above were confirmed by the histological score: when compared to vitamin E-coated mesh, plain mesh demonstrated a significantly greater degree of collagen organization, fibrosis, neovascularization and fatty infiltrates (Fig. 5.7).

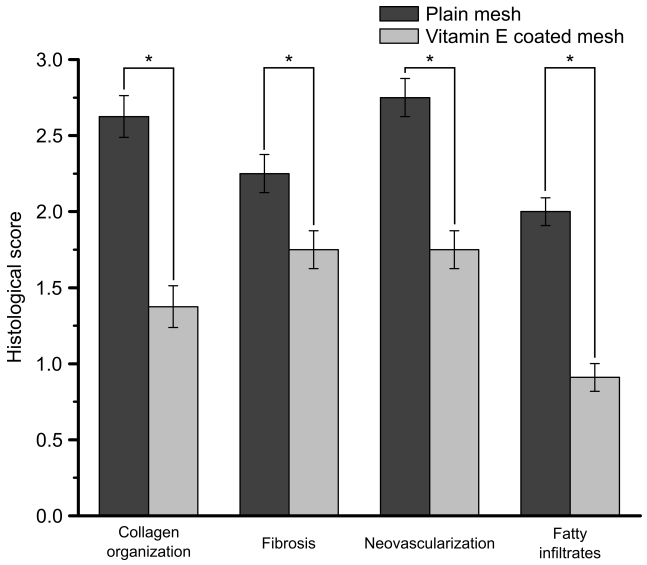

Fig. 5.7. Semi-quantitative histological assessment of the tissue surrounding plain and Vitamin E coated meshes. Histopathological score was obtained for the following parameter: collagen organization, fibrosis, neovascularization and fatty infiltrates. Asterisks represent statistically significant difference between plain and Vitamin E coated meshes (*$p<0.05$, $n=12$*). Error bars were calculated based on the standard deviation values.

Due to the wound healing process and the inflammation associated with it, collagen characteristics, in particular the ratio of mature to immature collagen, can be altered when compared to the normal tissue. Picrosirius red staining (PSR) was used to analyze the maturity of collagen surrounding the implants. Since collagen is a strongly anisotropic molecule it appears to be birefractive. Its birefringent

properties depend on several factors, such as maturity of fibers, package density, fiber alignment and thickness. Generally, mature collagen (MC) possesses stronger birefringence when compared with immature collagen (IC). Picrosirius red molecules also appear to be elongated and, when attached to collagen, enhance its birefringency. Due to this, mature collagen fibers, which are thick, aligned and densely packed, possess strong birefringent properties (intensified by PSR) and colored yellowish-orange or dark under polarized light. At the same time, immature fibers, which are loose and contain procollagens as well as intermediate collagens, appear greenish under polarized light. Fig. 5.8 shows images of histological slides stained with PSR for plain and coated mesh.

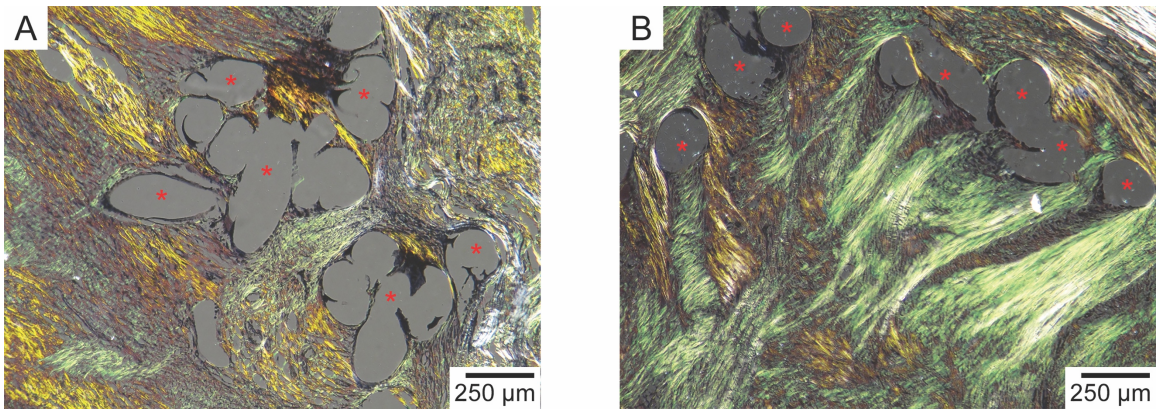

Fig. 5.8. Photomicrographs of histological slides stained with picrosirius red at 40x. Pictures were made through crossed polars. Asterisks show the area where mesh fibers were originally. Green areas correspond to immature collagen. Yellowish and dark areas are ascribed to mature collagen. (A) Polypropylene mesh coated with vitamin E. (B) Plain polypropylene mesh.

Fig. 5.9 shows the ratio of mature and immature collagen in the vicinity of the meshes calculated using the hue analysis. The mean percentage of mature

collagen (MC) surrounding plain mesh was calculated to be 57.3 ± 6.9%; the mean value for immature collagen (IC) was equal to 42.6 ± 6.9%, corresponding to the ratio of 1.34 ± 0.44. Collagen content in the tissue around vitamin E-coated mesh showed a higher percentage of mature fibers (69.0 ± 6.1%), while the percentage of immature collagen reduced to 31.0 ± 6.1%. The resulting MC/IC ratio was equal to 2.22 ± 0.81. The difference between the MC/IC ratios for coated and plain meshes was found to be statistically significant (*p=0.004, n=12*).

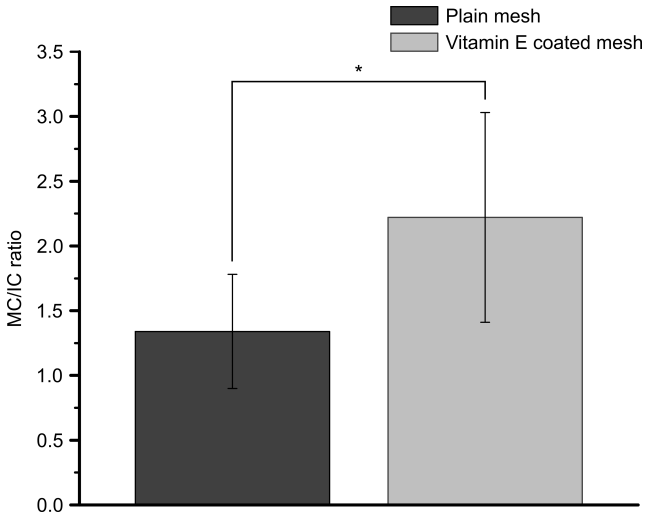

Fig. 5.9. The ratio of mature and immature collagen in the tissue surrounding plain and Vitamin E coated mesh. Asterisk represents statistically significant difference between plain and Vitamin E coated meshes (*p=0.004, n=12*). Error bars were calculated based on the standard deviation values.

Increased percentage of IC results in the formation of non-polymeric soluble collagen, which, according to the previous studies, can lead to the deterioration of biomechanical properties of abdominal wall [237].

5.4. Discussion

In 1958, Dr. Francis Usher introduced polyethylene for the reinforcement of hernia defects. This synthetic polymer provided several advantages over the metallic meshes, which were available at the time. The prospective evaluation of tissue repair versus mesh hernioplasty by Dr. Luijendijk and colleagues established an improved outcome in hernia repair with the use of synthetic mesh [238]. Over time, many different types of hernia repair mesh were introduced. Unfortunately, none of the hernia repair meshes is without disadvantages, resulting in a complication rate of approximately 30% [191]. Some of the complications, including chronic pain, tissue adhesion and recurrence, are closely related to oxidative stress. Recently, it was shown that antioxidants are highly effective against oxidative stress occurring during inflammation [211,212]. Thus, coating hernia repair meshes with antioxidant agents could be a useful strategy to reduce the rate of post-surgical complication [239]. In this part of the dissertation we focused on potential benefits of using vitamin E as a coating for hernia repair meshes to reduce host-tissue response following hernioplasty.

Vitamin E refers to a family of 8 tocopherols and tocotrienols, which have similar structure with different degree of methylation. These compounds are widely used antioxidants and known to possess pronounced anti-inflammatory properties [232]. α-tocopherol and γ-tocopherol are the two major forms of vitamin E in mammals. It was shown that these tocopherols possess the strongest anti-inflammatory properties in both animal and clinical studies [232,240]. Furthermore,

vitamin E has been successfully incorporated into implants, including titanium orthopedic implants, UHMWPE acetabular liners, breast implants, tympanostomy tubes and dialysis membranes[241–244].

Although all tocopherols are able to reduce inflammation, the mechanism of their anti-inflammatory action can vary. Studies conducted with α-tocopherol (α-T) showed that this compound is able to inhibit protein kinase C (PKC), which is responsible for activation and transcription of several pro-inflammatory molecules, such as IL-1β and cyclooxygenase [245]. Reduced PKC activity leads to the decreased phosphorylation of the NADPH oxidase subunit $p47^{phox}$, which, in turn, reduces the production of superoxide (O_2^-) in human monocytes and neutrophils [245]. Similarly, α-tocopherol was found to inhibit PKC in platelets leading to reduced cell aggregation [246]. Along with PKC, α-T down-regulates protein kinase B (Akt) [247], which is responsible for production of pro-inflammatory markers; Akt also controls a variety of downstream effectors, such as nuclear factor - κB (NFκB). This factor plays a crucial role in regulating the expression of various pro-inflammatory stimuli. It was demonstrated that α-T can drastically decrease the adhesion of various types of cells by inhibiting NFκB and, as a result, reducing the expression of several integrins such as CD11a, CD11b, and CD11c [248]. Thus, it can be expected that α-T possesses anti-adhesion properties, and such characteristics were in fact confirmed in the literature [249,250].

Taking into account all the background data along with vitamin E known safety record, it appears to be an excellent candidate for anti-inflammatory

coatings on hernia repair meshes. Slow release of poorly water-soluble vitamin E directly to the implant site could improve its ability to reduce host response to the implants.

In this work, a 3 x 3 cm piece of Prolene® mesh was coated with vitamin E and implanted in a rabbit model. Since 100 mg/ml vitamin E solution was initially used and binding yield of tocopherol was calculated to be ≈6 mg/in^2, the total dose of vitamin E adsorbed on the implant was ≈9 mg. According to the majority of the reports in the literature, tocopherols are typically administrated orally [232,240]. The therapeutic dose of vitamin E in a coating has not yet been established. However, Yetkin *et al.* [235] reported that intraperitoneal injection of 10 mg of vitamin E provides therapeutic effect in a rat hernia implant model. Assuming physiological concentration of vitamin E to be around 1 mg/dl [251], 9 mg of α-tocopherol introduced with the hernia repair implant in this study was expected to provide a reasonable local therapeutic dose, even assuming an incomplete (30%) release rate observed in a 10 day in vitro experiment.

The first 10 days following the surgery were identified as the most crucial period in terms of the long-lasting success of the implantation [235]. Therefore, the anti-inflammatory coating has to be stable, which requires that there is a sufficient amount of drug absorbed on the implant both during and after the ten-day period. Lack of stability is the major drawback of passive coatings, which reduces their efficacy when compared to active coatings [239]. The *in vitro* drug release profile for vitamin E-coated meshes showed that almost 70% of vitamin E remain

adsorbed on the mesh even after incubation in BSA solution for 10 days. Such a prolonged release rate is not unexpected since vitamin E is poorly soluble in water. These results indicate that α-tocopherol absorbed on the implant can potentially provide a prolonged release profile *in vivo*. Since oxidative stress is mostly caused by macrophages and neutrophils in the vicinity of the implant, prolonged drug release to the surrounding tissues is expected to suppress the inflammatory response and improve long-term outcomes of the surgery.

Elastic modulus and tensile strength of hernia repair meshes are of particular importance, since impaired mechanical properties can lead to mesh failure. Thus, we evaluated the effect of the coating on the mechanical properties of the meshes. According to the results of tensile testing, neither elastic modulus nor tensile strength of the implants were affected by the presence of vitamin E coating.

As the purpose of this research was to compare the tissue response to plain and α-tocopherol - coated meshes, histopathological analysis was of particular importance. Both implants demonstrated significantly different host response. The plain implant appeared to induce greater inflammatory response, as indicated by the larger number of macrophages infiltrating mesh-tissue interface. At the same time, there was no significant difference in FBGC response between the two implants.

Compared to vitamin E-coated mesh, the plain sample contained more fatty infiltrates, which correlates with enhanced connective tissue deposition and poor implant biocompatibility [252]. Also, a significantly higher level of

neovascularization was found around the plain mesh. On the one hand, adequate neovascularization indicates normal tissue integration and good biocompatibility of an implant, which is beneficial [253]. On the other hand, it was shown that excessive vascularization is often an indication of decreased biocompatibility [193]. Furthermore, increased neovascularization can be caused by an excessive host tissue response due to elevated level of vascular endothelial growth factor [254].

The uncoated implant was surrounded by heavier fibrosis and collagen encapsulation when compared to the vitamin E-coated mesh. According to the literature, highly organized collagen and heavy fibrosis encompassing hernia meshes are undesirable since it may lead to implant shrinkage and could also be correlated with the incidence of adhesions [64,255].

Analysis of the collagen framework at the surgical site was of particular interest since biomechanical strength in wound tissue, in many ways, is defined by collagen architecture and organization. After the first incision is made, fibroblasts that are recruited to the injury site begin secreting procollagen, which has high levels of lysine and proline. These amino acids, upon hydroxylation, are converted to hydroxylysine and hydroxyproline, which facilitate the transition of procollagen to tropocollagen. Collagen forms when several tropocollagen molecules become aligned and strong cross-links are created, increasing the tensile strength of the entire structure. When the maturation phase of healing begins, these immature collagen fibers are aligned towards tension lines, become thicker and more

compact, and the stability of the framework drastically increases, forming mature collagen. There are many factors, which may compromise fibrillogenesis, for instance cigarette smoking, genetic influence or activity of macrophages and neutrophils during acute phase of inflammation [237]. These aspects can alter the IC to MC ratio, increasing the percentage of disorganized collagen fibers, which may result in the formation of non-polymeric soluble collagen. This results in a deterioration of the biomechanical properties of the *transversus abdominus aponeurosis*. D. DuBay *et al.* [256] showed that it can lead to the decrease of abdominal wall compliance, as well as unequal distribution of pressure inside the abdominal cavity. In this study, an increased content of IC in the vicinity of the plain mesh was observed compared to the vitamin E-coated mesh. The observed effect can be closely related to the reduced inflammatory response associated with the implantation of modified hernia repair mesh. Based on the discussion above, higher MC/IC ratio could be beneficial and is expected to reduce the incidence rate of post-surgical complications.

Study described in this chapter has several limitations. The most important one is that only a single-animal pilot experiment was conducted. Although we showed indications that Vitamin E-coated mesh improves wound healing process following hernioplasty, single animal experiments cannot provide enough statistical data to support the claim. Multiple animal experiments are required to provide meaningful relationships among Vitamin E coating and host-body response.

Therefore, we conducted 5-animal experiment according to the protocol described in sec. 5.2.2, 5.2.5-5.2.8.

We used H&E staining to evaluate macrophage response towards the plain and Vitamin E-coated meshes. One-way ANOVA was used for statistical analysis of the obtained data. Mean values of the macrophage count obtained for each animal were treated as independent and used for the comparison of Vitamin E-coated and plain meshes. The results are shown in table 5.5.

Table 5.5. Macrophage response towards the studied meshes as assessed in the 5-animal experiment

Number of cells per high powered (400 x) field						
	Plain		Coated		N	P-value
	Mean	St.dev.	Mean	St.dev.		
1 rabbit	31	5	22	4	6	0.023
2 rabbit	23	4	17	3	6	0.015
3 rabbit	37	4	31	5	6	0.045
4 rabbit	48	5	31	5	6	0.0001
5 rabbit	28	5	21	3	6	0.018
Average	32	9	25	6	5	0.015

When compared with the plain mesh, a significant drop in the number of macrophages around the Vitamin E-coated mesh was observed ($p = 0.015$, $n=5$). These results are indicative of the reduced inflammatory response towards Vitamin E-coated meshes.

H&E and Masson's stainings were used to characterize newly-formed tissues in the vicinity of the implanted meshes. Semi-quantitative characterization of neovascularization, fatty infiltrates and collagen organization was conducted by an experienced histologist in a double-blinded manner according to the grading rubric provided in sec. 5.2.5. (table 5.1). The results are demonstrated in table 5.6.

Table 5.6. Semi-quantitative histological assessment of the tissue surrounding plain and Vitamin E coated meshes as assessed in the 5-animal experiment

Parameter		Histological score				N	P-value
		Plain		Coated			
		Mean	St.dev.	Mean	St.dev.		
Collagen organization	1 rabbit	2.3	0.3	1.8	0.2	6	0.04
	2 rabbit	2.6	0.3	2.1	0.1	6	0.03
	3 rabbit	2.3	0.3	2.0	0.1	6	0.09
	4 rabbit	2.2	0.3	1.8	0.3	6	0.02
	5 rabbit	2.6	0.6	1.9	0.3	6	0.03
	Average	2.3	0.3	1.9	0.2	5	0.02
Neo-vascularization	1 rabbit	2.1	0.5	1.7	0.3	6	0.021
	2 rabbit	2.4	0.3	1.7	0.2	6	0.031
	3 rabbit	2.3	0.4	1.8	0.3	6	0.022
	4 rabbit	2.0	0.3	1.7	0.2	6	0.033
	5 rabbit	2.4	0.4	1.9	0.4	6	0.021
	Average	2.2	0.3	1.7	0.2	5	0.015
Fatty infiltrates	1 rabbit	2.3	0.3	1.6	0.2	6	0.04
	2 rabbit	2.5	0.6	1.7	0.3	6	0.047
	3 rabbit	2.5	0.3	2	0.3	6	0.075
	4 rabbit	2.2	0.3	1.6	0.2	6	0.02
	5 rabbit	2.5	0.5	2.1	0.4	6	0.33
	Average	2.4	0.3	1.8	0.3	5	0.01

It is important to underline that for the rabbit #3 there was no significant difference ($p>0.05$, $n=6$) in terms of fatty infiltrates and collagen organization when comparing plain and Vitamin E-coated meshes. However, when comparing all 5 animals, there was a significant difference in case of all 3 histological parameters assessed in this part of the study. Vitamin E-coated mesh was found to be surrounded by tissues with a significantly lower degree of collagen organization when compared with the plain mesh. Moreover, significantly higher levels of neovascularization and fatty infiltrates were observed in the vicinity of the plain mesh as compared with the Vitamin E-coated implant. As discussed above, these effects are indicatives of an improved healing process in the case of Vitamin E-

coated mesh. Therefore, results of the 5-animal experiment are in good agreement with those of a single-animal experiment discussed above. At the same time, addition studies are required to support the claim that Vitamin E coating affects collagen architecture and decreases fibrotic response following hernioplasty.

5.5. Conclusions

In conclusion, Vitamin E-coated hernia repair meshes were produced, and their performance was evaluated *in vitro* and *in vivo*. It was found that use of an α-tocopherol - coated mesh reduced the inflammatory response when compared to a plain polypropylene implant. Subsequently, the reduced inflammatory response positively affected the healing process. Thus, data obtained herein serve as a foundation for further animal and clinical studies of tocopherol – coated hernia repair meshes.

CHAPTER 6

CONCLUSIONS AND RECOMMENDATIONS FOR FUTURE STUDIES

Over the past decades, many strategies to address the high incidence rate of postoperative complications related to medical implants have been developed. However, despite recent progress, post-surgical complications continue to be an important problem. In the present dissertation, we focused on developing novel, more effective approaches to prevent and treat common complications. In particular, the scope of this study was concentrated on the infections following orthopaedic surgeries, as well as chronic pain after hernia repair surgeries.

The first part of this work was focused on the prevention and treatment of orthopaedic implant–associated infections. Here, Kirchner wires were chosen as a model orthopaedic implant, as K-wiring procedures are often associated with a high incidence rate of infections. We proposed to coat the wires with a monolaurin – compound with the pronounced antibacterial activity against various pathogens. Comprehensive antibacterial studies showed excellent antimicrobial activity of the monolaurin coating against MRSA, MSSA and *S. epidermidis*—three pathogens that account for more than 80% of pin-site infections. At the same time, monolaurin coating exhibited little to no cytotoxicity to osteoblasts and excellent biocompatibility, which was shown to be the Achilles' heel of many antimicrobial agents currently used. Taking into account the obtained results, the approach proposed in this work can have a huge potential in orthopaedic applications.

At the same time, additional cell culture studies are required to fully evaluate the biocompatibility of the monolaurin coating. When implanted, K-wires are in contact with osteoblasts, fibroblasts and epithelial cells. Therefore, studies with epithelial cells and fibroblasts are necessary to assess the potential cytotoxicity of the monolaurin coating. Besides that, future studies should focus on three aspects: 1) drug loading increase; 2) the control of drug release kinetics; 3) the increase of the mechanical stability of the coating. The latter objective is particularly important, since many orthopaedic implant are exposed to the high shear stress during implantation. Thereby, the coating should be mechanical robust to withstand high shear stress. This can be done by incorporating therapeutic compounds into a polymeric matrix. Moreover, this approach promises the control over drug release kinetics, as well as the optimization of drug loading. Finally, animal studies are necessary to evaluate the antibacterial activity of the monolaurin coated K-wires, as well as the foreign body response towards the modified implants.

In the second part of the dissertation we addressed the incidence of postoperative chronic pain following hernia repair surgeries. We focused on the susceptibility of polymeric hernia meshes to the oxidative stress. Here, Composix™ and UltraPro® meshes were analyzed. In order to mimic natural body response to foreign objects we used two model systems that simulate the effect of reactive oxygen species and myeloperoxidase on hernia repair meshes. We showed these treatments cause substantial alterations of chemical, structural and physical properties of the meshes. For instance, mesh stiffening was observed.

We believe that this is due to the formation of various types of cross-links between polymer chains. Moreover, we have shown that Composix™ meshes are more susceptible to reactive oxygen species and hypochlorite anions when compared with UltraPro® implants, which is in a good agreement with clinical observations. This supports the predictive power of the model systems used in this study.

Future studies should focus on two major objectives: 1) additional physicochemical characterization of the treated meshes; and 2) analysis of the most widely used hernia repair meshes. The former objective is important for supporting the proposed mechanism of hernia mesh deterioration. In particularly, more detailed quantitative study of mesh surface composition should be conducted by means of high-resolution XPS. This allows accurate evaluation of the chemical groups that are introduced due to the oxidative stress. Moreover, additional mechanical measurements should be conducted. In the present work, we analyzed mesh stiffness using conventional tensile testing. However, this test does not expose meshes to the physiologically relevant types of mechanical loading. Future studies should involve ball burst testing, which was shown to better mimic *in vivo* loadings applied to hernia repair meshes [224]. Furthermore, environmental stress cracking experiments can provide a better insight on the mechanism of hernia mesh degradation. In the present work, meshes were not exposed to the mechanical stress while treated in the oxidative media. Future studies should assess the synergetic effect of statistic/dynamic mechanical loadings and oxidative insult. In addition, the analysis of a broad range of hernia repair meshes available

on the market should be performed using the methodology proposed in this work. The goal of this experiments is to rank hernia repair implants according to their susceptibility to oxidative stress. This will provide useful information for surgeons in selecting the appropriate implants for hernia repair surgeries.

The third part of the study focused on the mitigation of inflammation following hernia repair surgeries. We proposed to modify polypropylene hernia repair meshes with a Vitamin E-coating. A pilot animal study was conducted to evaluate the efficacy of the proposed approach. Based on the histopathological analysis, we observed that α-tocopherol-coated mesh induced less inflammatory response when compared to the plain implant. Therefore, the Vitamin E-coating positively affected the wound healing process, potentially improving the outcomes of hernia repair surgery.

Future studies should involve the analysis of the effect of Vitamin E coating on collagen architecture and fibrin content in the newly-formed tissues. Moreover, additional animal studies are required to assess the short- and long-term effects of a Vitamin E-coating. In the present study, we evaluated host-tissue response 5 weeks after the surgery. The effect of Vitamin E on an acute inflammatory response should also be assessed. This is generally done by explanting meshes within a few days after the initial surgery, and conducting histological evaluations. Moreover, long-term integration of the modified meshes and the presence of chronic inflammation should be evaluated by explanting the samples 6 months after the surgery.

Vitamin E coating was shown to positively affect the healing process by reducing the inflammatory response. At the same time, mitigation of the body's inflammatory response can potentially make Vitamin E-coated meshes more susceptible to postoperative infections. Therefore, animal studies employing bacteria-challenged models are necessary to evaluate the potential effect of Vitamin E coating on the infection incidence rate.

REFERENCES

[1] M.E. Falagas, G.C. Makris, Mesh-related infections after hernia repair, Hernia Repair Sequelae. (2010) 97–102.

[2] S. Nienhuijs, E. Staal, L. Strobbe, C. Rosman, H. Groenewoud, R. Bleichrodt, Chronic pain after mesh repair of inguinal hernia: a systematic review, Am. J. Surg. 194 (2007) 394–400.

[3] H. Sharma, G.R. Taylor, N.M.P. Clarke, A review of K-wire related complications in the emergency management of paediatric upper extremity trauma, Ann. R. Coll. Surg. Engl. 89 (2007) 252–258.

[4] N. Ferreira, L.C. Marais, Prevention and management of external fixator pin track sepsis, Strateg. Trauma Limb Reconstr. 7 (2012) 67–72.

[5] T. Jennison, M. McNally, H. Pandit, Prevention of infection in external fixator pin sites, Acta Biomater. 10 (2014) 595–603.

[6] M. Murray, J. Pizzorno, L. Pizzorno, The Encyclopedia of Healing Foods, New York, 2005.

[7] E.A. Mueller, P.M. Schlievert, Non-aqueous glycerol monolaurate gel exhibits antibacterial and anti-biofilm activity against gram-positive and gram-negative pathogens, PLoS One. 10 (2015) 1–12.

[8] U. Klinge, B. Klosterhalfen, A. P. Ottinger, K. Junge, V. Schumpelick, PVDF as a new polymer for the construction of surgical meshes., Biomaterials. 23 (2002) 3487–93.

[9] M.J. Cozad, D. A. Grant, S.L. Bachman, D.N. Grant, B.J. Ramshaw, S.

Grant, Materials characterization of explanted polypropylene, polyethylene terephthalate, and expanded polytetrafluoroethylene composites: spectral and thermal analysis, J. Biomed. Mater. Res. Part B Appl. Biomater. 94B (2010) 455–462.

[10] D.J. Hackett, A.C. Rothenberg, A.F. Chen, C. Gutowski, D. Jaekel, I.M. Tomek, B.S. Parsley, P. Ducheyne, P. a Manner, The Economic Significance of Orthopaedic Infections, J. Am. Acad. Orthop. Surg. 23 (2015) 1–7.

[11] B.H. Kapadia, R.A. Berg, J.A. Daley, J. Fritz, A. Bhave, M.A. Mont, Periprosthetic joint infection, Lancet. 387 (2016) 386–394.

[12] N.J. Hickok, I.M. Shapiro, Immobilized antibiotics to prevent orthopaedic implant infections, Adv. Drug Deliv. Rev. 64 (2012) 1165–1176.

[13] T. Bhattacharyya, R. Iorio, W.L. Healy, Rate of and risk factors for acute inpatient mortality after orthopaedic surgery., J. Bone Joint Surg. Am. 84–A (2002) 562–72.

[14] I. Collins, J. Wilson-MacDonald, G. Chami, W. Burgoyne, P. Vineyakam, T. Berendt, J. Fairbank, The diagnosis and management of infection following instrumented spinal fusion, Eur. Spine J. 17 (2008) 445–450.

[15] L. Pulido, E. Ghanem, A. Joshi, J.J. Purtill, J. Parvizi, Periprosthetic joint infection: The incidence, timing, and predisposing factors, Clin. Orthop. Relat. Res. 466 (2008) 1710–1715.

[16] S. Ahmed, S. Meghji, R.J. Williams, B. Henderson, J.H. Brock, S.P. Nair, Staphylococcus aureus fibronectin binding proteins are essential for

internalization by osteoblasts but do not account for differences in intracellular levels of bacteria, Infect. Immun. 69 (2001) 2872–2877.

[17] V.K. Aggarwal, H. Bakhshi, N.U. nter Ecker, J. Parvizi, T. Gehrke, D. Kendoff, Organism profile in periprosthetic joint infection: pathogens differ at two arthroplasty infection referral centers in Europe and in the United States, J. Knee Surg. 27 (2014) 399–406.

[18] T.E. Callahan, W.P. Schecter, J.K. Horn, Necrotizing soft tissue infection masquerading as cutaneous abcess following illicit drug injection., Arch. Surg. 133 (1998) 812-7-9.

[19] J. Parvizi, I.M. Pawasarat, K.A. Azzam, A. Joshi, E.N. Hansen, K.J. Bozic, Periprosthetic joint infection: The economic impact of methicillin-resistant infections, J. Arthroplasty. 25 (2010) 103–107.

[20] D. Gil, S. Shuvaev, A. Frank-Kamenetskii, V. Reukov, C. Gross, A. Vertegel, Novel Antibacterial Coating on Orthopedic Wires To Eliminate Pin Tract Infections, 61 (2017) 1–14.

[21] C. Toulson, S. Walcott-Sapp, J. Hur, E. Salvati, M. Bostrom, B. Brause, G.H. Westrich, Treatment of Infected Total Hip Arthroplasty With a 2-Stage Reimplantation Protocol. Update on “Our Institution’s” Experience From 1989 to 2003, J. Arthroplasty. 24 (2009) 1051–1060.

[22] C.E. Edmiston, O. Okoli, M.B. Graham, S. Sinski, G.R. Seabrook, Evidence for Using Chlorhexidine Gluconate Preoperative Cleansing to Reduce the

[23] B. AlBuhairan, D. Hind, a Hutchinson, Antibiotic prophylaxis for wound

infections in total joint arthroplasty: a systematic review., J. Bone Joint Surg. Br. 90 (2008) 915–919.

[24] N.M. Brown, C.A. Cipriano, M. Moric, S.M. Sporer, C.J. Della Valle, Dilute Betadine Lavage Before Closure for the Prevention of Acute Postoperative Deep Periprosthetic Joint Infection, J. Arthroplasty. 27 (2012) 27–30.

[25] B.H. Kapadia, R. Pivec, A.J. Johnson, K. Issa, Q. Naziri, J.A. Daley, M.A. Mont, Infection prevention methodologies for lower extremity total joint arthroplasty, Expert Rev. Med. Devices. 10 (2013) 215–224.

[26] A. Bistolfi, G. Massazza, E. Verné, A. Massè, D. Deledda, S. Ferraris, M. Miola, F. Galetto, M. Crova, Antibiotic-loaded cement in orthopedic surgery: a review., ISRN Orthop. 2011 (2011) 290851.

[27] C.P. Scott, P.A. Higham, J.H. Dumbleton, Effectiveness of bone cement containing tobramycin in an vitro susceptibility study of 99 organisms found in infected joint arthroplasty, J Bone Jt. Surg [Br]. 81 (1999) 440–3.

[28] E.S. Zhu, G.R. Thompson, C. Kreulen, E. Giza, Amphotericin B-impregnated bone cement to treat refractory coccidioidal osteomyelitis, Antimicrob. Agents Chemother. 57 (2013) 6341–6343.

[29] C.S. Adams, V. Antoci, G. Harrison, P. Patal, T.A. Freeman, I.M. Shapiro, J. Parvizi, N.J. Hickok, S. Radin, P. Ducheyne, Controlled release of vancomycin from thin sol-gel films on implant surfaces successfully controls osteomyelitis, J. Orthop. Res. 27 (2009) 701–709.

[30] V. Antoci, C.S. Adams, N.J. Hickok, I.M. Shapiro, J. Parvizi, Vancomycin

bound to Ti rods reduces periprosthetic infection: preliminary study., Clin. Orthop. Relat. Res. 461 (2007) 88–95.

[31] C. Ketonis, C.S. Adams, S. Barr, A. Aiyer, I.M. Shapiro, J. Parvizi, N.J. Hickok, Antibiotic modification of native grafts: improving upon nature's scaffolds., Tissue Eng. Part A. 16 (2010) 2041–2049.

[32] C.P. Chen, E. Wickstrom, Self-protecting bactericidal titanium alloy surface formed by covalent bonding of daptomycin bisphosphonates, Bioconjug. Chem. 21 (2010) 1978–1986.

[33] J.A. Lyndon, B.J. Boyd, N. Birbilis, Metallic implant drug/device combinations for controlled drug release in orthopaedic applications, J. Control. Release. 179 (2014) 63–75.

[34] W.H. Kim, S.B. Lee, K.T. Oh, S.K. Moon, K.M. Kim, K.N. Kim, The release behavior of CHX from polymer-coated titanium surfaces, Surf. Interface Anal. 40 (2008) 202–204.

[35] J.S. Suwandi, R.E.M. Toes, T. Nikolic, B.O. Roep, Inducing tissue specific tolerance in autoimmune disease with tolerogenic dendritic cells, Clin. Exp. Rheumatol. 33 (2015) 97–103.

[36] S.C. Von Plocki, D. Armbruster, K. Klein, K. Kämpf, K. Zlinszky, M. Hilbe, P. Kronen, E. Gruskin, B. Von Rechenberg, Biodegradable Sleeves for Metal Implants to Prevent Implant-Associated Infection: An Experimental In Vivo Study in Sheep, Vet. Surg. 41 (2012) 410–421. doi:10.1111/j.1532-950X.2011.00943.x.

[37] H. Gollwitzer, K. Ibrahim, H. Meyer, W. Mittelmeier, R. Busch, A. Stemberger, Antibacterial poly(D,L-lactic acid) coating of medical implants using a biodegradable drug delivery technology, J. Antimicrob. Chemother. 51 (2003) 585–591. doi:10.1093/jac/dkg105.

[38] M. Miranda, A. Fernández, S. Lopez-Esteban, F. Malpartida, J.S. Moya, R. Torrecillas, Ceramic/metal biocidal nanocomposites for bone-related applications, J. Mater. Sci. Mater. Med. 23 (2012) 1655–1662.

[39] M. Stigter, J. Bezemer, K. De Groot, P. Layrolle, Incorporation of different antibiotics into carbonated hydroxyapatite coatings on titanium implants, release and antibiotic efficacy, J. Control. Release. 99 (2004) 127–137.

[40] V. Alt, A. Bitschnau, J. Österling, A. Sewing, C. Meyer, R. Kraus, S.A. Meissner, S. Wenisch, E. Domann, R. Schnettler, The effects of combined gentamicin-hydroxyapatite coating for cementless joint prostheses on the reduction of infection rates in a rabbit infection prophylaxis model, Biomaterials. 27 (2006) 4627–4634.

[41] J. Gallo, M. Holinka, C.S. Moucha, Antibacterial surface treatment for orthopaedic implants, 2014.

[42] C. Rungsiyakull, Q. Li, G. Sun, W. Li, M. V. Swain, Surface morphology optimization for osseointegration of coated implants, Biomaterials. 31 (2010) 7196–7204.

[43] L. Nyhus, R. Condon, Hernia, 1995.

[44] W. Halsted, Surgical papers by William Stewart Halsted: the operative

treatment of inguinal hernia, John Hopkins Press, 1924.

[45] A. Lyons, R. Petrucelli, Medicine: an illustrated history, Harry N Abrams Publishers, New York, 1987.

[46] Hippocratic Writings. Edited with an introduction by GER Lloyd, Penguin Books, New York, 1983.

[47] R.A. Leonardo, History of surgery, Froben Press, New York, 1943.

[48] G. Campanelli, M. Canziani, F. Frattini, M. Cavalli, S. Agrusti, Inguinal hernia: State of the art, Int. J. Surg. 6 (2008) S26–S28.

[49] A. Pare, The apologie and treatise: containing the voyages made into divers places many of his writings upon surgery, Falcon Educational Books, London, 1951.

[50] R. Read, The centenary of Bassini's contribution to inguinal herniorrhaphy, Am. J. Surg. 153 (1987) 324.

[51] H. Cushing, The Employment of Local Anaesthesia in the Radical Cure of Certain Cases of Hernia, with a Note upon the Nervous Anatomy of the Inguinal Region., Ann. Surg. 31 (1900) 1–34.

[52] O.J. Usher F., Use of marlex mesh in the repair of incisional hernias, Am. Surg. 24 (1958) 969–974.

[53] R.C. Read, The contributions of Usher and others to the elimination of tension from groin herniorrhaphy, Hernia. (2005) 208–211.

[54] R. Bendavid, Abdominal wall hernias: principles and methods, New York, 2001.

[55] E. Aasvang, H. Kehlet, Chronic postoperative pain: the case of inguinal herniorrhaphy, Br. J. Anaesth. 95 (2005) 69–76.

[56] C.J. Filipi, Laparoscopic hiatal hernia repair: why they fail, Hernia. 4 (2000) 219–222.

[57] Retrieved on 8/30/2017 from http://www.scottishhernia.com/hernia_symptoms.html

[58] N.A. Henriksen, Systemic and local collagen turnover in hernia patients, Dan. Med. J. 63 (2016) 1–20.

[59] P.L. Jansen, P.R. Mertens, U. Klinge, V. Schumpelick, The biology of hernia formation, Surgery. 136 (2004) 1–4.

[60] D.R. Flum, K. Horvath, T. Koepsell, Have outcomes of incisional hernia repair improved with time? A population-based analysis., Ann. Surg. 237 (2003) 129–135.

[61] J. Höer, G. Lawong, U. Klinge, V. Schumpelick, Factors influencing the development of incisional hernia. A retrospective study of 2,983 laparotomy patients over a period of 10 years, Der Chir. 73 (2002) 474–480.

[62] N. a Henriksen, J.H. Mortensen, L.T. Sorensen, A.C. Bay-Jensen, M.S. Ågren, L.N. Jorgensen, M. a Karsdal, The collagen turnover profile is altered in patients with inguinal and incisional hernia., Surgery. 157 (2015) 312–21.

[63] A.B. Casanova, E.N. Trindade, M.R.M. Trindade, Collagen in the transversalis fascia of patients with indirect inguinal hernia: a case-control study, Am. J. Surg. 198 (2009) 1–5.

[64] Y.W. Novitsky, A.G. Harrell, J. a Cristiano, B.L. Paton, H.J. Norton, R.D. Peindl, K.W. Kercher, B.T. Heniford, Comparative evaluation of adhesion formation, strength of ingrowth, and textile properties of prosthetic meshes after long-term intra-abdominal implantation in a rabbit., J. Surg. Res. 140 (2007) 6–11.

[65] F. García-Moreno, P. Pérez-López, S. Sotomayor, B. Pérez-Köhler, Y. Bayon, G. Pascual, J.M. Bellón, Comparing the host tissue response and peritoneal behavior of composite meshes used for ventral hernia repair., J. Surg. Res. 193 (2015) 470–82.

[66] P. Wagh, A. Leverich, C. Sun, H. White, R. Read, Direct Inguinal Herniation in Men: A disease of Collagen, J. Surg. Res. 433 (1974) 435–433.

[67] P. V. Wagh, R.C. Read, Defective collagen synthesis in inguinal herniation, Am. J. Surg. 124 (1972) 819–822.

[68] K. Junge, U. Klinge, R. Rosch, P.R. Mertens, J. Kirch, B. Klosterhalfen, P. Lynen, V. Schumpelick, Decreased collagen type I/III ratio in patients with recurring hernia after implantation of alloplastic prostheses, Langenbeck's Arch. Surg. 389 (2004) 17–22.

[69] J.M. Bellón, A. Bajo, N. Ga-Honduvilla, M.J. Gimeno, G. Pascual, A. Guerrero, J. Buján, Fibroblasts from the transversalis fascia of young patients with direct inguinal hernias show constitutive MMP-2 overexpression., Ann. Surg. 233 (2001) 287–91.

[70] V. Jain, R. Srivastava, S. Jha, M. Misra, N. Rawat, D. Amla, Study of Matrix

Metalloproteinase-2 in Inguinal Hernia, J. Clin. Med. Res. 1 (2009) 285–289.

[71] H. Zheng, Z. Si, R. Kasperk, R.S. Bhardwaj, V. Schumpelick, U. Klinge, B. Klosterhalfen, Recurrent inguinal hernia: Disease of the collagen matrix?, World J. Surg. 26 (2002) 401–408.

[72] G.A. Antoniou, I.K. Tentes, S.A. Antoniou, C. Simopoulos, M.K. Lazarides, Matrix Metalloproteinase Imbalance in Inguinal Hernia Formation, J. Investig. Surg. 24 (2011) 145–150.

[73] A. Kingsnorth, K. LeBlanc, Hernias: Inguinal and incisional, Lancet. 362 (2003) 1561–1571.

[74] A. Anitha, K. Babu, S. Ballal, M. Vankalakunti, V. Siddini, R. Bonu, Type III collagen disorders: A case report and review of literature, Indian J. Pathol. Microbiol. 0 (2016) 0.

[75] C.N. Brown, J.G. Finch, Which mesh for hernia repair?, Ann. R. Coll. Surg. Engl. 92 (2010) 272–278.

[76] U. Klinge, M. Binnebösel, R. Rosch, P. Mertens, Hernia recurrence as a problem of biology and collagen, J. Minim. Access Surg. 2 (2006) 151–154.

[77] H. Patel, D.R. Ostergard, G. Sternschuss, Polypropylene mesh and the host response, Int. Urogynecol. J. 23 (2012) 669–679.

[78] O. Guillaume, J.-P. Lavigne, O. Lefranc, B. Nottelet, J. Coudane, X. Garric, New antibiotic-eluting mesh used for soft tissue reinforcement., Acta Biomater. 7 (2011) 3390–7.

[79] C.R. Deeken, M.S. Abdo, M.M. Frisella, B.D. Matthews, Physicomechanical

evaluation of polypropylene, polyester, and polytetrafluoroethylene meshes for inguinal hernia repair., J. Am. Coll. Surg. 212 (2011) 68–79.

[80] R. Rosch, U. Klinge, Z. Si, K. Junge, B. Klosterhalfen, V. Schumpelick, A role for the collagen I/III and MMP-1/-13 genes in primary inguinal hernia?, BMC Med. Genet. 3 (2002) 2.

[81] U.K. Saarialho-Kere, Patterns of matrix metalloproteinase and TIMP expression in chronic ulcers., Arch. Dermatol. Res. 290 Suppl (1998) S47-54.

[82] P. Lynen Jansen, U. Klinge, P.R. Mertens, Hernia disease and collagen gene regulation: Are there clues for intervention?, Hernia. 10 (2006) 486–

[83] K. Junge, M. Binnebösel, K.T. Von Trotha, R. Rosch, U. Klinge, U.P. Neumann, P.L. Jansen, Mesh biocompatibility: Effects of cellular inflammation and tissue remodelling, Langenbeck's Arch. Surg. 397 (2012) 255–270.

[84] Y. Bilsel, I. Abci, The search for ideal hernia repair; mesh materials and types., Int. J. Surg. 10 (2012) 317–21.

[85] S.P. Lake, S. Ray, A.M. Zihni, D.M. Thompson, J. Gluckstein, C.R. Deeken, Pore size and pore shape-but not mesh density-alter the mechanical strength of tissue ingrowth and host tissue response to synthetic mesh materials in a porcine model of ventral hernia repair, J. Mech. Behav. Biomed. Mater. 42 (2015) 186–97.

[86] W.S. Cobb, K.W. Kercher, B.T. Heniford, The argument for lightweight

polypropylene mesh in hernia repair., Surg. Innov. 12 (2005) 63–69.

[87] U. Klinge, Mesh for hernia repair, Br. J. Surg. 95 (2008) 539–540.

[88] S. Post, B. Weiss, M. Willer, T. Neufang, D. Lorenz, Randomized clinical trial of lightweight composite mesh for Lichtenstein inguinal hernia repair, Br. J. Surg. 91 (2004) 44–48.

[89] P.J. O'Dwyer, A.N. Kingsnorth, R.G. Molloy, P.K. Small, B. Lammers, G. Horeyseck, Randomized clinical trial assessing impact of a lightweight or heavyweight mesh on chronic pain after inguinal hernia repair, Br. J. Surg. 92 (2005) 166–170.

[90] S. Hasegawa, T. Yoshikawa, Y. Yamamoto, N. Ishiwa, S. Morinaga, Y. Noguchi, H. Ito, N. Wada, K. Inui, T. Imada, Y. Rino, Y. Takanashi, Long-term outcome after hernia repair with the Prolene Hernia System, Surg. Today. 36 (2006) 1058–1062.

[91] P.J. Emans, M.H.F. Schreinemacher, M.J.J. Gijbels, G.L. Beets, J.W.M. Greve, L.H. Koole, N.D. Bouvy, Polypropylene meshes to prevent abdominal herniation. Can stable coatings prevent adhesions in the long term?, Ann. Biomed. Eng. 37 (2009) 410–418.

[92] S. Bringman, S. Wollert, J. Österberg, S. Smedberg, H. Granlund, T.J. Heikkinen, Three-year results of a randomized clinical trial of lightweight or standard polypropylene mesh in Lichtenstein repair of primary inguinal hernia, Br. J. Surg. 93 (2006) 1056–1059.

[93] D. Gil, J. Rex, W. Cobb, V. Reukov, A. Vertegel, Anti-inflammatory coatings

of hernia repair meshes: A pilot study, J. Biomed. Mater. Res. - Part B Appl. Biomater. (2017) 1–9.

[94] S.F. Thames, J.B. White, K.L. Ong, The myth : in vivo degradation of polypropylene-based meshes, Int. Urogynecol. J. (2016).

[95] R. Gonzalez, K. Fugate, D. McClusky, E.M. Ritter, A. Lederman, D. Dillehay, C.D. Smith, B.J. Ramshaw, Relationship between tissue ingrowth and mesh contraction, World J. Surg. 29 (2005) 1038–1043.

[96] G.J. Morris-Stiff, L.E. Hughes, The outcomes of nonabsorbable mesh placed within the abdominal cavity: Literature review and clinical experience, J. Am. Coll. Surg. 186 (1998) 352–367.

[97] G. Riepe, J. Loos, H. Imig, A. Schroder, E. Schneider, J. Petermann, A. Rogge, M. Ludwig, A. Schenke, R. Nassutt, N. Chakfe, M. Morlock, Long-term in vivo alterations of polyester vascular grafts in humans, Eur. J. Vasc. Endovasc. Surg. 13 (1997) 540–548.

[98] R. Simmermacher, B. van der Lei, J. Schakenraad, R. Bleichrodt, Improved tissue in growth and anchorage of expanded polytetrafluoroethylene by perforation: an experimental study in the rat, Biomaterials. 12 (1991) 22–24.

[99] R.L.P. Romao, A. Nasr, P.P.L. Chiu, J.C. Langer, What is the best prosthetic material for patch repair of congenital diaphragmatic hernia? Comparison and meta-analysis of porcine small intestinal submucosa and polytetrafluoroethylene, J. Pediatr. Surg. 47 (2012) 1496–1500.

[100] D.L. Sanders, A.N. Kingsnorth, Prosthetic mesh materials used in hernia

surgery, Expert Rev. Med. Devices. 9 (2012) 159–179.

[101] J.M. Bellón, A. García-Carranza, N. García-Honduvilla, A. Carrera-San Martín, J. Buján, Tissue integration and biomechanical behaviour of contaminated experimental polypropylene and expanded polytetrafluoroethylene implants, Br. J. Surg. 91 (2004) 489–494.

[102] K. Junge, U. Klinge, R. Rosch, P. Lynen, M. Binnebösel, J. Conze, P.R. Mertens, R. Schwab, V. Schumpelick, Improved collagen type I/III ratio at the interface of gentamicin- supplemented polyvinylidenfluoride mesh materials, Langenbeck's Arch. Surg. 392 (2007) 465–471.

[103] D. Berger, M. Bientzle, Polyvinylidene fluoride: A suitable mesh material for laparoscopic incisional and parastomal hernia repair!, Hernia. 13 (2009) 167–172.

[104] R.H. Fortelny, A.H. Petter-Puchner, K.S. Glaser, F. Offner, T. Benesch, M. Rohr, Adverse effects of polyvinylidene fluoride-coated polypropylene mesh used for laparoscopic intraperitoneal onlay repair of incisional hernia, Br. J. Surg. 97 (2010) 1140–1145.

[105] C.F. Bellows, A. Smith, J. Malsbury, W.S. Helton, Repair of incisional hernias with biological prosthesis: a systematic review of current evidence., Am. J. Surg. 205 (2013) 85–101.

[106] M. López Cano, M. Armengol Carrasco, M.T. Quiles Pérez, M.A. Arbós Vía, Biological Implants in Abdominal Wall Hernia Surgery, Cirugía Española (English Ed. 91 (2013) 217–223.

[107] D. Le, C.W. Deveney, N.L. Reaven, S.E. Funk, K.J. McGaughey, R.G. Martindale, Mesh choice in ventral hernia repair: so many choices, so little time., Am. J. Surg. 205 (2013) 602–607.

[108] N.J. Smart, M. Marshall, I.R. Daniels, Biological meshes: a review of their use in abdominal wall hernia repairs., Surgeon. 10 (2012) 159–71.

[109] D. Seker, H. Kulacoglu, Long-Term Complications of Mesh Repairs for Abdominal-Wall Hernias, J. Long. Term. Eff. Med. Implants. 21 (2011) 205–218.

[110] S.C. Lehr, A.L. Schuricht, A Minimally Invasive Approach For Treating Postoperative Seromas After Incisional Hernia Repair, J. Soc. Laparoendosc. Surg. (2001) 267–271.

[111] J.M. Bellón, L.A. Contreras, C. Sabater, J. Buján, Pathologic and clinical aspects of repair of large incisional hernias after implant of a polytetrafluoroethylene prosthesis, World J. Surg. 21 (1997) 402–6.

[112] E. Chrysos, E. Athanasakis, Z. Saridaki, A. Kafetzakis, O. Zoras, Surgical repair of incisional ventral hernias: Tension-free technique using prosthetic materials (expanded Polytetrafluoroethylene Gore-Tex Dual Mesh), J. Gastrointest. Surg. 8 (2004) 369–370.

[113] C. Brochhausen, V.H. Schmitt, T.K. Rajab, C.N.E. Planck, M. Wallwiener, H. Hierlemann, C.J. Kirkpatrick, Intraperitoneal adhesions — An ongoing challenge between biomedical engineering and the life sciences, J. Biomed. Mater. Res. Part A. 98A (2011) 143–156.

[114] S. Muller, T. Langø, R. Brekken, B. Ystgaard, Degree of adhesions after repair of incisional hernia, JSLS. 14 (2010) 399–404.

[115] F.E. Primus, H.W. Harris, A critical review of biologic mesh use in ventral hernia repairs under contaminated conditions., Hernia. 17 (2013) 21–30.

[116] O. Guillaume, A.H. Teuschl, S. Gruber-blum, R.H. Fortelny, H. Redl, A. Petter-puchner, Emerging Trends in Abdominal Wall Reinforcement : Bringing Bio-Functionality to Meshes, Adv. Healthc. Mater. (2015) 1763–1789.

[117] C.R. Costello, S.L. Bachman, B.J. Ramshaw, S.A. Grant, Materials characterization of explanted polypropylene hernia meshes, J. Biomed. Mater. Res. - Part B Appl. Biomater. 83 (2007) 44–49.

[118] A.C. Wang, L.Y. Lee, C.T. Lin, J.R. Chen, A histologic and immunohistochemical analysis of defective vaginal healing after continence taping procedures: A prospective case-controlled pilot study, Am. J. Obstet. Gynecol. 191 (2004) 1868–1874.

[119] H.F. Kucuk, H.E. Sikar, N. Kurt, H. Uzun, M. Eser, F. Tutal, Y. Tuncer, Lichtenstein or darn procedure in inguinal hernia repair: A prospective randomized comparative study, Hernia. 14 (2010) 357–360.

[120] J. Gillion, G. Begin, C. Marecos, G. Fourtanier, Expanded polytetrafluoroethylene patches used in the intraperitoneal or extraperitoneal position for repair of incisional hernias of the anterolateral abdominal wall, Am. J. Surg. 174 (1997) 16–19.

[121] B.R. Swenson, T.R. Camp, D.P. Mulloy, R.G. Sawyer, Antimicrobial-Impregnated Surgical Incise Drapes in the Prevention of Mesh Infection after Ventral Hernia Repair, 9 (2008).

[122] G.E. Leber, J.L. Garb, A.I. Alexander, W.P. Reed, Long-term complications associated with prosthetic repair of incisional hernias., Arch. Surg. 133 (1998) 378–382.

[123] B. Perez-Kohler, Y. Bayon, J.M. Bello, Mesh Infection and Hernia Repair: A Review, Surg. Infect. (Larchmt). 17 (2016) 124–137.

[124] W.S. Cobb IV, J.B. Harris, J.S. Lokey, E.S. Mcgill, K.L. Klove, Incisional herniorrhaphy with intraperitoneal composite mesh: A report of 95 cases, in: Am. Surg., 2003: pp. 784–787.

[125] S.G. Taylor, P.J. O'Dwyer, Chronic groin sepsis following tension-free inguinal hernioplasty, Br. J. Surg. 86 (1999) 562–565.

[126] A. Çakmak, Y. Çirpanli, E. Bilensoy, K. Yorganci, S. Çaliş, Z. Saribaş, V. Kaynaroğlu, Antibacterial activity of triclosan chitosan coated graft on hernia graft infection model, Int. J. Pharm. 381 (2009) 214–219.

[127] D. Kilic, C. Agalar, E. Ozturk, E.B. Denkbas, A. Cime, F. Agalar, Antimicrobial activity of cefazolin-impregnated mesh grafts, ANZ J. Surg. 77 (2007) 256–260.

[128] W.S. Cobb, B.L. Paton, Y.W. Novitsky, M.J. Rosen, K.W. Kercher, T.S. Kuwada, B.T. Heniford, Intra-abdominal placement of antimicrobial-impregnated mesh is associated with noninfectious fever, Am. Surg. 72

(2006) 1205–1208.

[129] J. Raphel, M. Holodniy, S.B. Goodman, S.C. Heilshorn, Multifunctional coatings to simultaneously promote osseointegration and prevent infection of orthopaedic implants, Biomaterials. 84 (2016) 301–314.

[130] R. Satishkumar, a a Vertegel, Antibody-directed targeting of lysostaphin adsorbed onto polylactide nanoparticles increases its antimicrobial activity against S. aureus in vitro., Nanotechnology. 22 (2011) 505103.

[131] Y. Yurko, K. McDeavitt, R.S. Kumar, T. Martin, A. Prabhu, A.E. Lincourt, A. Vertegel, B.T. Heniford, Antibacterial mesh: a novel technique involving naturally occurring cellular proteins., Surg. Innov. 19 (2012) 20–6.

[132] M. Fernandez-Gutierrez, E. Olivares, G. Pascual, J.M. Bellon, J. San Román, Low-density polypropylene meshes coated with resorbable and biocompatible hydrophilic polymers as controlled release agents of antibiotics., Acta Biomater. 9 (2013) 6006–18.

[133] C.J. Brandt, D. Kammer, A. Fiebeler, U. Klinge, Beneficial effects of hydrocortisone or spironolactone coating on foreign body response to mesh biomaterial in a mouse model, J. Biomed. Mater. Res. - Part A. 99 A (2011) 335–343.

[134] C. Hu, S. Liu, Y. Zhang, B. Li, H. Yang, C. Fan, W. Cui, Long-term drug release from electrospun fibers for in vivo inflammation prevention in the prevention of peritendinous adhesions, Acta Biomater. 9 (2013) 7381–7388.

[135] I. Kourtzelis, S. Rafail, R.A. DeAngelis, P.G. Foukas, D. Ricklin, J.D.

Lambris, Inhibition of biomaterial-induced complement activation attenuates the inflammatory host response to implantation, FASEB J. 27 (2013) 2768–

[136] M.E. Franklin, B.D. Matthews, The Benefits of Omega-3 Fatty Acid-Coated Mesh in Ventral Hernia Repair, 2010.

[137] C.Y. Kong, L.L. Lai, A. Yin, Y. Khoo, N.A. Rahman, K.F. Chin, Inflammatory reaction to fish oil coated polypropylene mesh used for laparoscopic incisional hernia repair: a case report, BMC Surg. (2016) 4–9.

[138] Retrieved on 8/30/2017 from https://hollislawfirm.com/case/hernia-mesh-lawsuit/cqur/

[139] M.T. Wolf, C.L. Dearth, C.A. Ranallo, S.T. LoPresti, L.E. Carey, K.A. Daly, B.N. Brown, S.F. Badylak, Macrophage polarization in response to ECM coated polypropylene mesh, Biomaterials. 35 (2014) 6838–6849.

[140] B. Du, Z. Bian, B. Xu, Skin health promotion effects of natural Beta-Glucan derived from cereals and microorganisms: A review, Phyther. Res. 28 (2014) 159–166.

[141] G. Champault, C. Barrat, Inguinal hernia repair with beta glucan-coated mesh: Results at two-year follow up, Hernia. 9 (2005) 125–130.

[142] M. Chen, P.O. Zamora, P. Som, L. a Peña, S. Osaki, Cell attachment and biocompatibility of polytetrafluoroethylene (PTFE) treated with glow-discharge plasma of mixed ammonia and oxygen., J. Biomater. Sci. Polym. Ed. 14 (2003) 917–935.

[143] A. Sannino, F. Conversano, A. Esposito, A. Maffezzoli, Polymeric meshes

for internal sutures with differentiated adhesion on the two sides, J. Mater. Sci. Mater. Med. 16 (2005) 289–296.

[144] H. Gerullis, E. Georgas, C. Eimer, C. Arndt, D. Barski, B. Lammers, B. Klosterhalfen, M. Borós, T. Otto, Coating with autologous plasma improves biocompatibility of mesh grafts in vitro: Development stage of a surgical innovation, Biomed Res. Int. 2013 (2013).

[145] N. Udpa, S.R. Iyer, R. Rajoria, K.E. Breyer, H. Valentine, B. Singh, S.P. McDonough, B.N. Brown, L.J. Bonassar, Y. Gao, Effects of Chitosan Coatings on Polypropylene Mesh for Implantation in a Rat Abdominal Wall Model, Tissue Eng. Part A. 19 (2013) 2713–2723.

[146] G. Champault, C. Polliand, F. Dufour, M. Ziol, L. Behr, A “self adhering” prosthesis for hernia repair: Experimental study, Hernia. 13 (2009) 49–52.

[147] B. Veleirinho, D.S. Coelho, P.F. Dias, M. Maraschin, R. Pinto, E. Cargnin-Ferreira, A. Peixoto, J. a Souza, R.M. Ribeiro-do-Valle, J. a Lopes-da-Silva, Foreign body reaction associated with PET and PET/chitosan electrospun nanofibrous abdominal meshes., PLoS One. 9 (2014) e95293.

[148] G. Pascual, S. Sotomayor, M. Rodríguez, Y. Bayon, J.M. Bellón, Behaviour of a new composite mesh for the repair of full-thickness abdominal wall defects in a rabbit model, PLoS One. 8 (2013) 1–16.

[149] K.L. Townsend, A. Race, M. Keane, W. Miller, L. Dishaw, E.R. Fisher, D.S. Russell, M.J. Allen, A novel hydrogel-coated polyester mesh prevents postsurgical adhesions in a rat model, J. Surg. Res. 167 (2011) e117–e124.

[150] J.W.A. Burger, J.A. Halm, A.R. Wijsmuller, S. Ten Raa, J. Jeekel, Evaluation of new prosthetic meshes for ventral hernia repair, Surg. Endosc. Other Interv. Tech. 20 (2006) 1320–1325.

[151] S. Gruber-Blum, A.H. Petter-Puchner, J. Brand, R.H. Fortelny, N. Walder, W. Oehlinger, F. Koenig, H. Redl, Comparison of three separate antiadhesive barriers for intraperitoneal onlay mesh hernia repair in an experimental model, Br. J. Surg. 98 (2011) 442–449.

[152] M.P. Diamond, E.L. Burns, B. Accomando, S. Mian, L. Holmdahl, Seprafilm?? adhesion barrier: (2) A review of the clinical literature on intraabdominal use, Gynecol. Surg. 9 (2012) 247–257.

[153] T. Karaca, A.U. Gözalan, Ö. Yoldaş, B.Ç. Bilgin, A. Tezer, Effects of tamoxifen citrate on postoperative intra-abdominal adhesion in a rat model, Int. J. Surg. 11 (2013) 68–72.

[154] A.H. MacIver, M.D. McCall, R.L. Edgar, A.L. Thiesen, D.L. Bigam, T.A. Churchill, A.M.J. Shapiro, Sirolimus drug-eluting, hydrogel-impregnated polypropylene mesh reduces intra-abdominal adhesion formation in a mouse model, Surgery. 150 (2011) 907–915.

[155] J. Zhu, Y. Zhao, L. Yang, S. Hou, Y. Su, R. Yang, Antibacterial Modification of Kirschner Wires with Polyluteolin toward Methicillin-Resistant Staphylococcus Aureus (MRSA), Materials (Basel). 8 (2015) 4876–4883.

[156] G. Schmidmaier, M. Lucke, B. Wildemann, N.P. Haas, M. Raschke, Prophylaxis and treatment of implant-related infections by antibiotic-coated

implants: a review., Injury. 37 Suppl 2 (2006) S105-12.

[157] D.G. Hargreaves, S.J. Drew, R. Eckersley, Kirschner wire pin tract infection rates: A randomized controlled trial between percutaneous and buried wires, J. Hand Surg. Am. 29 (2004) 374–376.

[158] L.P. Hsu, E.G. Schwartz, D.M. Kalainov, F. Chen, R.L. Makowiec, Complications of K-wire fixation in procedures involving the hand and wrist, J. Hand Surg. Am. 36 (2011) 610–616.

[159] S.M. Kurtz, E. Lau, H. Watson, J.K. Schmier, J. Parvizi, Economic burden of periprosthetic joint infection in the United States., J. Arthroplasty. 27 (2012)

[160] R. Wang, X. He, Y. Gao, X. Zhang, X. Yao, B. Tang, Antimicrobial property, cytocompatibility and corrosion resistance of Zn-doped ZrO2/TiO2 coatings on Ti6Al4V implants, Mater. Sci. Eng. C. 75 (2017) 7–15.

[161] V.R. Muzykantov, NO gets a test ride on high-tech transporting nanodevices: A commentary on “Sustained-release nitric oxide from long-lived circulating nanoparticles,” Free Radic. Biol. Med. 49 (2010) 528–529.

[162] Y. Li, G. Liu, Z. Zhai, L. Liu, H. Li, K. Yang, L. Tan, P. Wan, X. Liu, Z. Ouyang, Z. Yu, T. Tang, Z. Zhu, X. Qu, K. Dai, Antibacterial properties of magnesium in vitro and in an in vivo model of implant-associated methicillin-resistant Staphylococcus aureus infection, Antimicrob. Agents Chemother. 58 (2014) 7586–7591.

[163] R. Kuehl, P.S. Brunetto, A.K. Woischnig, M. Varisco, Z. Rajacic, J. Vosbeck, L. Terracciano, K.M. Fromm, N. Khanna, Preventing Implant-Associated

infections by silver coating, Antimicrob. Agents Chemother. 60 (2016) 2467–2475.

[164] K.-H. Park, K.E. Greenwood-Quaintance, A.N. Schuetz, J.N. Mandrekar, R. Patela, Activity of Tedizolid in Methicillin- Resistant Staphylococcus epidermidis Experimental Foreign Body-Associated Osteomyelitis Kyung-Hwa, Antimicrob. Agents Chemother. 61 (2017) 1–8.

[165] E.M. Hetrick, M.H. Schoenfisch, Reducing implant-related infections: active release strategies., Chem. Soc. Rev. 35 (2006) 780–9.

[166] C.L. Romanò, S. Scarponi, E. Gallazzi, D. Romanò, L. Drago, Antibacterial coating of implants in orthopaedics and trauma: a classification proposal in an evolving panorama, J. Orthop. Surg. Res. 10 (2015) 1–11.

[167] A. Ruzin, R.P. Novick, Equivalence of Lauric Acid and Glycerol Monolaurate as Inhibitors of Signal Transduction in Staphylococcus aureus Equivalence of Lauric Acid and Glycerol Monolaurate as Inhibitors of Signal Transduction in Staphylococcus aureus, J. Bacteriol. 182 (2000) 2668–2671.

[168] V.M. Verallo-Rowell, K.M. Dillague, B.S. Syah-Tjundawan, Novel antibacterial and emollient effects of coconut and virgin olive oils in adult atopic dermatitis, J. Drugs Dermatology. 19 (2008) 308–315.

[169] M.L. Peterson, P.M. Schlievert, Glycerol Monolaurate Inhibits the Effects of Gram Positive Select Agents on Eukaryotic Cells, Biochemistry. 45 (2006) 2387–2397.

[170] Q. Li, J.D. Estes, P.M. Schlievert, L. Duan, J. Amanda, P.J. Southern, C.S.

Reilly, M.L. Peterson, N. Schultz-, K.G. Brunner, K.R. Nephew, S. Pambuccian, J.D. Lifson, J. V Carlis, A.T. Haase, Glycerol monolaurate prevents mucosal SIV transmission, Nature. 458 (2009) 1034–1038.

[171] H.G. Preuss, B. Echard, A. Dadgar, N. Talpur, V. Manohar, M. Enig, D. Bagchi, C. Ingram, Effects of essential oils and monolaurin on Staphylococcus aureus: In vitro and in vivo studies, Toxicol. Mech. Methods. 15 (2005) 279–285.

[172] P.M. Schlievert, M.L. Peterson, Glycerol monolaurate antibacterial activity in broth and biofilm cultures, PLoS One. 7 (2012) e40350.

[173] N. Borodinov, A.P. Soliani, Y. Galabura, B. Zdyrko, C. Tysinger, S. Novak, Q. Du, Y. Huang, V. Singh, Z. Han, J. Hu, L. Kimerling, A.M. Agarwal, K. Richardson, I. Luzinov, Gradient Polymer Nanofoams for Encrypted Recording of Chemical Events, ACS Nano. (2016)

[174] J. Merritt, D. Kadouri, G. O'Toole, Growing and Analyzing Static Biofilms, Curr. Protoc. Microbiol. (2015) 1–29.

[175] O. Guillaume, X. Garric, J.-P. Lavigne, H. Van Den Berghe, J. Coudane, Multilayer, degradable coating as a carrier for the sustained release of antibiotics: preparation and antimicrobial efficacy in vitro., J. Control. Release. 162 (2012) 492–501.

[176] H. Kobayashi, M. Oethinger, M.J. Tuohy, G.W. Procop, T.W. Bauer, Improved detection of biofilm-formative bacteria by vortexing and sonication: A pilot study, Clin. Orthop. Relat. Res. 467 (2009) 1360–1364.

[177] S. El Abed, S.K. Ibnsouda, H. Latrache, F. Hamadi, Scanning Electron Microscopy (SEM) and Environmental SEM: Suitable Tools for Study of Adhesion Stage and Biofilm Formation, in: Scan. Electron Microsc., 2012: pp. 717–730.

[178] X. Chen, D. Hou, L. Wang, Q. Zhang, J. Zou, G. Sun, Antibacterial Surgical Silk Sutures Using a High-Performance Slow-Release Carrier Coating System, ACS Appl. Mater. Interfaces. 7 (2015) 22394–22403.

[179] G. Meng, J. He, Y. Wu, F. Wu, Z. Gu, Antibiotic-loaded chitosan hydrogel with superior dual functions: Antibacterial efficacy and osteoblastic cell responses, ACS Appl. Mater. Interfaces. 6 (2014) 10005–10013.

[180] K.T. Holland, D. Taylor, A.M. Farrell, The effect of glycerol monolaurate on growth of, and production of toxic shock syndrome toxin-1 and lipase by, staphylococcus aureus, J. Antimicrob. Chemother. 33 (1994) 41–55.

[181] H.G. Preuss, B. Echard, M. Enig, I. Brook, T.B. Elliott, Minimum inhibitory concentrations of herbal essential oils and monolaurin for gram-positive and gram-negative bacteria, Mol. Cell. Biochem. 272 (2005) 29–34.

[182] Y.C. Lin, P.M. Schlievert, M.J. Anderson, C.L. Fair, M.M. Schaefers, R. Muthyala, M.L. Peterson, Glycerol monolaurate and dodecylglycerol effects on Staphylococcus aureus and toxic shock syndrome toxin-1 in vitro and in vivo, PLoS One. 4 (2009) 2–11.

[183] T. Nakatsuji, M.C. Kao, J.-Y. Fang, C.C. Zouboulis, L. Zhang, R.L. Gallo, C.-M. Huang, Antimicrobial Property of Lauric Acid Against Propionibacterium

Acnes: Its Therapeutic Potential for Inflammatory Acne Vulgaris, J. Invest. Dermatol. 129 (2009) 2480–2488.

[184] S. Lieberman, M.G. Enig, H.G. Preuss, A Review of Monolaurin and Lauric Acid, Altern. Complement. Ther. 12 (2006) 310–315.

[185] A. Abron, M. Hopfensperger, J. Thompson, L.F. Cooper, Evaluation of a predictive model for implant surface topography effects on early osseointegration in the rat tibia model, J. Prosthet. Dent. 85 (2001) 40–46.

[186] J.H. Yu, L.C. Wu, J.T. Hsu, Y.Y. Chang, H.H. Huang, H.L. Huang, Surface roughness and topography of four commonly used types of orthodontic archwire, J. Med. Biol. Eng. 31 (2011) 367–370.

[187] D. Campoccia, L. Montanaro, C.R. Arciola, The significance of infection related to orthopedic devices and issues of antibiotic resistance., Biomaterials. 27 (2006) 2331–9.

[188] A. Gristina, Biomaterial-centered infection: microbial adhesion versus tissue integration, Science. 237 (1987) 1588–1595.

[189] A. Delaune, O. Poupel, A. Mallet, Y.M. Coic, T. Msadek, S. Dubrac, Peptidoglycan crosslinking relaxation plays an important role in staphylococcus aureus walkr-dependent cell viability, PLoS One. 6 (2011).

[190] C.C.B. Pereira, M.A.P. da Silva, M.A.P. Langone, Enzymatic Synthesis of Monolaurin, Appl. Biochem. Biotechnol. 113–116 (2004).

[191] J. Jenkins, P. O'Dwyer, Inguinal hernias, Bmj. 336 (2008) 269–272.

[192] A. Serrero, S. Trombotto, Y. Bayon, P. Gravagna, S. Montanari, L. David,

Polysaccharide-based adhesive for biomedical applications: correlation between rheological behavior and adhesion., Biomacromolecules. 12 (2011) 1556–66.

[193] S.B. Orenstein, E.R. Saberski, D.L. Kreutzer, Y.W. Novitsky, Comparative analysis of histopathologic effects of synthetic meshes based on material, weight, and pore size in mice., J. Surg. Res. 176 (2012) 423–9.

[194] A.J. Wood, M.J. Cozad, D.A. Grant, A.M. Ostdiek, S.L. Bachman, S.A. Grant, Materials characterization and histological analysis of explanted polypropylene, PTFE, and PET hernia meshes from an individual patient., J. Mater. Sci. Mater. Med. 24 (2013) 1113–22.

[195] FDA, Urogynecologic Surgical Mesh Implants.

[196] H. Patel, G. Sternschuss, D.R. Ostergard, Post-Implantation Alterations of Polypropylene in the Human, J. Urol. 188 (2012) 27–32.

[197] G. Sternschuss, D.R. Ostergard, H. Patel, Post-implantation alterations of polypropylene in the human, J. Urol. 188 (2012) 27–32.

[198] A.J. Coury, Chemical and biochemical degradation of polymers intended to be biostable, in: Biomater. Sci. An Introd. to Mater. Med., Third Edit, Elsevier, 2013: pp. 696–715.

[199] J.M. Anderson, A. Rodriguez, D.T. Chang, Foreign body reaction to biomaterials., Semin. Immunol. 20 (2008) 86–100.

[200] M.D. Rees, C.L. Hawkins, M.J. Davies, Hypochlorite and superoxide radicals can act synergistically to induce fragmentation of hyaluronan and chondroitin

sulphates, Biochem. J. 184 (2004) 175–184.

[201] W.S. Cobb, J.M. Burns, R.D. Peindl, A.M. Carbonell, B.D. Matthews, K.W. Kercher, B.T. Heniford, Textile analysis of heavy weight, mid-weight, and light weight polypropylene mesh in a porcine ventral hernia model., J. Surg. Res. 136 (2006) 1–7.

[202] C.R. Costello, S.L. Bachman, B.J. Ramshaw, S.A. Grant, Materials characterization of explanted polypropylene hernia meshes, J. Biomed. Mater. Res. B. Appl. Biomater. 83 (2007) 44–49.

[203] R.J. Fitzgibbons, A.T. Richards, T.H. Quinn, Open hernia repair, ACS Surg. Princ. Pract. (2003) 1–22.

[204] Q. Zhao, J. Casas-Bejar, P. Urbanski, K. Stokes, Glass Wool–H2O2/CoCl2 test system for in vitro evaluation of biodegradative stress cracking in polyurethane elastomers, J. Biomed. Mater. Res. 29 (1995) 467–475.

[205] J. Štikarová, R. Kotlín, T. Riedel, J. Suttnar, K. Pimková, L. Chrastinová, J.E. Dyr, The effect of reagents mimicking oxidative stress on fibrinogen function, Sci. World J. 2013 (2013) 1–8.

[206] R. Nisticò, M.G. Faga, G. Gautier, G. Magnacca, D. D'Angelo, E. Ciancio, G. Piacenza, R. Lamberti, S. Martorana, Physico-chemical characterization of functionalized polypropylenic fibers for prosthetic applications, Appl. Surf. Sci. 258 (2012) 7889–7896.

[207] C.S. Brazel, N.A. Peppas, Mechanisms of solute and drug transport in relaxing, swellable, hydrophilic glassy polymers, Polymer (Guildf). 40 (1999)

3383–3398.

[208] L.M. Valenzuela, G. Zhang, C. Flach, S. Murthy, R. Mendelsohn, B. Michniak-Kohn, J. Kohn, Multiscale analysis of water uptake and erosion in biodegradable polyarylates., Polym. Degrad. Stab. 97 (2012) 410–420.

[209] S.V. Gopal, A. Warrier, Recurrence after groin hernia repair-revisited., Int. J. Surg. 11 (2013) 374–7.

[210] S. Kumar, R.G. Wilson, S.J. Nixon, I.M.C. Macintyre, Chronic pain after laparoscopic and open mesh repair of groin hernia., Br. J. Surg. 89 (2002) 1476–9.

[211] V. Shuvaev, J. Han, K.J. Yu, S. Huang, B.J. Hawkins, M. Madesh, M. Nakada, V.R. Muzykantov, PECAM-targeted delivery of SOD inhibits endothelial inflammatory response., FASEB J. 25 (2011) 348–57.

[212] E.D. Hood, M. Chorny, C.F. Greineder, I. S. Alferiev, R.J. Levy, V.R. Muzykantov, Endothelial targeting of nanocarriers loaded with antioxidant enzymes for protection against vascular oxidative stress and inflammation, Biomaterials. 35 (2014) 3708–3715.

[213] R. van Lith, E.K. Gregory, J. Yang, M.R. Kibbe, G. a Ameer, Engineering biodegradable polyester elastomers with antioxidant properties to attenuate oxidative stress in tissues., Biomaterials. 35 (2014) 8113–22.

[214] A. Coda, R. Bendavid, F. Botto-Micca, M. Bossotti, A. Bona, Structural alterations of prosthetic meshes in humans., Hernia. 7 (2003) 29–34.

[215] E.B. Deerenberg, J. Verhelst, S.E.R. Hovius, J.F. Lange, Mesh expansion

as the cause of bulging after abdominal wall hernia repair, Int. J. Surg. Case Rep. 28 (2016) 200–203.

[216] Q. Zhao, A. McNally, Human plasma α2-macroglobulin promotes in vitro oxidative stress cracking of pellethane 2363-80A: In vivo and in vitro correlations, J. Biomed. Mater. Res. 27 (1993) 379–388.

[217] M.A. Schubert, M.J. Wiggins, J.M. Anderson, A. Hiltner, Role of oxygen in biodegradation of poly(etherurethane urea) elastomers, J. Biomed. Mater. Res. 34 (1997) 519–530.

[218] L.J. Hazell, J.J. van den Berg, R. Stocker, Oxidation of low-density lipoprotein by hypochlorite causes aggregation that is mediated by modification of lysine residues rather than lipid oxidation, Biochem. J. 302 (1994) 297–304.

[219] U. Panzenboeck, S. Raitmayer, H. Reicher, H. Lindner, O. Glatter, E. Malle, W. Sattler, Effects of reagent and enzymatically generated hypochlorite on physicochemical and metabolic properties of high density lipoproteins, J. Biol. Chem. 272 (1997) 29711–29720.

[220] M. Katrantzis, M.S. Baker, C.J. Handley, D.A. Lowther, The oxidant hypochlorite (OCl-), a product of the myeloperoxidase system, degrades articular cartilage proteoglycan aggregate, Free Radic. Biol. Med. 10 (1991)

[221] H. Otaguro, L.F.C.P. de Lima, D.F. Parra, a. B. Lugão, M. a. Chinelatto, S.V. Canevarolo, High-energy radiation forming chain scission and branching in polypropylene, Radiat. Phys. Chem. 79 (2010) 318–324.

[222] S. Alariqi, P. Kumar, B.S. Rao, R.P. Singh, Effect of γ-dose rate on crystallinity and morphological changes of γ-sterilized biomedical polypropylene, Polym. Degrad. Stab. 94 (2009) 272–277.

[223] L.H. Sperling, Introduction to Physical Polymer Science, New York, 2006. http://pubs.acs.org/doi/abs/10.1021/ed078p1469.1.

[224] S. Lyu, D. Untereker, Degradability of polymers for implantable biomedical devices., Int. J. Mol. Sci. 10 (2009) 4033–65.

[225] J. Skrobot, L. Zair, M. Ostrowski, M. El Fray, New injectable elastomeric biomaterials for hernia repair and their biocompatibility, Biomaterials. 75 (2016) 182–192.

[226] O. Sánchez, V. Rodríguez-Sureda, C. Domínguez, T. Fernández-Figueras, A. Vilches, E. Llurba, J. Alijotas-Reig, Study of biomaterial-induced macrophage activation, cell-mediated immune response and molecular oxidative damage in patients with dermal bioimplants., Immunobiology. 217 (2012) 44–53.

[227] S. Lyu, D. Untereker, Degradability of Polymers for Implantable Biomedical Devices, Int. J. Mol. Sci. 10 (2009) 4033–4065.

[228] N. Bryan, H. Ahswin, N.J. Smart, Y. Bayon, J. a Hunt, In vitro activation of human leukocytes in response to contact with synthetic hernia meshes., Clin. Biochem. 45 (2012) 672–6.

[229] C. Petro, E. Nahabet, C. Criss, S. Orenstein, H. von Recum, Y. Novitsky, M. Rosen, Central failures of lightweight monofilament polyester mesh causing

hernia recurrence: a cautionary note, Hernia. 19 (2015) 155–159.

[230] A. Carbonell, B. Matthews, D. Dréau, M. Foster, C. Austin, K. Kercher, R. Sing, B. Heniford, The susceptibility of prosthetic biomaterials to infection, Surg. Endosc. 19 (2005) 430–435.

[231] B.T. Heniford, K.B. Williams, J.F. Bradley, Ventral and Incisional Hernia Repair with Preperitoneal Mesh Placement: Outcomes from a Prospective Study in Complex Hernia Repair, in: Oral Present. South. Surg. Assoc. Annu. Meet., 2013.

[232] Q. Jiang, Natural forms of vitamin E: metabolism, antioxidant, and anti-inflammatory activities and their role in disease prevention and therapy, Free Radic. Biol. Med. 72 (2014) 76–90.

[233] A. Beharka, D. Wu, M. Serafini, S. Meydani, Mechanism of vitamin E inhibition of cyclooxygenase activity in macrophages from old mice: role of peroxynitrite, Free Radic Biol Med. 32 (2002) 503–511.

[234] G. Javad, K. Reza, Farid Hossiani Alireza, R. Negin, Nahanmoghadam Ebrahim, Salehifar Houshang, Vitamin e supplementation, lung functions and clinical manifestations in children with moderate asthma: a randomized double blind placebo-controlled trial, Iran. J. Allergy, Asthma Immunol. 13 (2014) 98–103.

[235] G. Yetkin, M. Uludag, B. Citgez, S. Karakoc, N. Polat, F. Kabukcuoglu, Prevention of peritoneal adhesions by intraperitoneal administration of vitamin E and human amniotic membrane., Int. J. Surg. 7 (2009) 561–5.

[236] D. A MacKenna, J.H. Omens, A. D. McCulloch, J.W. Covell, Contribution of collagen matrix to passive left ventricular mechanics in isolated rat hearts., Am. J. Physiol. 266 (1994) H1007-18.

[237] R. Raymond, Metabolic aspects of hernia disease, in: Abdom. Wall Hernias Princ. Manag., 2000: pp. 139–142.

[238] J. Burger, R. Luijendijk, W. Hop, J. Halm, E. Verdaasdonk, J. Jeekel, Long-term follow-up of a randomized controlled trial of suture versus mesh repair of incisional hernia, Ann. Surg. 240 (2004) 578–583.

[239] A.W. Bridges, A.J. García, Anti-inflammatory polymeric coatings for implantable biomaterials and devices., J. Diabetes Sci. Technol. 2 (2008) 984–94.

[240] E. Reiter, Q. Jiang, S. Christen, Anti-inflammatory properties of α- and γ-tocopherol, Mol. Aspects Med. 28 (2007) 668–691.

[241] M. Cook, N. Johnson, H.D. Zegzula, M. Schray, M. Glissmeyer, L. Sorenson, Prophylactic use of pentoxifylline (Trental) and Vitamin E to prevent capsular contracture after implant reconstruction in patients requiring adjuvant radiation, Am. J. Surg. 211 (2016) 854–859.

[242] K. ichiro Yamamoto, M. Matsuda, M. Okuoka, T. Yakushiji, M. Fukuda, T. Miyasaka, Y. Matsumoto, K. Sakai, Antioxidation property of vitamin E-coated polysulfone dialysis membrane and recovery of oxidized vitamin E by vitamin C treatment, J. Memb. Sci. 302 (2007) 115–118.

[243] P. Bracco, E. Oral, Vitamin E-stabilized UHMWPE for total joint implants: A

review, Clin. Orthop. Relat. Res. 469 (2011) 2286–2293.

[244] C. Uneri, M. Sari, J. Akboğa, M. Yüksel, Vitamin e-coated tympanostomy tube insertion decreases the quantity of free radicals in tympanic membrane., Laryngoscope. 116 (2006) 140–3.

[245] C.L. Cachia, O., Benna, J.E., Pedruzzi, E., Descomps, B., Gougerot-Pocidalo, M.A., Leger, Alpha- tocopherol inhibits the respiratory burst in human monocytes. Attenuation of p47(phox) membrane translocation and phosphorylation, J. Biol. Chem. 273 (1998) 32801–32805.

[246] J.F. Freedman, J.E., Farhat, J.H., Loscalzo, J., Keaney Jr., Alpha-tocopherol inhibits aggregation of human platelets by a protein kinase C-dependent mechanism, Circulation. 94 (1996) 2434–2440.

[247] J.M. Kempna, P., Reiter, E., Arock, M., Azzi, A., Zingg, InhibitionofHMC-1mastcell proliferationby vitamin E: involvement of the protein kinaseB pathway, J. Biol. Chem. 279 (2004) 50700–50709.

[248] I. Islam, K.N., Devaraj, S., Jialal, Alpha-tocopherol enrichment of monocytes decreases agonist- induced adhesion to human endothelial cells, Circulation. 98 (1998) 2255–2261.

[249] S. Sury, M.D., Frese-Schaper, M., Muhlemann, M.K., Schulthess, F.T., Blasig, I.E., Tauber, M.G., Shaw, S.G., Christen, Evidence that N-acetylcysteine inhibits TNF-alpha-induced cerebrovascular endothelin-1 upregulation via inhibition of mitogen- and stress-activated protein kinase, Free Radic. Biol. Med. 41 (2006) 1372–1383.

[250] G.D. Hooker, B.M. Taylor, D.K. Driman, Prevention of adhesion formation with use of sodium hyaluronate–based bioresorbable membrane in a rat model of ventral hernia repair with polypropylene mesh—A randomized, controlled study, Surgery. 125 (1999) 211–216.

[251] G. Vatassery, A. Krezowski, J. Eckfeldt, Vitamin E concentrations in human blood plasma and platelets, Am. J. Clin. Nutr. 37 (1983) 1020–1024.

[252] S. Wilkosz, J. Epstein, A. De Giorgio-Miller, W. McLean, G. Ireland, S. Herrick, Remodelling of adipose tissue during experimental omental adhesion formation, Br. J. Surg. 95 (2008) 387–396.

[253] F.S. Ayubi, P.J. Armstrong, M.S. Mattia, D.M. Parker, Abdominal wall hernia repair: A comparison of Permacol and Surgisis grafts in a rat hernia model, Hernia. 12 (2008).

[254] K. Dee, D. Puleo, R. Bizios, An Introduction To Tissue-Biomaterial Interactions, 2002.

[255] G. Welty, U. Klinge, B. Klosterhalfen, R. Kasperk, V. Schumpelick, Functional impairment and complaints following incisional hernia repair with different polypropylene meshes, Hernia. 5 (2001) 142–147.

[256] D. DuBay, W. Choi, M. Urbanchek, X. Wang, B. Adamson, Incisional Herniation Induces Decreased Abdominal Wall Compliance via Oblique Muscle Atrophy and Fibrosis, Ann. Surg. 45 (2007) 140–147.